

https://dspace.org/

An initial estimation of the concentrations of methane (CH4) emitted from the Wakkerstroom wetland and Majuba power station in Mpumalanga province, South Africa

Bobo, Christine

2024-08

University of the Witwatersrand, Johannesburg

https://hdl.handle.net/10539/45212

Bobo, Christine. (2024). An initial estimation of the concentrations of methane (CH4) emitted from the Wakkerstroom wetland and Majuba power station in Mpumalanga province, South Africa. [Master's dissertation, University of the Witwatersrand, Johannesburg]. WIReDSpace. https://hdl.handle.net/10539/45212

Downloaded from a DSpace repository. https://dspace.org/



An initial estimation of the concentrations of methane (CH_4) emitted from the Wakkerstroom wetland and Majuba power station in Mpumalanga province, South Africa.

by

Ms Christine Bobo

(Person No. 1606543)

Submitted in fulfilment of the requirements for the Degree

Master of Science

in

Animal, Plant and Environmental Sciences

in the Faculty of Science, University of Witwatersrand, Johannesburg, South Africa

Supervisors: Professor Mary. C. Scholes and Dr David. G. Furniss

August 2024

DECLARATION

I, **Christine Bobo** (student ID: 1606543), am currently enrolled in the MSc program for Animal, Plant, and Environmental Sciences for the year 2024. I hereby affirm the following:

- I acknowledge that plagiarism, defined as the unauthorized use of another person's work without proper acknowledgement, is unethical.
- I verify that all materials submitted for evaluation in the aforementioned course are entirely my own, except where explicitly stated otherwise.
- I have adhered to the prescribed referencing guidelines when incorporating the ideas and words of others.
- I am aware that any suspicion of academic dishonesty or failure to attribute sources appropriately may result in disciplinary measures by the University of the Witwatersrand.

Signature: 

Date: 26 August 2024

ABSTRACT

The continuous increase in methane (CH_4) emissions to the atmosphere poses a formidable challenge to Earth's climate resilience and exacerbates the impacts of global warming. This study compared microbial CH_4 concentrations from the Wakkerstroom wetland to fossil fuel concentrations from the coal stockpiles at the Majuba power station in Mpumalanga, South Africa, using three methodological approaches: flexfoil bags, isotopic analysis, and satellite data. Seasonal ground measurements were collected in 3L flexfoil bags and analysed for CH_4 mole fraction using a Picarro 2301 calibrated to the WMO X2004A CH_4 scale. Samples were prepared for isotopic analysis by continuous-flow isotope-ratio mass spectrometry using an Isoprime Trace Gas system. Findings from ground sampling measurements showed that for three out of the four seasons, *Phragmites australis* at the Wakkerstroom wetland had the highest CH_4 concentration [spring (0.209 ± 0.076 ppm), autumn (0.537 ± 0.239 ppm), and winter (0.132 ± 0.065 ppm)], and the coal stockpiles at the Majuba power station had the lowest CH_4 concentration [summer (0.022 ± 0.021 ppm), autumn (0.014 ± 0.053 ppm), and winter (0.002 ± 0.004)]. Isotopic measurements, which identify and differentiate gas sources by examining distinct isotopic signatures, showed that the Wakkerstroom wetland had consistently light, ^{13}C depleted isotopic signatures seasonally ranging between -61.4‰ to -55.6‰. In contrast to this, the Majuba power station coal stockpiles had inconsistent isotopic signatures through the sampling seasons- heavier CH_4 emission isotopic signatures with ^{13}C enrichment during spring and summer at -35.3 ± 1.0 ‰ and -43.5 ± 3.5 ‰ respectively, and lighter isotopic signatures with ^{13}C depletion during autumn and winter of - 62.0 ± 1.6 ‰ and - 87.0 ± 10.3 ‰ respectively.

On a larger temporal and spatial scale, satellite-based measurements from the Tropospheric Monitoring Instrument (TROPOMI) showed no significant differences between Wakkerstroom (1855.4 ± 18.0 ppb) and Majuba power station (1857.1 ± 22.9 ppb) in terms of the total column averaged dry-air mole fraction of methane (XCH_4). An increasing trend in CH_4 mole fraction, in Southern Africa as measured at Cape Point Global Atmospheric Watch (GAW) station over a 39-year period was also observed. Meteorological variables, particularly wind direction, had a more significant impact on CH_4 mole fractions at Cape Point than at the Wakkerstroom wetland. The multi-faceted approach of utilizing the three measurement techniques provided a comprehensive view of atmospheric CH_4 showing that wetlands could be more significant CH_4 hotspots in comparison to coal stockpiles at power stations. Measuring methane concentrations is challenging due to its inherent complexity, thus the utilisation of different measurement

methodologies further highlighted the spatial and temporal variability of CH_4 concentrations at both the wetland and the coal stockpiles.

Key words

Methane, wetland, coal stockpiles, source isotopic signature, TROPOMI, GAW.

To my mother**, Nontozanele Gerty Bobo**, sister, **Thembeka Bobo**, and niece, **Nonceba "Jane" Bobo**. Your teaching will forever inspire me to approach knowledge with a compassionate heart and a quest for wisdom that transcends the confines of the academic realm.

"***My mom did what school didn't. She taught me how to think"***. – [Trevoh Noah]

To my dearest friend, Hlumisa Ntsangani, who passed away during this dissertation and whose radiant spirit illuminated my darkest days and whose unwavering support fuelled my academic journey. Though you are no longer physically present, your indomitable strength and enduring friendship will forever reside in the words etched within these pages.

ACKNOWLEDGEMENTS

I would like to thank the Lord Almighty for giving me strength to pull through and finish this dissertation.

I would further like to extend gratitude he following people:

- Prof. Mary Scholes: For supervision, guidance, emotional and financial support. Thank you for giving me a chance at this project, it would have never begun without you.
- Dr. David Furniss: For supervision, guidance, emotional and financial support from my Honours year until present. Thank you for your constant encouragement, you've reminded me of the reasons I enjoy science.
- Prof. Euan Nisbet (Royal Holloway, University of London): For supplying flexfoil bags for sampling, analysis of the methane gas samples, paying for the costs of shipment throughout the project. Thank you for also constantly answering questions I had on the data at times I was unsure. This project would not have occurred without you.
- Dr. Rebecca Fisher (Royal Holloway, University of London): For ensuring that gas samples were collected and analysed on time throughout the project. Thank you for also attending meetings to help me in understanding my data and results. It's enjoyable working with you.
- Casper Labuschagne: Thank you for helping me access all data from Cape Point and reading my work.
- Hugo De Lemos: For helping me with TROPOMI data accessing and analysis.
- Carol Preston: Thank you for lending me the boat for sampling in the autumn and winter seasons. It helped achieve my research objectives.
- This work is based on the research supported in part by the National Research Foundation (NRF) South Africa (Grant number: MND210427597639).

Contents

1. INTRODUCTION 14
1.1. Overview 14
1.2. Rationale 16
1.3. Aim 16
1.4. Research objectives 16
1.5. Key research questions. 17
2. LITERATURE REVIEW 18
2.1. Global climate change and the global CH_4 budget 18
2.2. Methane emissions in South Africa 20
2.3. Methane production and emissions in the South African coal sector. 22
2.4. Methane production and concentrations in South African wetland ecosystems 22
2.5. Approaches to measuring wetland and coalbed methane concentrations. 24
2.6. Closed chamber method. 24
2.7. Flexfoil bag sampling method. 26
2.8. Effect of various plant communities on methane concentrations. 28
2.9. Isotopic signatures and their use. 31
2.10. Satellite approaches to methane emission quantification using TROPOMI. 34
2.11. The Cape Point Global Atmospheric Watch (GAW) station in South Africa. 36
2.12. Concluding summary 38
3. MATERIALS AND METHODS 39
3.1. Study sites 39
3.2. Wakkerstroom wetland 39
3.3. Majuba power station 40
3.4. Study species 43
3.5. Typha Capensis 43
3.6. *Phragmites australis* 45
3.7. Schoenoplectus decipiens 48
3.8. Experimental design and protocol 50
3.9. Set-up of sampling equipment on sampling sites 50
3.10. Sampling at the Wakkerstroom wetland sites 51
3.11. Sampling at the Majuba power station 52
3.12. Standard trace gas analysis at Royal Holloway, University of London (RHUL) 57
3.13. Determination of isotopic source signatures using the Keeling plot technique. 59
3.14. Data analyses 60

3.15. Regression analysis for Keeling plot computation 60
3.16. Wakkerstroom weather station data 62
3.17. Measurement principles of the TROPOMI instrument 62
3.18. TROPOMI CH_4 product 63
3.19. TROPOMI data collection and processing 65
3.20. TROPOMI Data analyses 65
3.21. The Cape Point Global Atmospheric Watch (GAW) station. 66
3.23. Data analyses for the Cape Point GAW data. 67
4. RESULTS 69
4.1. SECTION A: Ground field concentrations and isotope data from the Wakkerstroom wetland plant communities and the Majuba power station coal stockpile. 69
4.2. Meteorological variables at the Wakkerstroom wetland. 77
4.3. Seasonal wind patterns at the Wakkerstroom wetland 77
4.4. Temperature and rainfall data at Wakkerstroom, Mpumalanga. 79
4.5. Relative humidity at Wakkerstroom, Mpumalanga. 80
4.6. SECTION B: TROPOMI measurements 82
4.7. SECTION C: GAW measurements. 89
4.8. Annual reported mole fraction of CH_4 at Cape Point for 39 years (1983 - 2021). ..90
4.9. Wind roses at Cape Point 92
4.10. Atmospheric transport to Cape Point, South Africa. 94
4.11. Air temperature at Cape Point 95
4.12. Relative humidity (%) at Cape Point. 95
5. DISCUSSION 97
5.1. Methane concentrations from the Wakkerstroom wetland and coal stockpile at the Majuba power station. 97
5.2. Source carbon isotopic signatures in CH_4 ($S13CCH4$) at the Wakkerstroom wetland and Majuba power station coal stockpiles 102
5.3. Satellite based measurements of CH_4 mole fractions using TROPOMI 104
5.4. Cape Point GAW CH_4 data. 106
5.5. Limitations and suggestions for future work. 108
6. CONCLUSION 108
7. REFERENCES 110

LIST OF FIGURES:

Figure 1: Diagram illustrating the greenhouse effect. Image from: https://forces.si.edu/atmosphere/02_04_07.html 19
Figure 2: Global methane budget 2008-2017 as report in the study by Saunois *et al.* (2020). The emission range is indicated by the numbers in parenthesis, and the numbers on the left and right represent bottom-down and top-down estimations, respectively. 20
Figure 3: Sources of CH_4 by sector in South Africa as reported by Shikwambana *et al.* (2022) 21
Figure 4: The range of $S^{13}C_{CH_4}$ values for various sources of methane, including microbial (red), abiotic (grey), eukaryotic (green), atmospheric (blue), and fungal (orange) origins, is presented based on findings by Moritz Schroll *et al.* (2020). The combination of microbial and abiotic methane formation processes for gas hydrates is indicated by the red and grey dashed bars, referring to Kvenvolden (1995). Data regarding these signatures were compiled from studies by Brownlow *et al.* (2017), Keppler *et al.* (2006, 2016), Kvenvolden (1995), Nisbet *et al.* (2016), Quay *et al*. (1999), and Vigano *et al.* (2009). 33
Figure 5: Map showing the location of the Wakkerstroom wetland and the Majuba power station in Mpumalanga province, South Africa. 41
Figure 6: Trucks delivering coal at Majuba power station. Image captured on 26 January 2023.....42
Figure 7: *Typha Capensis* sampling sites at the Wakkerstroom wetland. Top left: Typha water sampling site. 44
Figure 8:*Phragmites* on the wetland bank at the Wakkerstroom wetland**.** 46
Figure 9:Water *Phragmites australis* sampling site.....47
Figure 10: Mixed vegetation (*Typha* and *Schoenoplectus)* sampling site at Wakkerstroom wetland during the spring season (left) and during the autumn season (right). 49
Figure 11:Sampling equipment (flexfoil bag, fishing rod, and 6V battery operated pump**)**...50
Figure 12: Google Earth image of the location of where the samples were collected for the vegetation communities along the Wakkerstroom wetland in Mpumalanga province, South Africa 52
Figure 13:Location of where the samples were collected at Majuba power station in Mpumalanga province, South Africa. 54
Figure 14: Downwind sampling locations at Majuba power station during the 4 seasons of sampling: spring (top left), summer (top right), autumn (bottom left), winter (bottom right).55

Figure 15: Upwind sampling locations at Majuba power station during the 4 seasons of sampling: spring (top left), summer (top right), autumn (bottom left), winter (bottom right).56
Figure 16: Diagram of the sampling equipment for CH_4 analysis set-up at RHUL. Adapted from Fisher *et al*. (2006). 58
Figure 17: Diagram of the sampling equipment for CH_4 analysis set-up at RHUL. Adapted from Fisher *et al*. (2006). 58
Figure 18: Image showing the CH_4 analyser during sample analysis. Adapted from Fisher *et al.* (2006).....59
Figure 19: TROPOMI measurement principle (Apituley *et al.,* 2022).....63
Figure 20:Map showing the location of the Cape Point GAW station (Labuschagne *et al.,* 2018). 66
Figure 21: Cape Point GAW station sampling instrumentation (source: Alban Thollot: "https://www.ige-grenoble.fr/Cape-Point-South-Africa").....67
Figure 22: Concentration (ppm) measurements collected from various vegetation communities at the Wakkerstroom wetland and coal stockpiles at the Majuba power station in the spring (9-10 September 2022), summer (25-26 January 2023), autumn (22-23 April 2023) and winter(22-23 July 2023).....71
Figure 23: Keeling plots representing the source carbon isotopic source signatures of the Wakkerstroom wetland in the spring, summer, autumn, and winter seasons. 74
Figure 24: Keeling plots representing the carbon isotopic source signatures of the Majuba power station in the spring, summer, autumn, and winter seasons.....76
Figure 25:Seasonal wind rose plots at Wakkerstroom, Mpumalanga (SON: September, October, November; DJF: December, January, February; MAM: March, April, May; JJA: June, July, August).....78
Figure 26:Seasonal temperature pattern (°C) at Wakkerstroom, Mpumalanga on January 2022 – August 2023 with red arrows indicating field sampling days in each season. 79
Figure 27:Seasonal rainfall pattern at Wakkerstroom, Mpumalanga from January 2022-August 2023 with red arrows indicating field sampling days in each season. 80
Figure 28:Relative humidity at Wakkerstroom, Mpumalanga from January 2022-August 2023 with red arrows indicating field sampling days in each season. 81
Figure 29: Boxplot showing the Total column averaged dry-air mole fraction of methane at Wakkerstroom and Majuba power station in Mpumalanga province, South Africa as measured using TROPOMI.....83
Figure 30: Map produced from TROPOMI total column averaged dry-air mole fraction of

methane product (spring 2022)**.** 85
Figure 31: Map produced from TROPOMI total column averaged dry-air mole fraction of methane product (summer 2023). 86
Figure 32: Map produced from TROPOMI total column averaged dry-air mole fraction of methane product (autumn 2023). 87
Figure 33: Map produced from tropomi total column averaged dry-air mole fraction of methane product (winter 2022). 88
Figure 34: Monthly reported mole fraction of CH_4 at Cape Point GAW station during 2014-2021 90
Figure 35:Reported mole fraction of methane (ppb) at Cape Point for the years 1983 – 2021. 91
Figure 36: Seasonal wind rose plots for Cape Point GAW station (SON: September, October, November; DJF: December, January, February; MAM: March, April, May; JJA: June, July, August) 93
Figure 37: HYSPLIT backward trajectory analysis for the summer (20 January 2021) and winter (15 August 2021) representative days at Cape Point, South Africa. 94
Figure 38:Seasonal air temperature graph for the Cape Point GAW station in Cape Town, South Africa for the years 2020 - 2022**.** 95
Figure 39: Seasonal/monthly relative humidity (%) patterns at Cape Point GAW station, South Africa. 96
Figure 40: Diagram illustrating humidity-induced convection in Phragmites plants (van den Berg et al., 2020). N_2 and O_2 move through stomata in the leaf sheath, driven by the diffusion gradient. Living plants generate higher pressure in the stem (ΔP), causing airflow towards the rhizome, venting through old and damaged stems (red arrows). O_2 is conveyed to the soil, while CH_4 diffusing into the rhizome is transported to the atmosphere. Where O_2 and CH_4 coexist, CH_4 oxidation takes place. 99

LIST OF TABLES

Table 1: GWP of greenhouse gases as reported by the IPCC (2022). Image from: https://erce.energy/erceipccsixthassessment/ _____15

Table 2: Mean and standard deviation table for seasonal concentration (ppm) data. _____72

Table 3: Descriptive statistics of the total column averaged dry-air mole fraction of methane distribution at Majuba power station and Wakkerstroom. _____83

LIST OF ABBREVIATIONS

- GAW: Global Atmospheric Watch
- GHG: Greenhouse gas
- GWP: Global Warming Potential
- IPCC: Intergovernmental Panel on Climate Change
- LAN: Lin'an
- LFS: Longfengshan
- NPP: National Polar-orbiting Partnership
- NWA: National Water Act
- PA: Paris Agreement
- S5P: Sentinel 5 Precursor
- SAAQIS: South African Air Quality Information System
- SAWS: South African Weather Services
- SDGs: Sustainable Development Goals
- TROPOMI: Tropospheric Monitoring Instrument
- UNEP: United Nations Environment Programme
- UNFCCC: United Nations Framework Convention on Climate Change
- VIIRS: Visible Infrared Imager Radiometer Suite instrument.
- WDCGG: World Data Centre for Greenhouse Gases
- WLG: Waliguan
- WMO: World Meteorological Organisation
- XCH_4: Total column averaged dry-air mole fraction of methane.

LIST OF SYMBOLS

- $\delta^{13}CH_4$: Carbon isotopic signature in methane.

1. INTRODUCTION

1.1. Overview

The Climate Change Bill of South Africa has a broad main purpose to "*enable the development of an effective climate change response and a long-term transition to a low carbon and climate-resilient economy and society for South Africa in the context of sustainable development.*" (Climate Change Bill, 2022).

The Intergovernmental Panel on Climate Change (IPCC) reported that, by 2017, anthropogenic warming rose by approximately 1 °C over pre-industrial levels, with an approximate annual rate of increase of 0.2 °C (IPCC, 2018). Should global warming keep increasing at its current rate, it is predicted to reach 1.5°C between the years 2030 and 2052 (Masson-Delmotte *et al.*, 2022). Warming from pre-industrial to current emissions will last for centuries to millennia and will continue to cause additional long-term changes in the climate system, which include sea level rise, with related effects (Masson- Delmotte *et al.*, 2022). Various greenhouse gases (GHG), including methane (CH_4), contribute to this warming through the greenhouse effect which subsequently leads to climate change. Methane concentrations in the atmosphere exacerbate global warming, necessitating regulation to avoid and mitigate adverse climate impacts. Methane is primarily produced through natural processes such as microbial activity in wetlands (Krüger *et al.*, 2013) and enteric fermentation in ruminants (Moeletsi and Tongwane, 2015). Additionally, anthropogenic activities such as coal mining (Zhu *et al.*, 2017), coal stockpiling (Kozinc *et al.*, 2004), fossil fuel extraction (Brantley *et al.*, 2014), and the increase in the number of landfill sites (Bakkaloglu *et al.*, 2021) also contribute to CH_4 emissions. Methane accounts for approximately 17% of the radiative forcing experienced by the lower atmosphere (Rubino *et al.*, 2019). Methane plays an important role in atmospheric chemistry and as a greenhouse gas. As a known ozone precursor, CH_4 reacts with hydroxyl radicals to decrease the atmosphere's oxidizing capacity and capacity to produce ozone in the troposphere (Kirschke *et al.* 2013; Crutzen and Lelieveld, 2001). This methane-hydroxyl reaction may also have an effect on the production of secondary organic aerosols (Crutzen and Lelieveld, 2001). Reducing methane emissions would lead to a notable enhancement in air quality and climate resilience.

The term "Global Warming Potential" (GWP) refers to a metric used to compare how well different greenhouse gases retain heat in the atmosphere (IPCC, 2022). The GWP is determined by comparing each gas's radiative efficiency (the capacity to absorb heat) and decay rate (the

amount that can be removed from the atmosphere over a certain time period) to that of carbon dioxide CO_2 (IPCC, 2022). Global warming potential offers a method for converting different gas emissions into a mutual or standard metric, allowing the radiative effects of different greenhouse gases to be combined into a single, uniform measure that is expressed in carbon (C) or carbon dioxide (CO_2) equivalents. Methane exhibits a higher GWP than CO_2 per molecule, with its GWP being 28 times higher than that of CO_2 over 100 years (IPCC, 2022), and 84-86 times over 20 years (IPCC, 2022) (Table 1).

Table 1: GWP of greenhouse gases as reported by IPCC (2022). The different years are the years of publication of the IPCC assessment reports (AR). Image from: https://erce.energy/erceipccsixthassessment/.

Greenhouse Gas	100-Year Time Period				20-Year Time Period			
	AR4 2007	AR5 2014	AR6 2021		AR4 2007	AR5 2014	AR6 2021	
	Feedback Not Included		*Feedback Included*		*Feedback Not Included*		*Feedback Included*	
CO_2	1	1	1	1	1	1	1	1
$CH_{4\ fossil\ origin}$	25	28	34	29.8	72	84	86	82.5
$CH_{4\ non\ fossil\ origin}$				27.2				80.8
N_2O	298	265	298	273	289	264	268	273

Methane has an atmospheric residence time of approximately 8-10 years (Mayer *et al.*, 1982). This extended residence time is concerning because if CH_4 remains in the atmosphere for 10 years or longer, it can contribute significantly to global warming and climate change during that period. A longer atmospheric residence time means that any reduction efforts will take longer to have an impact on atmospheric CH_4 concentrations.

The detection and quantification of CH_4 is quite demanding because CH_4 is thoroughly mixed in the atmosphere, and only slight changes within large background concentrations are utilized for detection. This makes CH_4 measurement a challenging task to perform accurately (Hu *et al.*, 2018; Shen *et al.,* 2021; Plant *et al.,* 2022, Nisbet *et al.*, 2023).

1.2. Rationale

Global methane emissions have more than doubled since the year 1750, with wetlands responsible for approximately 13 % of the global CH_4 emissions, and fossil fuels responsible for approximately 34 % of global CH_4 emissions (Zhang *et al.,* 2022). Ranked as the 14t^{h} largest global GHG emitter, South Africa is quite limited on studies centred on CH_4 sources and emissions. Methane emission research is essential to comprehending and mitigating South Africa's role in climate change (Gütschow *et al.*, 2021). South Africa is committed to global climate agreements, such as the Paris Agreement (PA), and strives for a resilient, low-carbon economy to comply with the sustainable development goals (SDGs). To achieve sustainable development objectives and make well-informed mitigation decisions, more studies/research on GHG's such as CH_4 sources in the country are required.

1.3. Aim

The aim of this research is to compare CH_4 concentrations and isotopic signatures from a wetland, which primarily involves microbial processes, with those from coal stockpiles at a coal-fired power station in South Africa. Comparing methane concentrations from coal stockpiles and wetlands is valuable as there is limited data on either source and comparing them can provide new insights and fill gaps in the current understanding of methane concentrations from these two sources in a South African context. This study serves as one the very few measurements from a South African wetland and the first data on comparisons of CH_4 concentrations from microbial wetland concentrations versus anthropogenic coal stockpile concentrations in South Africa.

1.4. Research objectives

a) To measure the CH_4 concentrations (ppm) from two sources: the Wakkerstroom wetland vegetation communities and downwind of the coal bed at the Majuba power station.
b) To measure the ^{13}C isotopes in collected air samples from the Wakkerstroom wetland and downwind of the coal bed at the Majuba power station to establish each sites' methane carbon isotopic signature ($\delta^{13}CH_4$) through Keeling curves. This is to distinguish between different sources of methane (i.e., wetlands and coal stockpiles) based on their unique isotopic compositions.

c) To calculate and present the total column averaged dry-air mole fraction of CH_4 (ppb) as measured by the Tropospheric Monitoring Instrument (TROPOMI) at the Wakkerstroom wetland and Majuba power station to assess seasonal variations.
d) To calculate and present the reported CH_4 mole fraction (ppb) from data collected at the Cape Point Global Atmospheric Watch (GAW) station in order to assess seasonal CH_4 trends in a "clean" undisturbed atmosphere from 1983 – 2021.

1.5. Key research questions.

a) What are the seasonal concentrations (ppm) for the CH_4 inputs to the air above the Wakkerstroom wetland and the Majuba Power Station coal bed?
b) How does the water depth at which plants are rooted affect the observed CH_4 concentration at the Wakkerstroom wetland?
c) What are the seasonal variations in each sites' methane carbon isotopic signature ($\delta^{13}CH_4$) for the CH_4 concentrations at the Wakkerstroom wetland and Majuba Power Station coal bed?
d) Are there differences in the total column averaged dry-air mole fraction of CH_4 (ppb) at the Wakkerstroom wetland and Majuba power station as measured by TROPOMI?
e) What trends exist in the reported CH_4 mole fraction (ppb) of the "clean" atmosphere as measured at the Cape Point Global Atmospheric Watch (GAW) station?

2. LITERATURE REVIEW

The literature review provides the background to understanding methane concentrations and the methods for measuring the concentrations of wetland and coal origin.

2.1. Global climate change and the global CH_4 budget

Global warming, as defined by Masson-Delmotte *et al.* (2022), refers to the collective increase in surface air and sea surface temperatures observed worldwide over a 30-year timeframe. Climate change, a broader concept encapsulating various long-term alterations in Earth's climate systems, including temperature, precipitation, and wind patterns (Masson-*Delmotte et al.,* 2022; Mikhaylov *et al*., 2020; Abbass *et al*., 2022), acknowledges the interconnected nature of these changes. While global warming emphasizes temperature rise, climate change recognizes its multifaceted impacts on different components of the Earth's climate system (Weber and Stern, 2011), such as shifts in precipitation, sea level changes, alterations in extreme weather events, and disturbances to ecosystems (Masson-Delmotte et al., 2022; Mikhaylov *et al.,* 2020; Abbass *et al*., 2022; Bandh *et al.,* 2021).

Natural factors contributing to global climate change include microbial activity in wetlands and sporadic volcanic eruptions (Hardy, 2003; Hegerl *et al*., 2019; Masson-Delmotte *et al*., 2022), while human activities like fossil fuel combustion, deforestation, and inadequate waste management, particularly through landfill sites, serve as anthropogenic drivers (Stern, 2014; Hornsey and Fielding, 2020; Masson-Delmotte *et al.,* 2022). These activities release greenhouse gases like CH_4 and CO_2 into the atmosphere, creating a greenhouse effect wherein heat is trapped, leading to atmospheric and surface temperature increases (Masson-Delmotte *et al.*, 2022). The "greenhouse effect", illustrated in figure 1, involves the accumulation of gases in Earth's atmosphere that trap heat. Initially, shortwave radiation penetrates the atmosphere, warming the Earth's surface, which then emits longwave radiation. This longwave radiation becomes trapped in the atmosphere, causing heat to be re-radiated back to the Earth's surface, ultimately resulting in elevated atmospheric and surface temperatures, and contributing to global warming.

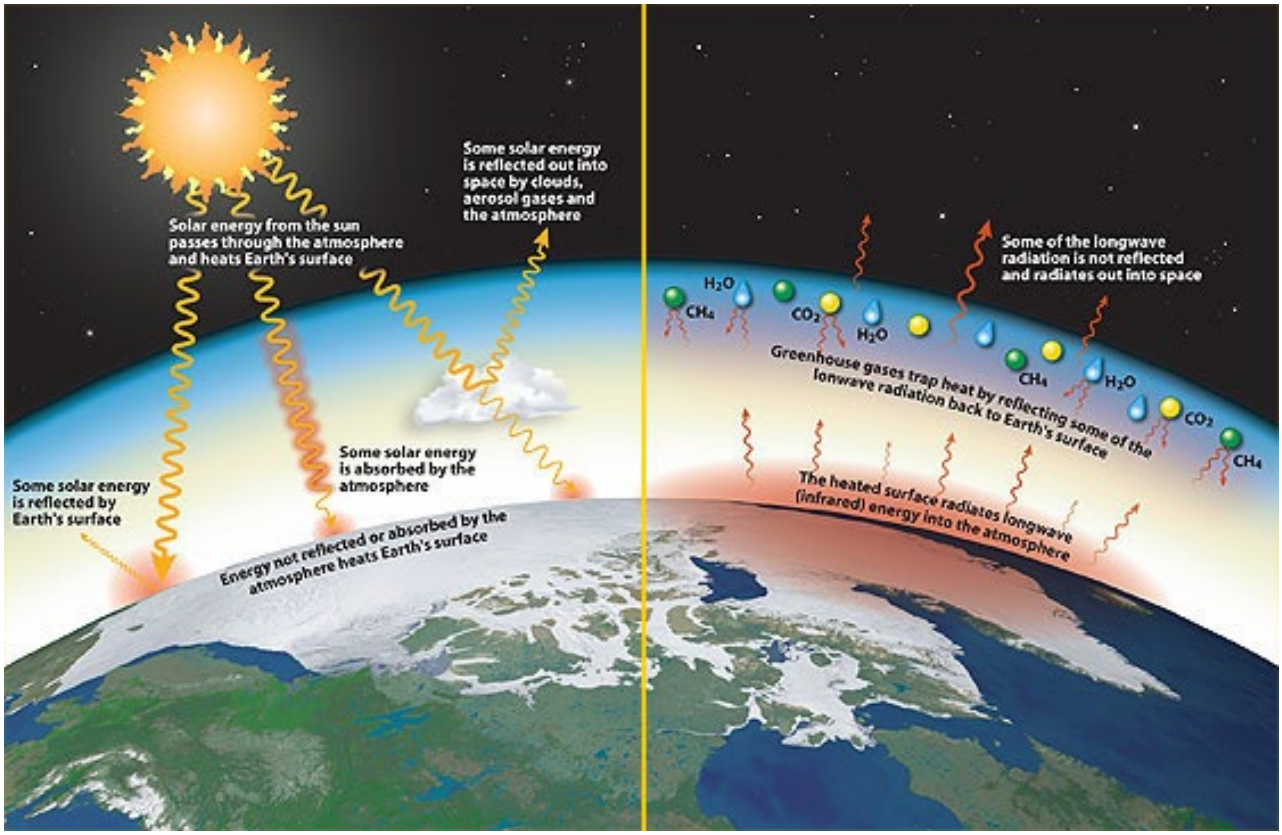


Figure 1: Diagram illustrating the greenhouse effect. Image from: https://forces.si.edu/atmosphere/02_04_07.html

The primary source of uncertainty in the methane budget (Figure 2) is natural concentrations, namely from wetlands and rivers. Between 2000 and 2017, the estimated global emission range from natural wetlands was 101–179 Tg CH_4 yr^{-1}, with an average of 149 Tg CH_4 yr^{-1}. On the other hand, coal provides between 29 to 61 Tg CH_4 yr^{-1} globally, on average 42 Tg CH_4 yr^{-1}.

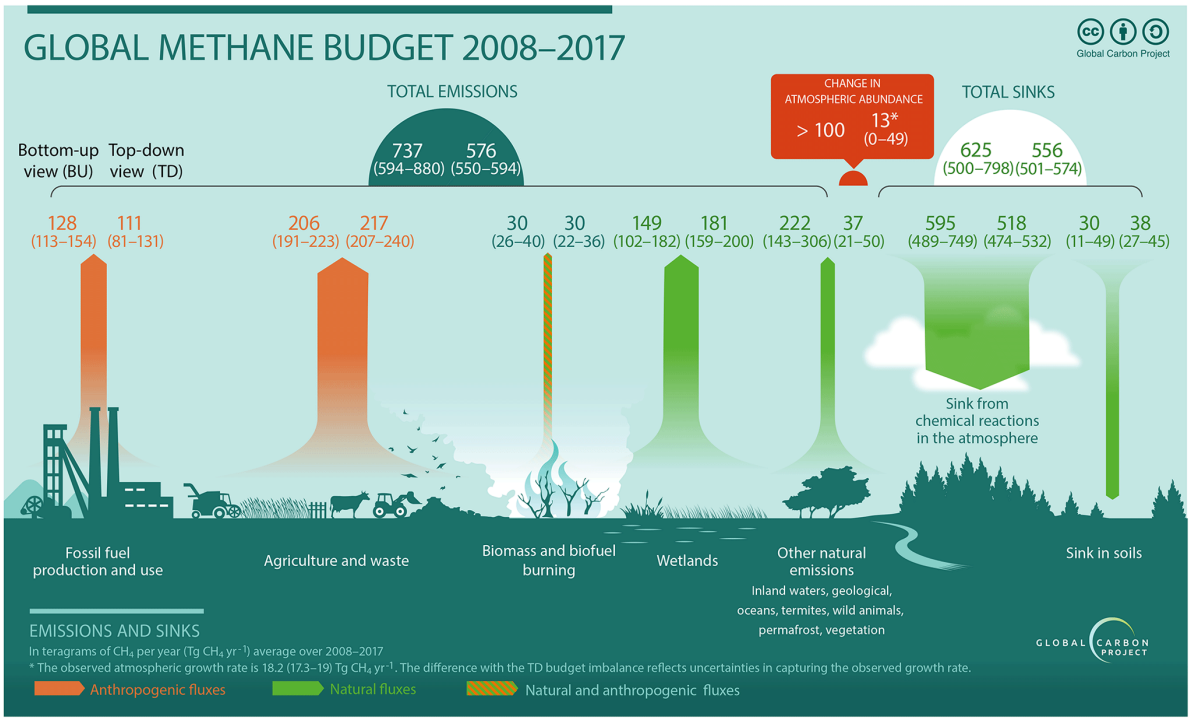


Figure 2: The global methane budget, 2008-2017, the emission range is indicated by the numbers in parenthesis, and the numbers on the left and right represent bottom-down and top-down estimations (Saunois *et al.* (2020)).

2.2. Methane emissions in South Africa

Agricultural activities, particularly livestock farming, stand out as the biggest source of methane (CH_4) emissions in South Africa (Tongwane and Moeletsi *et al.,* 2022; Shikwambana *et al.*, 2020). Within this sector, enteric emissions from livestock represent the largest contributor, accounting for 52% of total emissions (Shikwambana *et al.*2022; Figure 3). Findings have also been made in another study that commercial beef cattle accounted for 48% of the 0.87 million tons of CH_4 emissions from enteric fermentation in 2018, while subsistence beef and dairy cattle contributed 36% and 17%, respectively (Tongwane and Moeletsi, 2020). Following closely, landfill sites emerge as the second-largest source, generating 40% of South Africa's total CH_4 emissions. Livestock manure contributes 5% to the overall CH_4 emissions, while energy production and wastewater each contribute 2% (Shikwambana *et al.*, 2022).

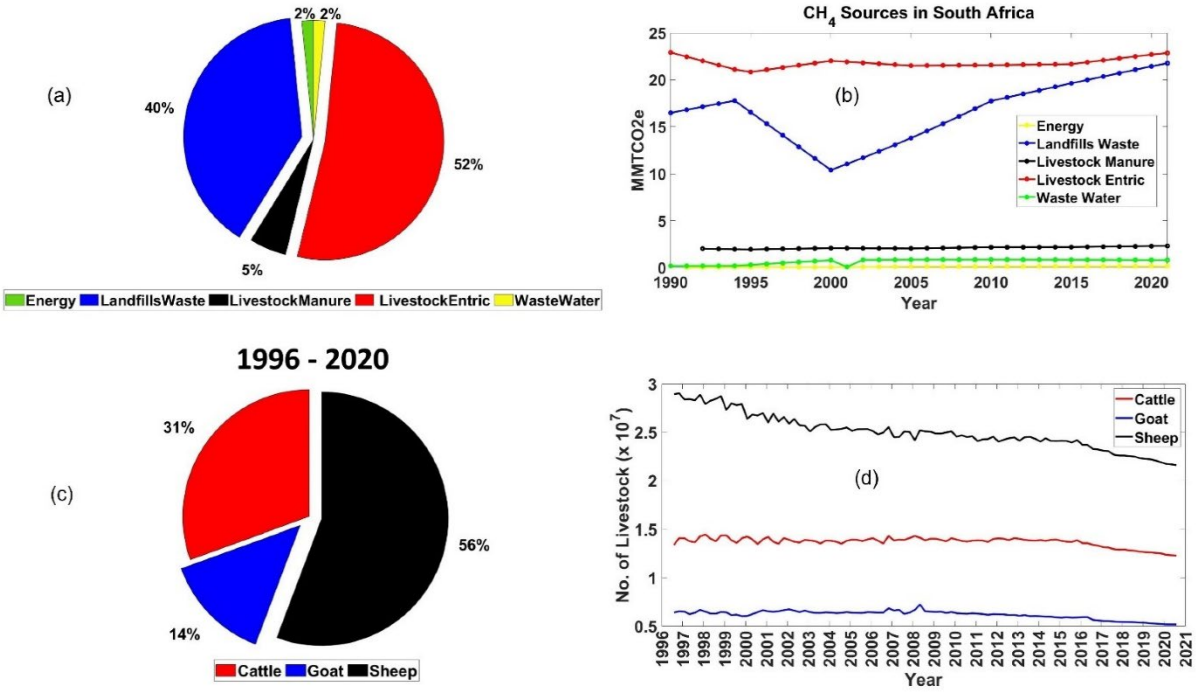


Figure 3: Sources of CH_4 by sector in South Africa (Shikwambana *et al*. (2022)).

2.3. Methane production and emissions in the South African coal sector.

Atmospheric pollution from energy production, inclusive of coal mining and coal stockpiling is of global concern. Methane gas emission from coal supply refers to emissions originating from coal seams, released during exploration, venting of seams, and ventilation of shafts. Methane gas emissions from coal also include emissions from coal stockpiling at coal-fired power stations (Cohen and Winkler, 2014).

In underground coal mining, most emissions stem from methane previously trapped in the coal seam, which is released through venting in South African mines. Conversely, in open-cast mines, methane emissions released from the coal seam constitute a small fraction of the overall GHG emissions (less than 2%) (Cohen and Winkler, 2014).

Methane is produced in a power station during the process of stockpiling, through the process of gasification. The reaction is as follows:

$2C_{(s)} + 2H_2O_{(l)} = CH_{4(g)} + CO_{2(g)}$ → ***equation 1.***

At the coal stockyard, the coal is dumped by a tipper in a flat area designated for the stockpiling of coal. During the dumping process, cannons are used simultaneously for dust control whilst the wetness of the coal is increased for better compaction. Therefore, water mist is provided for supressing airborne dust and compaction of coal. This reaction between the water mist and coal produces CH_4 gas as shown in the equation 1.

In Africa, coal is the lowest CH_4 emitting sector (1 %), with the highest being oil and gas (48%), followed by municipal solid waste (35 %) and wastewater (16%). These values exclude those of livestock agriculture. About 80% of the continental emissions are produced by the top 10 emitters, which include South Africa, Egypt, and Nigeria (African Development Bank, 2022). Only two countries in Africa—South Africa and Zimbabwe—have substantial coal mining operations. Coal mining and fossil fuel power stations play a key role as the energy provider in South Africa. Approximately 80% of primary energy needs in South Africa are provided by coal (Makgetla and Patel, 2021) and approximately 28% of the coal produced in South Africa is exported and this makes South Africa the 4th largest coal exporting country in the world (Munnik *et al.*, 2010). South Africa, by far the greatest coal producer on the continent, is responsible for the majority of Africa's annual coal related CH_4 emissions, which were estimated to be 45 000 tons (1.6 Mt CO_2e) (African Development Bank, 2022).

2.4. Methane production and concentrations in South African wetland ecosystems.

Wetlands are ecosystems of diverse ecology where soil is usually covered by surface or even

groundwater or where this water covers the soil surface perennially or for varying time periods. Wetlands are categorised as aquatic ecosystems which are a transition between terrestrial ecosystems such as forests and grasslands, and fully aquatic ecosystems such as rivers and oceans. Approximately 3.8% of South Africa's surface area is made up of the 4 596 509 hectares (ha) of inland aquatic habitats and artificial wetlands (Van Deventer *et al.*, 2020). In terms of all inland wetlands, unchanneled valley bottom wetlands cover 1 908.8 ha (6.5 %) of land (Van Deventer *et al.*, 2020). Wetlands are protected under the National Water Act (Act 36 of 1998; RSA, 1998a). Wetlands are vital for the ecosystem services they provide, such as water filtration, flood prevention, pollution removal, erosion prevention, groundwater restoration, and climate change regulation (Bird, 2010; McCartney *et al.*, 2011). Wetlands are crucial biodiversity regions in many countries due to high floral and faunal diversity (Van Deventer *et al.*, 2020). The highveld of South Africa includes wetlands with large seasonal moisture deficits, high potential evapotranspiration, and relatively little rainfall (Bird, 2010).
Sources of CH_4 can be classified as pyrogenic (originating from fire), biogenic (originating from natural biological processes), and thermogenic (originating from a heat source). Wetlands are classified as a crucial biogenic source of CH_4 (Krüger *et al.*, 2012). Natural wetlands are a significant source of CH_4 emissions, accounting for 20–40% of worldwide emissions (Parker *et al.*, 2018). There are still a lot of unknowns about their unpredictability and responsiveness to climate change (Chanton, 2005; Nisbet, 2023; Wang *et al.,* 2023). In 2020, wetlands contributed 1 193 Gg CO_2e (57 Gg CH_4) to the total CH_4 produced in South Africa (Department of Forestry, Fisheries and the Environment, 2023) .Research to better understand CH_4 production and release in wetlands is thus crucial in solving the challenge of rising CH_4 emissions globally.

2.5. Approaches to measuring wetland and coalbed methane concentrations.

Archaea produce a significant amount of CH_4 in the anoxic sediments of wetland ecosystems (Svensson and Rosswall, 1984; Torres-Alvarado *et al*., 2005; Jeffrey *et al*., 2019). It is possible for vascular plants to release CH_4 into the atmosphere from sediments (Chanton, 2005; Bastviken *et al*., 2023). The oxic water-sediment interface is avoided by this route, as oxidative reactions may use up a significant amount of the generated CH4 there (Torres-Alvarado *et al*., 2005; Demirel and Scherer, 2008; Jeffrey *et al*., 2019). Aquatic plants may be the source of between 50 and 95% of the total CH_4 emitted from wetlands, with the remaining portion coming from diffusion processes through their stomata and/or mass flow (Dacey, 1981; Korrensalo *et al*., 2022). A common technique for measuring the amount of CH_4 that plants emit is to enclose whole plants, or parts of them, in sealed chambers, and then monitor the rate at which the concentration of CH_4 in the chamber increases over time (Knapp and Yavitt, 1992; Whiting and Chanton, 2001; Chang and Yang, 2003; Otter and Scholes, 2000; Krüger *et al.* 2012; Bansal *et al.*, 2020).

2.6. Closed chamber method.

In the field of wetland ecology, the closed chamber method emerges as an indispensable tool for assessing CH_4 concentrations within vascular plants. This method provides detailed insights into the complex relationship between plant physiology and wetland CH_4 concentrations. The closed chamber method is commonly used for CH_4 flux measurements, but sometimes also used to measure CH_4 concentrations. Methane flux refers to the rate at which methane is exchanged between a specific area (e.g., a wetland) and the atmosphere. Methane flux is quantified by measuring the quantity of methane entering or exiting a defined area within a specified duration. Methane flux measurements are advantageous in that they offer precise data on the actual amount of CH_4 emitted into the atmosphere per hour or year, which enables the assessment of flux rates over time. Methane concentration measurements on the other hand refer to the amount of methane present in a given volume of air in a specific location at a single moment in time.

The closed chamber technique for assessing CH_4 concentrations dates back to the 1990s (Whiting and Chanton, 1992; Schipper and Reddy, 1994; Van Der Gon and Neue, 1995; Van Der Nat *et al.*, 1998) and continues to be used in CH_4 concentration measurement from wetlands (Schultz and Pett *et al.*, 2018; Yang *et al.,* 2020; Gülşen and Yapıcıoğlu, 2021; Antonijević *et al.*, 2023). Environmental and plant physiological reactions were observed while utilizing closed chambers for measuring CH_4 concentrations from *Typha latifolia* (cattails)

from two wetlands – one in central New York, and the other northeast of Kansas (Knapp and Yavitt, 1992). A gas chromatograph was utilised to measure CH_4 in collected air samples. Once the chambers with *Typha* leaves were enclosed, there was a rapid increase in CH_4 concentration, ranging from 1.5 ppm to 3.5 ppm. With findings much similar to Knapp and Yavitt (1992), CH_4 concentrations from wetlands in Taiwan using the chamber method were investigated by Chang and Yang (2003) and their results showed that in the Kang-du wetland, Kang-nan wetland, and Kang-nan lake area, the atmospheric CH_4 concentrations were 0.8–2.7, 0.7–1.6, and 0.8–1.7 ppm, respectively.

Using the chamber method, the atmospheric global warming potentials of methane in relation to the annual methane emission/carbon dioxide exchange ratio across wetlands spanning from the boreal zone to the near subtropics were examined (Whiting and Chanton, 2001). The authors assessed CH_4 emission fluxes in this instance, where *Typha latifolia, Peltandra virginica, and Carex* were the dominant vegetation communities of the wetlands. The CH_4 fluxes from *Typha latifolia* dominated wetlands were 4.3 – 6.8 $mol.m^{-2}.yr^{-1}$ whereas those from *Peltandra virginica* were 6.8 – 11.0 $mol.m^{-2}.yr^{-1}$. The CH_4 fluxes from *Carex* dominated wetlands were 3.7 – 4.6 $mol.m^{-2}.yr^{-1}$.

During the early 2000s still, the closed chamber method was also used to quantify CH_4 fluxes and concentrations in South Africa. Over a two-year period, CH_4 fluxes and concentrations were examined at a South African floodplain and subtropical savanna site, the Nylsvley Nature Reserve, located approximately 200 km north of Johannesburg (Otter and Scholes, 2000). Collected air samples from savanna soil were assessed for CH_4 concentration. In the winter, when there was CH_4 consumption, soil depth profiles in the upland savannas revealed a consistent drop in CH_4 content with depth (to 0.4 ppm CH_4 at 0.5 metres). A rise in CH_4 content to 2.8 ppm was found at a depth of 0.05 - 0.10 metres during the summer months when CH_4 generation occurred. During these months of CH_4 generation, the soil profile's variability in CH_4 concentration increased, suggesting that there were localized pockets of variable CH_4 sources. The floodplain's CH_4 fluxes were found to be regulated by the depth of the water table. The greatest concentrations were when the water was at or slightly above the soil's surface (saturated soil). When the water level was more than 0.1 m below the soil's surface or 0.4 m above it, fluxes were almost zero. These findings were in agreement with Krüger *et al.* (2012) who assessed the carbon, nitrogen content of soil, ground water level (GWL- depth of the anaerobic soil zone), soil water chemistry, and soil temperature in two South African wetlands located in the Drakensberg also using the chamber method. They found that since anaerobic conditions predominate for longer periods of time, sites in the centre of the wetland with the

highest water table produced the highest source of atmospheric CH_4. In this way, both studies (Otter and Scholes, 2000; Krüger *et al.* 2012) showed that water depth/level has an effect on CH_4 emissions.

While static chamber methods are commonly used to measure methane concentrations from various ecosystems, they do have some disadvantages. The act of placing a chamber over the soil or vegetation can create a microenvironment within the chamber that differs from the surrounding area. This alteration may influence microbial activity and gas fluxes, potentially leading to inaccuracies in methane measurements (Yu *et al.*, 2013). The process of placing and retrieving static chambers can also be time and labour-intensive, especially when monitoring large study areas. This may limit the frequency of measurements and result in spatial gaps in data collection (Mu *et al.*, 2022).

2.7. Flexfoil bag sampling method.

Following the realisation of some disadvantages of the chamber method, ground measurement techniques for measuring CH_4 evolved since the late 1990s. Flexfoil bag (sometimes also referred to as a Tedlar bags) sampling emerged as a method for accurately quantifying CH_4 emission concentrations in various environmental settings and have been used in several studies (MacDonald *et al.*, 1998; Sriskantharajah *et al.*, 2012; Bakkaloglu *et al.*, 2022; Fiehn *et al.*, 2023; Juszczak and Augustin, 2013; Lu *et al.*, 2021; Gatland *et al.*, 2014). The advantages of using flexfoil bag sampling are numerous. Flexfoil bags are lightweight and easy to transport, making them suitable for field/ground measurement studies. Their simple design facilitates quick deployment and efficient data collection. Their versatility is also helpful as they can be applied to various ecosystems, including wetlands, agricultural fields, and even in mines without altering the environment of measurement.

Methane concentrations have been assessed using the flexfoil bag sampling technique at a Finnish subarctic wetland by Sriskantharajah *et al.* (2012). The findings showed that at diel (24-hour) periods, CH_4 concentrations ranged between 1.8 – 2.4 ppm. Their results were similar to Fisher *et al.* (2017) who also utilized the flexfoil bag sampling method to assess CH_4 concentrations in wetlands located in the Fennoscandian Arctic, showing CH_4 concentrations ranging at 1.85 – 1.94 ppm.

Tropical wetland ground-based and flight-based CH_4 emission measurement campaigns have also used the flexfoil bag sampling method. Methane fluxes and concentrations were presented for wetlands located in Boliva (France *et al.*, 2022b). The results showed that the range in CH_4 concentration for flights over wetlands at the city of Trinidad in Bolivia was 1.8-2.3 ppm. These

results by France *et al.* (2022b) were in close agreement with those of Shaw *et al.* (2022), who presented CH_4 concentration for Zambian wetlands, also using the flexfoil bag method, as 1.9 – 2.4 ppm for the Bangweulu, Lukanga, and Kafue wetlands.

The flexfoil method has also extended to being utilized for measurements of CH_4 concentrations from the coal mining sector (Center and Eltschlager, 2001; Forrester *et al.*, 2017; Kosmack, 2008; Silva *et al.*, 2010; Zazzeri *et al.*, 2015, Wali, 2022). When monitoring light hydrocarbons - specifically CH_4 in coal mines located in Brazil, Silva *et al.* (2010) utilised the flexfoil bag method too. In the underground mines, sampling was done at various time intervals (before and after blasting), at various points (mine entry, ventilation wells and outlet, rest area). Silva *et al.* (2010) then found varying levels in CH_4 concentrations ranging from 3 ppm – 470 ppm on the underground and surface mines. Along similar lines, a similar study of plume mapping of anthropogenic CH_4 concentrations in the United Kingdom found concentrations of CH_4 around the Thoresby colliery to range from 2.8 – 3 ppm (Zazzeri *et al.*, 2015). This was a mobile sampling campaign with samples taken a few kilometres from the coal mine itself.

2.8. Effect of various plant communities on methane concentrations.

The vascular gas transport systems of various plant species differ in efficiency of gas transport. Studies have assessed the influence of vegetation communities such as *Phragmites australis* and *Typha* species on CH_4 emission flux using closed chambers (Cao *et al.*, 2017; Lawrence *et al.*, 2017; Bansal *et al.*, 2020; Johnson *et al.*, 2021). In a study aimed at assessing wetland invasion by *Typha glauca,* findings showed that *Typha* had CH_4 fluxes triple (mean: 45.9 ± 16.7 mg CH_4-C m^{-2} h^{-1}) that of native wet meadow vegetation (15.0 ± 10.5 mg CH_4-C m^{-2} h^{-1}) from soils in three midwestern (USA) wetlands (Lawrence *et al.*, 2017). This occurred particularly under high water levels (> 10 cm), however the fluxes were almost negligible under low water levels (< 10 cm) (Lawrence *et al.*, 2017). Along similar lines, using clear flux chamber measurements immediately above *Typha* plants ("whole-plant"), next to *Typha* plants (where roots were present but no stems; "plant-adjacent"), and on soils devoid of plants ("control"), the effects of *Typha* on CH_4 flux were evaluated (Bansal *et al.*, 2020). In comparison to the plant-adjacent or control treatments, the CH_4 flux rates in the whole-plant treatment were nearly five times higher (51.78 ± 8.16 mg-C $m^{-2}day^{-1}$). This was mostly due to diffusive-only flux, with plant-mediated transport serving a minor contribution.

Zania latifolia and *Phragmites australis* were planted in artificial wetland microcosms, and the fluxes of CH_4 were assessed when wastewater was treated under different conditions of biological oxygen demand (BOD). According to Inamori *et al.* (2007), *Z. latifolia* units consistently exhibited a larger CH_4 flow than *P. australis* units (highest measurement of roughly 40 $mg.m^{-2}.h^{-1}$). The authors suggested that *P. australis* tends to reduce the activity of methane-producing bacteria due to its complex root zone and lower biological oxygen demand (BOD) concentration. The findings of *P. australis* having low CH_4 flux when compared to other plant species was also seen in a natural freshwater wetland located in Iganga District, Uganda (Were *et al.*, 2021). The findings indicated that *Papyrus* and *Typha* exhibited mean CH_4 fluxes (mg $C.m^{-2}.h^{-1}$) of 14.1 ± 0.8 and 13.5 ± 1.2, respectively, during the dry season. While there was no difference between these values, they were both significantly higher than *Phragmites'* (8.7 ± 0.5). However, there were only slight variations in the mean CH_4 fluxes among the three plant groups during the rainy season.

2.9. Impact of meteorological variables on CH_4 production in wetlands.

Apart from the presence of methanogenic archaea, the production and detection of CH_4 in wetlands is dependent on some meteorological variables namely temperature, rainfall, and wind. Laboratory experimental studies on the effect of these variables thus remains pivotal in the understanding of CH_4 emission dynamics in wetlands, as done by Deng *et al*. (2019). In an attempt to understand the impact of temperature on the microbes responsible for CH_4 production in an alkaline wetland located in the Tibetan plateau, Deng *et al*. (2019) incubated soil slurries for 100 days under anaerobic conditions at temperatures of 10, 20, 30 and 45 °C. An accumulation of CH_4 and stable isotope fractionation were quantified to determine the pathways for the CH_4 production. By sequencing methanogenic mcrA genes and/or transcripts as well as bacterial and archaeal 16S rRNA, the microbial community architectures were examined. In their results, it was stated that from 10 to 30 °C, the generation of CH_4 was accelerated, but at 45 °C, it nearly completely stopped and the precursor to methane, acetate, accumulated. Acetate only accumulated at lower temperatures if acetotrophic CH_4 generation was prevented by methyl fluoride. Soil temperature thus plays a role in CH_4 generation and should be accounted for in studies assessing CH_4 generation in wetlands.

The temperature of water in the wetland can also play a role in CH_4 emitted and detected. According to an assessment in a marsh by Huertas *et al*. (2019), CH_4 levels were strongly and positively associated with both water temperature and chlorophyll a levels, demonstrating that temperature controls sedimentary methanogenesis and that primary productivity increases the availability of organic materials. Despite the fact that temperature and productivity appeared to be the two environmental factors that most strongly influenced the accumulation of dissolved CH_4, the spatio-temporal patterns found indicate that CH_4 dynamics in wetlands and marshes are likely governed by a variety of mechanisms rather than by a single environmental factor.

Another meteorological factor to be considered in CH_4 concentration analysis is wind speed, which was found by Rey-Sanchez *et al*. (2018) to be the strongest meteorological driver of methane flux to the atmosphere, alongside temperature. In an estuarine wetland situated in Ohio, four main land-cover types—open water, emergent vegetation (*Typha* spp.), floating vegetation (Nelumbo spp.), and mud flats—monthly gas exchange sampling was carried out utilizing non-steady state chambers. They state that the rate of mixing at the top water layer and the amount of gas exchange between the surface and the atmosphere are both governed by wind speed. Thus, higher wind speeds mean higher rates of gaseous (CH_4) exchange with

the atmosphere. Wind can cause mixing in the surface layers of water bodies, bringing CH_4-rich water from deeper layers to the surface where it can escape into the atmosphere. Wind also reduces the boundary layer in the atmosphere at the water surface and maintains a steeper concentration gradient by removing CH_4 entering the atmosphere from the water surface.

It is vital that no meteorological variable is underestimated in its importance in the exchange of CH_4 between the atmosphere and wetlands. Poindexter and Variano (2013) find this to be the case for hydrodynamic transport of dissolved gas through the surface water. After laboratory analysis of quantifying gas transfer speeds for CH_4, CO_2 and O_2 in a model wetland, there was a weak, nonlinear relationship between wind speed and gas transport. The gas transport generally increased as wind speed increased. They also state that most hydrodynamic gas transport in wetlands is driven by thermal convection. However, the assumptions of Poindexter and Variano (2013) on the relationship between wind speed and gas transport rest on the assumption that the results in the laboratory analysis should be in line with those that would be observed in the wetland canopy in the field. Thus, field campaigns remain vital to accurately assess the relationship between wind speed and direction with CH_4 conentrations and CH_4 transport.

Listed under environmental factors that drive CH_4 flux by Rey-Sanchez *et al*. (2018) was also water level, which is at most times governed by rainfall. The fluctuations in water levels above the wetlands surface were found to have a weak impact on the fluxes of CH_4 in the wetland. In fact, they found that the water levels had a stronger impact on CH_4 fluxes at night than daytime, thus leading to higher CH_4 fluxes during the night. There seems to be compelling reason to argue that empirical models predicting effect of meteorological data in CH_4 wetland emissions remain crucial in understanding CH_4 dynamics in wetlands.

The effect of rainfall on atmospheric CH_4 growth (i.e., increase in atmospheric CH_4 concentrations) was also assessed by Nisbet *et al*. (2016), who conducted a study to isotopically assess the causes of CH_4 growth and the CH_4 isotopic shift more negative or lighter isotopic signatures for the period 2007 - 2014. In their results, apart from an increase in CH_4 agricultural sources, they state that the growth of biogenic CH_4, particularly in the Southern hemisphere and in the equatorial tropical regions, was strongly positively correlated with anomalies in rainfall. During the summer season of 2010-2011, in the Ascension island located in the Atlantic equatorial region, the averaged CH_4 mole fraction growth was most pronounced, and this was interpreted as a result of the strong southern hemisphere wet season from November to March each year. Nisbet *et al*. (2016), along with Dlugokencky *et al*.

(2009) strongly rate precipitation and temperature in Southern hemisphere and tropical wetlands as strong drivers of CH_4 growth.

2.10. Isotopic signatures and their use.

In order to mitigate CH_4 emissions, CH_4 sources have to be identified and isotopic analysis can aid in this. Methane carbon isotopic signatures ($\delta^{13}CH_4$) Methane carbon isotopic signature, which is commonly expressed as the ratio of carbon-13 to carbon-12, offers important insights into the origins and mechanisms of methane production. Methane contains carbon in the form of different isotopes, primarily carbon-12 (^{12}C) and carbon-13 (^{13}C). The isotopic signature is expressed as $\delta^{13}C$, which represents the deviation of the $^{13}C/^{12}C$ ratio in a sample from a standard reference material, usually the Pee Dee Belemnite (PDB) standard for carbon. Different sources of methane have distinct $\delta^{13}C$ values, allowing scientists to identify the origin of methane emissions.

The Keeling plot regression (Keeling, 1958) is utilised in the identification of source isotopic signatures of CH_4. A plot of the relative ^{13}C enrichment in a methane gas sample against the inverse of the CH_4 mole fraction or concentration (ppm) is used to calculate the isotopic source signature ($\delta^{13}CH_4$). The y-intercept in the Keeling plot gives the isotopic source signature of the CH_4, as shown in the equation.

$$\delta^{13}C_a = C_b(\delta^{13}C_b - \delta^{13}C_s) \times (\frac{1}{C_a}) + \delta^{13}C_s \quad \rightarrow \text{ equation 2 (France } \textit{et al.}\text{, 2022a)}$$

- C_a: Measured atmospheric concentration of CH_4 using flexfoil bags.
- C_b : Atmospheric background of CH_4 using flexfoil bags.
- $\delta^{13}C_a$: Measured isotopic composition.
- $\delta^{13}C_b$: Background atmospheric isotopic composition.
- $\delta^{13}C_s$: The source isotopic composition.

The carbon isotopic signature of atmospheric CH_4 has, in the recent years, shifted toward lighter (^{13}C-depleted) values, indicating a change in the dominating CH_4 sources (France *et al.*, 2022a), possibly, due to:

(i) An increase in biogenic emissions from sources such as wetlands and ruminants.

(ii) A shift in the atmospheric hydroxyl radical's (OH-) ability to oxidize emissions. A decrease in the OH- concentration or its reactivity leads to a longer atmospheric residence time for CH_4. Atmospheric hydroxyl radicals are determined by complex atmospheric chemistry processes.

(iii) Modifications in the relative intensities of emissions from fossil fuels, waste, and agriculture, among other anthropogenic sources (France *et al*., 2022a).

Studies (Ganesan *et al.*, 2018; Wesley *et al.*, 2023; MOYA/ZWAMPS Team *et al.*, 2022; Sriskantharajah *et al.,* 2012) have utilised the Keeling plot technique to determine the isotopic signatures of various wetlands globally. The $\delta^{13}CH_4$ data from wetlands located in Africa and South America has been analysed with findings highlighting that, for emissions from equatorial Nile wetlands and agricultural regions, the measured $\delta^{13}CH_4$ ranged from −55 to −49 ‰, whereas from Upper Congo and Zambezi wetlands, they were approximately -60 ± 1 ‰ (MOYA/ZWAMPS Team *et al.*, 2022). The Amazonian wetlands of northeast Bolivia had very similar $\delta^{13}CH_4$ values measured over them (around −59‰), and when the $\delta^{13}CH_4$ signatures from tropical wetlands in the southern Upper Congo and Upper Amazon drainage were plotted together, the overall $\delta^{13}CH_4$ result was -59 ± 2 ‰ (MOYA/ZWAMPS Team *et al.*, 2022). Along similar lines, methane source signatures from tropical wetland emissions showed that $\delta^{13}CH_4$ measurements of papyrus-rich tropical wetlands in Uganda and the Okavango appear to be ^{13}C enriched, with a bulk wetland signature of about -52 ± 2‰ (France *et al.*, 2022a).

The metabolic composition of the local vegetation plays a crucial role in generating unique isotopic signatures ($\delta^{13}CH_4$) at the regional level. In warm tropical grasslands, farms, and wetlands, the prevalence of C_4 plants such as maize, sugar, papyrus, and various pastoral grasses contributes to higher carbon content enriched in ^{13}C (Fisher *et al*., 2017). In contrast, trees, bushes, and vegetation such as reeds with C_3 metabolisms exhibit significant discrimination against ^{13}C (MOYA/ZWAMPS Team *et al*. 2022).

Coalbed CH_4 emissions are generally poorly characterised, thus their isotopic composition also requires more analysis through a series of sampling campaigns. However, CH_4 emission $\delta^{13}CH_4$ from coal mines have been assessed (Menound, 2021; Zazzeri *et al.*, 2016; Fiehn *et al.,* 2021; Zhang, 2022). Zazzeri *et al.* (2016) presents CH_4 emission measurements and isotopic signatures from coal mines in Poland, Australia, and the United Kingdom, with bituminous coal averaging −65‰ and −55‰ for open-cast and deep mines respectively, and anthracite averaging −40‰ and −30‰ for open-cast and deep mines respectively. Findings have also been made that the $\delta^{13}CH_4$ signals of coal seam gas sources in the Surat Basin located in Queensland, Australia range from −55.6 ‰ to −50.9 ‰ (Lu *et al.*, 2021). Altogether, it is evident that various sources of CH_4 have a distinct range of isotopic signatures which differ

from each other (Figure 4). This makes isotopic characterization a good technique that can be used to differentiate sources of CH_4.

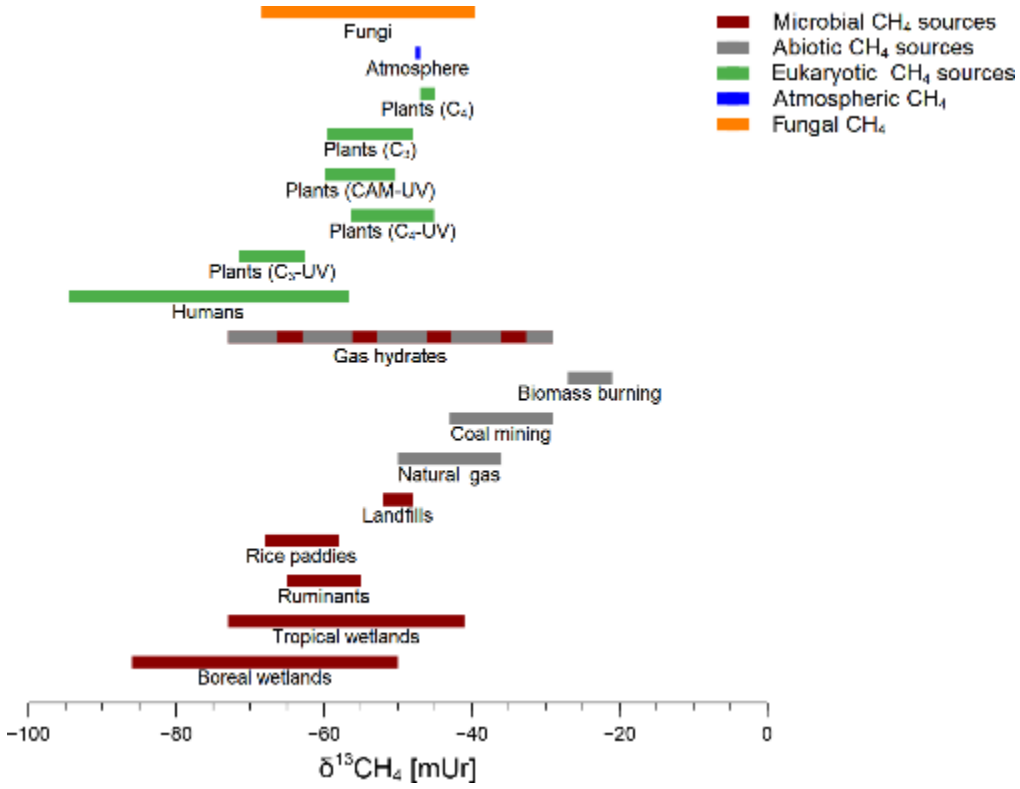


Figure 4: The range of $\delta^{13}CH_4$ values for various sources of methane, including microbial (red), abiotic (grey), eukaryotic (green), atmospheric (blue), and fungal (orange) origins, is presented based on findings by Schroll *et al*. (2020). The combination of microbial and abiotic methane formation processes for gas hydrates is indicated by the red and grey dashed bars, referring to Kvenvolden (1995). Data regarding these signatures were compiled from studies by Brownlow *et al*. (2017), Keppler *et al*. (2006, 2016), Kvenvolden (1995), Nisbet *et al.* (2016), Quay *et al*. (1999), and Vigano *et al*. (2009).

2.11. Satellite approaches to methane emission quantification using TROPOMI.

Satellite data retrieval is a crucial method to measure CH_4 emissions on larger spatial and temporal scales and can sometimes be used to validate ground measurement data. The Tropospheric Monitoring Instrument (TROPOMI), which is an instrument housed on the Sentinel 5 Precursor (S5P) satellite, is able to measure CH_4 mole fractions efficiently over diverse environments and CH_4 sources, and has been used in several studies to quantify CH_4 emissions (Plant *et al.,* 2022; Zhang *et al.,* 2022; De Gouw *et al.,* 2020; Shen *et al.,* 2021; Turner *et al.,* 2018).

TROPOMI provides CH_4 tropospheric column concentrations with adequate spatial-temporal coverage, and sufficient accuracy for CH_4 source detection. TROPOMI officially processed total column-averaged dry-air mole fraction of methane (XCH_4) in the offline data stream in April 2019. The total column averaged dry-air mole fraction of methane denotes the average CH_4 mole fraction in a vertical column of the earth's atmosphere, usually measured in parts per billion (ppb). This value accounts for the entire atmospheric column from the earth's surface to the troposphere, adjusts for water vapor's influence on gases such as methane, and expresses methane's proportion relative to the total dry air molecules. Monitoring this metric offers insights into methane's distribution, sources, and impact on climate change.

TROPOMI measurements have been validated and compared with other satellites to assess the accuracy of the instrument in CH_4 emission estimation, and when compared to the existing Greenhouse gases Observing Satellite (GOSAT) findings showed that there was indeed an agreement in the CH_4 products of both satellites. The average difference between their products was only 13.6 ppb (Hu *et al.,* 2018).

Methane emissions can be measured using TROPOMI from wetland ecosystems. Methane mole fractions were calculated using TROPOMI for wetlands located in South Sudan (Pandey *et al.*, 2022), where seasonal data of the total column averaged dry-air mole fraction of methane in the wetland areas were calculated. The lowest mole fractions were in the season with the highest rainfall and lowest temperature season (June - August) ranging at 1050 -2600 ppb in the winter of 2018 and 2019, with the highest mole fractions at 1870 - 2930 ppb in the months of September-November in 2018 and 2019. The authors further suggested that temperature was a strong regulator of emissions from wetlands in South Sudan. Along similar lines, Karoff and Vara-Vela (2023) reported wetlands as having the lowest levels of total column averaged dry-air mole fraction of methane when compared to various land cover types. The mole fraction of wetlands was reported for each continent and were at ~ 1800 ppb. In their study, Karoff and

Vara-Vela (2023) urged that researchers should be cautious when interpreting methane data from TROPOMI because of possible confounding variables that could cause errors in methane concentration estimates and slight uncertainty in retrieval algorithms.

There is a lack of studies on methane mole fractions from coal power stations using TROPOMI. However, TROPOMI has been utilized to assess mole fractions from coal mines. Methane mole fractions from coal mining in Queensland, Australia were analysed using TROPOMI, revealing total column averaged dry-air mole fraction of methane concentrations ranging from 1793 to 1828 ppb (Sadavarte *et al.*, 2021), while spatial-temporal distribution patterns of total column averaged dry-air mole fraction of methane in the Tarim, Sichuan, Central China, and North China basins were also examined, with recorded total column averaged dry-air mole fraction of methane values ranging from 1491 to 2352 ppb across the four basins (Zhang *et al.*, 2022).

South Africa lacks studies using TROPOMI data for CH_4 measurements. A study was recently conducted using TROPOMI to assess the distribution, trends, and sources of CH_4 in South Africa (Shikwambana *et al.*, 2022). Shikwambana *et al.* (2022) evaluated South Africa's average spatial distribution of CH_4 concentrations between 2018 and 2021 and the interior and northern regions of South Africa were found to have high mole fractions of CH_4, ranging between 1826–1850 ppb. The authors stated the lack of CH_4 emission data as one of the study's shortcomings. To completely comprehend the origins and trends of localized CH_4 emissions, the authors further suggested more CH_4 monitoring stations to be established and that a follow-up study ought to look into how CH_4 emissions relate to vegetation and meteorological factors as precipitation, temperature, and the Normalized Difference Vegetation Index (NDVI).

2.12. The Cape Point Global Atmospheric Watch (GAW) station in South Africa.

The World Meteorological Organization (WMO) Global Atmosphere Watch (GAW) stations hold immense importance in the realm of atmospheric environment monitoring and research. Positioned strategically across the globe, these stations serve as sentinel points for collecting continuous and comprehensive data on various atmospheric constituents, including greenhouse gases, aerosols, and ozone. Through sophisticated instrumentation and rigorous scientific protocols, GAW stations provide invaluable insights into atmospheric compositions of the earth, thereby facilitating understanding of atmospheric processes, quality of air, and changes in climate (Labuschagne *et al.*, 2018).

A collaboration occurred between the Atmospheric Sciences Division of the South African Council for Scientific and Industrial Research (CSIR) and the Max Plank Institute (MPI), Germany (which afterwards was named the Fraunhofer Institute for Atmospheric Environmental Research). This collaboration led to a baseline monitoring station which was established and located at Cape Point in South Africa. The observatory situated at the station in Cape point was later incorporated to the WMO's GAW in 1995.

Numerous partners from both South Africa and around the globe have collaborated and worked at Cape Point over the past four decades, providing reliable and quality data. As part of its mandate, the GAW station in Cape Point provides regional (southern hemisphere background) trace gas concentration data for prediction of potential changes in climate that may occur in the future (Labuschagne *et al.*, 2018). Additionally, the GAW Cape Point station complies with environmental agreements together with the World Data Centre (WDC) and the United Nations Framework Convention on Climate Change (UNFCCC) (Labuschagne *et al.*, 2018). These data are also easily accessible to the public through the South African regional Air Quality Information System (SAAQIS) and the World Data Centre for Greenhouse Gases (WDCGG). Data collected from the are valuable to both the United Nations Environment Programme (UNEP)/WMO ozone and IPCC Climate Assessments because the GAW station is based in a mostly untouched maritime environment with associated closeness to the Southern Ocean. It also acts as a benchmark for regional changes in the composition of the southern African atmosphere. (Labuschagne *et al.*, 2018). Various trace gas data is collected at the Cape Point GAW station, including the reported mole fraction of CH_4 (in ppb). There are two air-mass regimes at the Cape Point site- one is when the Cape Peninsular is buffeted by strong south easterly to south westerly winds during austral spring and autumn (November to April), and clean maritime air predominates (Labuschagne *et al.*, 2018). The advection of air towards Cape

Point from the southeast, which occurs during the austral spring and autumn seasons, is driven by high-pressure systems originating from the South Atlantic. Additionally, during the peak winter months (June–August), the South Atlantic High-Pressure system shifts toward the equator, leading to stronger westerly winds that pass over the southern tip of South Africa (Labuschagne *et al*., 2018). Therefore, there are changes in the prevailing directions of the wind from a north to a north westerly direction between autumn and spring which falls within the months of March-September. Thus, pollution from city of Cape Town is transported southward by the north westerly winds throughout the winter, and the Cape Point monitoring station detects this anthropogenic-derived pollution. Several factors including passing cold fronts moving from west to east and associated rainfalls affect the weather conditions at Cape Point. For the majority of the time at Cape Point, the wind and air masses come from the Southern Ocean, thus the station detects air before it gets polluted by anthropogenic activities. The GAW mandate is that only background atmospheric levels are of interest and that the baseline 39 year filtered data set is representative of the vast Southern Ocean to Antarctica and not an indication of continental sources. As such, maritime air is detected approximately 70% of the time and 30% of the time other continental air features are detected.

Research utilizing GAW CH_4 measurements suggests that the recent rise in CH_4 mole fractions after 2007 can be attributed to increased wetland mole fractions in tropical regions and human-induced sources in the mid-latitudes of the northern hemisphere (AK-BHD, 2021; Nisbet *et al.*, 2019). When characterising atmospheric CH_4 over the South African interior, Feig *et al.* (2016) found Cape Point to have the lowest concentration (1750 ppb) of CH_4 in comparison to regions dominated by power generation and industrial activity. Their study showed that Cape Point is thus an ideal and crucial background location to quantify the extent at which CH_4 emissions from various sources such as wetlands and fossil fuels differ from the undisturbed "clean" atmosphere. Measurements from other WMO GAW stations located across the globe are also available. Methane mole fraction data from three WMO GAW stations namely Lin'an (LAN), Longfengshan (LFS), and Waliguan (WLG) all located in China were assessed from the years 2009 to 2011 (Fang *et al.*, 2013). LAN is situated in a region in China with robust economic activities whereas LFS's location is within a intensive agricultural activity mostly cultivation of rice. WLG is in an isolated location around the northwest region of China. Across all seasons, consistently data from the LAN, revealed elevated mole-fractions of methane. The increased methane levels were attributed to surface winds originating from the northeast with a peak rise of 32 ± 15 ppb observed during summer. Within each season, a peak-to-peak increase in amplitude of about 77 ± 35 ppb was recorded. Conversely, at LFS, the amplitude of

the 24 hours cycle remained relatively unchanged throughout the year, except during the summer months where 196 ± 65 ppb was recorded. July marks the peak of CH_4 values at LFS, a deviation from the usual patterns seasonally observed in the northern hemisphere. Meanwhile, WLG exhibited the lowest CH_4 mole fractions and variability. Maximum values are observed during summer, contrasting with other WMO/GAW global stations in the northern hemisphere.

In-situ atmospheric methane measurements extensively conducted over a period of 26 years at the WLG station have further been presented by (Liu *et al.*, 2021). Over this period, a predominantly continuous atmospheric CH_4 levels uptrend was recorded at WLG, with an annual rate of growth mean value of 5.1±0.1 ppb between 1994 to 2019. However, there were specific intervals, such as 1999–2000 and 2004–2006, characterized by near-zero or negative growth rates. The recorded mean CH_4 mole fraction in 1994 stood at merely 1799.0±0.4 ppb, whereas by 2019, it had surged by approximately 133 ppb, reaching the highest number ever recorded in the WLG GAW data history of 1932.0±0.1 ppb. The mean CH_4 levels data recorded from different seasons ranges from the years 1994 -2018 at WLG were presented with the highest values of 1861.7±0.4 ppb obtained during summer and the lowest in spring (1853.1±0.3 ppb). An exception was noted during 1994–1997 when there was a peak during winter and a trough during autumn. The authors stated that local sources, such as human activities, increasingly influenced WLG.

Data from GAW stations worldwide can thus aid researchers in assessing long term global climatological variability. Studies inclusive of methane data from South Africa's GAW station are limited and Cape Point GAW station data should be continuously analysed and included in CH_4 source emission studies for a comprehensive view of atmospheric CH_4 emissions.

2.13. Concluding summary

It is evident from the literature review that studies using a multifaceted approach (flexfoil bag sampling, satellite, and isotope data) to assess CH_4 concentrations in South Africa are lacking. Improved characterization of methane concentrations from the country's wetlands and the coal industry is necessary to facilitate the reduction of methane. This study serves as one the very few measurements from a South African wetland and the first data on comparisons of CH_4 concentrations from microbial wetland emissions versus anthropogenic coal stockpile emissions in South Africa.

3. MATERIALS AND METHODS

In this chapter, the methodologies employed to address the research objectives outlined in the preceding chapters are detailed. The methodological framework guiding the study encompasses the research design, data collection methods, sampling strategies, and analytical techniques.

3.1. Study sites

3.2. Wakkerstroom wetland

The Wakkerstroom wetland (commonly referred to as the *Wakkerstroom vlei*) is located in the South-eastern region of the Mpumalanga province, on the highveld in South Africa (Figure 5). The wetland's co-ordinates are 27˚ 22'S; 30˚ 07'E. The Wakkerstroom wetland's main body is subdivided into three major hydrogeomorphic units. The uppermost 1 kilometre and the lowermost 2 kilometres of the wetland system is defined as the floodplain whereas the middle reaches of it is defined as the unchanelled valley bottom wetland (Joubert and Ellery, 2013).

The Tugela River upper catchment includes the Wakkerstroom wetland, with the wetland forming part of the Tugela River's upper basin (Stockdale *et al.*, 2021). The primary wetland body is around 4.5 metres deep, with peat accumulation reaching a depth of 2 metres (Joubert and Ellery, 2013). The Thaka river, which drains into Zaaihoek Dam, emerges from the Wakkerstroom wetland south of the R543. The majority of water input of the Wakkerstroom wetland occurs through the Wakkerstroom Dam which is located immediately upstream of the wetland along with minor tributary streams along hills surrounding the wetland (Joubert and Ellery, 2013). The annual potential evapotranspiration at the Wakkerstroom wetland is approximately double the average annual precipitation, at 1715.2 mm (Stockdale *et al.*, 2021). The Wakkerstroom wetland is not a region characterized by high floral diversity (Kotze *et al.*, 1994), however it provides a habitat suitable for foraging and nesting many bird species including the rare and threatened white-winged flufftail. Other bird species present in the wetland include the African marsh harrier and the grey crowned crane (Kotze *et al.* 1994; BirdLife South Africa, 2006). The wetland area increased in size by 0.483 km^2 between 1938 and 2009. It changed from 3.769 km^2 in 1938 to 4.252 km^2 in 2009 possibly due to the boundary of the wetland being non-static and fluctuations in climate conditions leading to irregular shifts in the wetland extent (Stockdale *et al.*, 2021).

3.3. Majuba power station

The Majuba power station, located in Mpumalanga province, South Africa (27°6′2″S 29°46′17″E), lies between Volksrust and Amersfoort. It is the southernmost among Eskom's 11 operational coal-fired power stations. Operational since 2001, it ranks as the second largest power plant, boasting an installed capacity of 4,110 MW. Presently, Majuba power station does not possess its own dedicated mine, instead acquiring coal via short to medium term supply contracts from a pool of 15 suppliers (source: https://www.eskom.co.za/eskom-divisions/gx/coal-fired-power-stations/). Consequently, Majuba power station sources coal from various origins. Coal delivery occurs monthly, facilitated by both rail (0.42 MT) and road (0.74 MT), with around 700 trucks making deliveries per day (Figure 6).

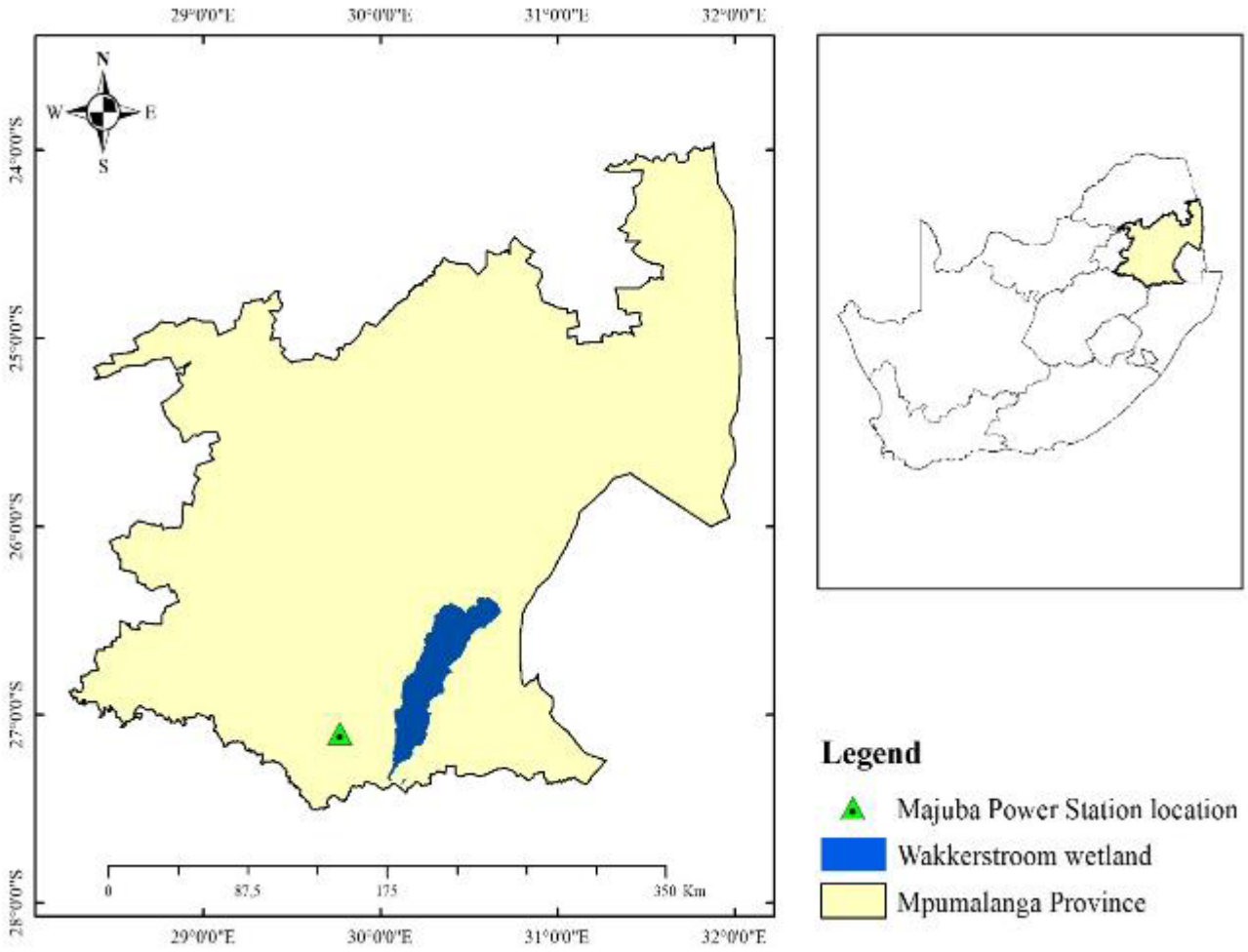


Figure 5: Map showing the location of the Wakkerstroom wetland and the Majuba power station in Mpumalanga province, South Africa.



Figure 6: Trucks delivering coal at Majuba power station. Image captured on 26 January 2023.

3.4. Study species

3.5. Typha capensis

The family *Typhaceae* consists of one genera and approximately 10 -15 species (Masoko *et al.*, 2008). The individual plants are tall with the capability to reproduce clonally by rhizomes which are submerged forming dense stands. The plant leaves are diuretic. The species of focus for purposes of this study is *Typha capensis* (Rohrb. N.E.Br), commonly known as *bulrush. T. capensis* is generally found in shallow, wet regions such as marshes, swamps, and any other slow moving or stagnant water regions. It is a robust, reed-like plant sparsely distributed in the Northwestern Cape region but very common all around the inland region of South Africa (Van Wyk *et al.*, 1997). *Typha* is also a C_3 monocot (Farnsworth and Meyerson, 2003; Jones, 1988; Schweingruber *et al.*, 2020; Musara and Aladejana, 2020) that inhabits both brackish and freshwater tidal marshes. *T. capensis* is mostly found in the sedge marsh belt of the Wakkerstroom wetland (Figure 7).







Figure 7: Typha Capensis sampling sites at the Wakkerstroom wetland. Top left: *Typha* water sampling site.

3.6. ***Phragmites australis***

Phragmites australis (Cav. Steud) (Figures 8 and 9), known as the common reed, is a species which often dominates in freshwater wetlands (Adams and Bate, 1999). While typically associated with the C_3 photosynthetic pathway (Hough and Wetzel, 1977; Mal and Narine, 2004; Kiviat, 2013; Get *et al*., 2014), there has been ongoing debate regarding its photosynthetic mechanisms. Some studies suggest similarities to the C_4 pathway in terms of photosynthetic rates and the presence of mature chloroplasts in the bundle sheath (Antonielli *et al*., 2002; Milke *et al*., 2020; Srivastava *et al*., 2014; Raghuvanshi *et al.,* 2023). *Phragmites australis* is widely distributed along South African riverbanks and is frequently found in monospecific stands (Laing *et al*., 2003; Raghuvanshi *et al*., 2023). *Phragmites* demonstrates tolerance to low pH levels and is recognized as a viable plant for phytoremediation purposes (Van Deventer and Cho, 2014). In the Wakkerstroom wetland, while the edges are characterized by grassland, the majority of the wetland, including its interior, is dominated by *Phragmites australis* (Cav. Steud) (Stockdale *et al*., 2021).







Figure 8: Photographs of *Phragmites* on the wetland bank at the Wakkerstroom wetland**.**



Figure 9:Water *Phragmites australis* sampling site.

3.7. ***Schoenoplectus decipiens***

Schoenoplectus decipiens (Nees) J. Raynal (Figure. 10) is a C_3 sedge (Snowden, 2009; Bruhl and Wilson, 2007; Whigham *et al.,* 2023) found in Africa, India and Pakistan which are tropical regions (Jiménez-Mejías *et al.*, 2007). *S. decipiens* grows in the sedge meadow and wet grassland in a large area near and in the Wakkerstroom vlei. Another *Schoenoplectus* species, *Schoenoplectus brachyceras* (A. Rich.) K. Lye exists in the deeper, open waters further into the Wakkerstroom vlei and covers a dense sedge marsh. The two plant species are sympatric in Wakkerstroom. The height of *Schoenoplectus* species varies between 80 – 2400 mm and the achene surface of the plant is defined as smooth to regulose (Browning, 1992). *S. brachyceras* consist of inflorescence of a pseudolateral anthela with 1-10 branches and *S. decipiens* consists of a pseudolateral head, occasionally an anthela with 1 - 3 branches (Browning, 1992).



Figure 10: Mixed vegetation (*Typha* and *Schoenoplectus*) sampling site at Wakkerstroom wetland during the spring season (left) and during the autumn season (right).

3.8. Experimental design and protocol

3.9. Set-up of sampling equipment on sampling sites

The sampling equipment consists of a 6V battery operated air pump, a two-metre pole (a fishing rod was utilised in this study), and 3-litre SKC flexfoil plus bags (Figure 11). The pump has an outlet tube that directs air that has been sucked in from within the canopy of the vegetation into the 3 litre flexfoil bag. The pump was allowed to fill the bag up to 2.25 litres (75% capacity) in approximately 40 seconds. The flexfoil bags could not be filled to 100% capacity as they were to be inside an airplane for analysis at the laboratory. Thus, the pressure on the outside of the bags could drop causing the bags to expand and burst leading to bag failure. The failure of the bags was however accounted for by having, at minimum, three bags being used to sample at each of the vegetation communities.

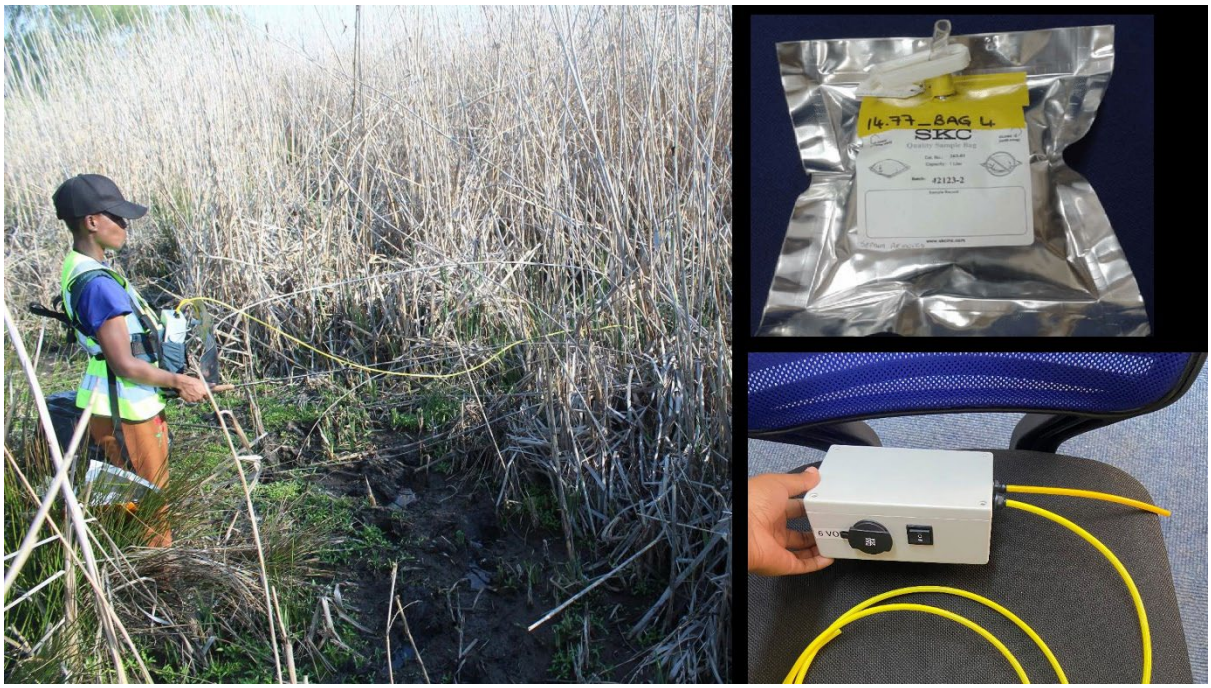


Figure 11:Sampling equipment (flexfoil bag, fishing rod, and 6V battery operated pump).

3.10. Sampling at the Wakkerstroom wetland sites

The sampling dates were 09 September 2022 for spring, 25 January 2023 for summer, 22 April 2023 for autumn and 22 July 2023 for winter. The Wakkerstroom wetland samples were taken at the vegetation community sites downwind and inside the wetland - namely *Typha*, *Phragmites*, and a mixed site of *Typha* and *Schoenoplectus* since a pure *Schoenoplectus* site was difficult to locate. For this study, the sampling sites at the wetland will be referred to as *Phragmites*, *Typha*, and Mixed (*Schoenoplectus* + *Typha*). During the autumn and winter season, in order to assess the effect of water depth on CH_4 concentrations, additional air samples of *Phragmites* and *Typha* were taken where the water was deeper. These samples are referred to as "*Typha* water" and "water *Phragmites*" in this study. The samples also included background air samples which were taken upwind of the Wakkerstroom wetland. The sampling locations, at fixed GPS co-ordinates for vegetation communities at the Wakkerstroom wetland were used.

The pump was held within the near vicinity approximately 0-1 metres above the vegetation. A stopwatch was used to record the time taken (~ 40 s) to fill each bag to 75% capacity. Prior to sample collection at each location, the pump was flushed for 2 minutes with air from the vicinity of the vegetation sample that was going to be collected. This was done to ensure that the air that will be collected was that of the current location with minimal to no contamination of residual air from previous sampling sessions. At each vegetation community location downwind of the wetland, at least three sampling bags at minimum were filled with air. Background air samples were collected at approximately four kilometres upwind of the wetland and three bags were also utilised for this.

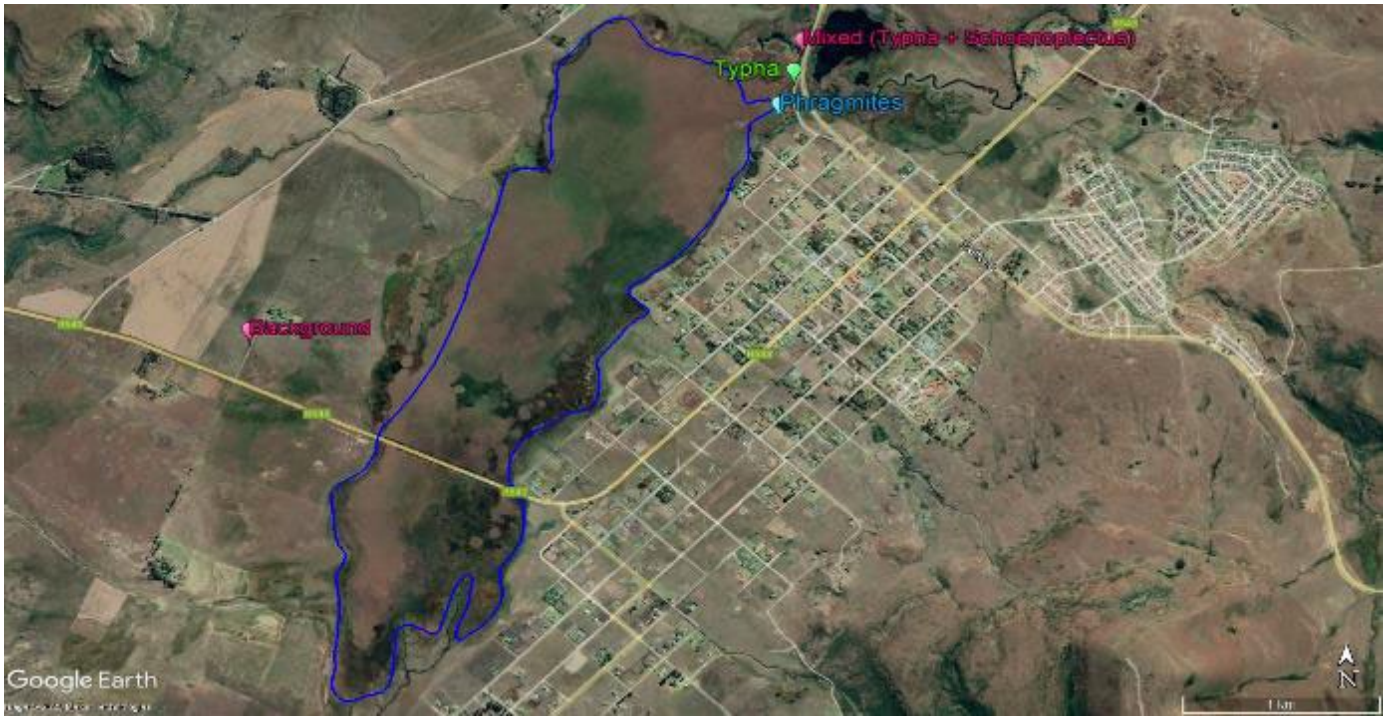


Figure 12: Google Earth image of the location of where the samples were collected for the vegetation communities along the Wakkerstroom wetland in Mpumalanga province, South Africa

3.11. Sampling at the Majuba power station.

The sampling dates were 10 September 2022 for spring, 26 January 2023 for summer, 23 April 2023 for autumn and 23 July 2023 for winter. The location of sampling varied seasonally at the power station according to abiotic factors such as wind direction, temperature, and wind speed (Figure 13). The downwind location (Figure 14) of sampling at the Majuba power station varied depending on wind direction and accessibility (1.71 km's from the stockpile in spring, 6.8 km's from the coal stockpile in summer, 2.65 km's from the stockpile in autumn). Given that the CH_4 concentrations and their associated isotopic signatures are known to originate from the coal stockpiles, it was necessary to position oneself as close as possible in the downwind direction. The background (upwind) sampling location (Figure 15) also varied according to wind direction on each sampling day in each season. During each sampling season, three replicates of background (upwind) air samples were collected, and three replicates were collected for downwind concentration samples. A total of six sampling bags were utilised for the Majuba power station each season of sampling. Once air sampling was completed at both the Majuba power station and the Wakkerstroom wetland, the flexfoil bags were all packaged into boxes and sent to Royal Holloway, University of London (RHUL) for isotopic analysis

and CH_4 concentration analysis.



Figure 13: Location of the samples collected at Majuba power station in Mpumalanga province, South Africa.



Figure 14: Downwind sampling locations at Majuba power station during the 4 seasons of sampling: spring (top left), summer (top right), autumn (bottom left), winter (bottom right).



Figure 15: Upwind sampling locations at Majuba power station during the 4 seasons of sampling: spring (top left), summer (top right), autumn (bottom left), winter (bottom right).

3.12. Standard trace gas analysis at Royal Holloway, University of London (RHUL)

Royal Holloway, University of London is situated in Egham, Surrey in the United Kingdom (51.4257° N, 0.5631°W). In the Royal Holloway (RHUL) greenhouse gas laboratory, the IsoPrime mass spectrometer and GV Instruments Trace Gas preconcentrator were first installed in March 2003. The instruments are all joined in a continuous-flow set-up (Figure 16). The laboratory concentration and isotopic analysis of gas samples collected in this study followed the procedure outlined by Fisher *et al.* (2006). The samples were prepared for isotopic analysis by continuous-flow isotope-ratio mass spectrometry using an IsoPrime Trace Gas system (Figure 17 and 18).

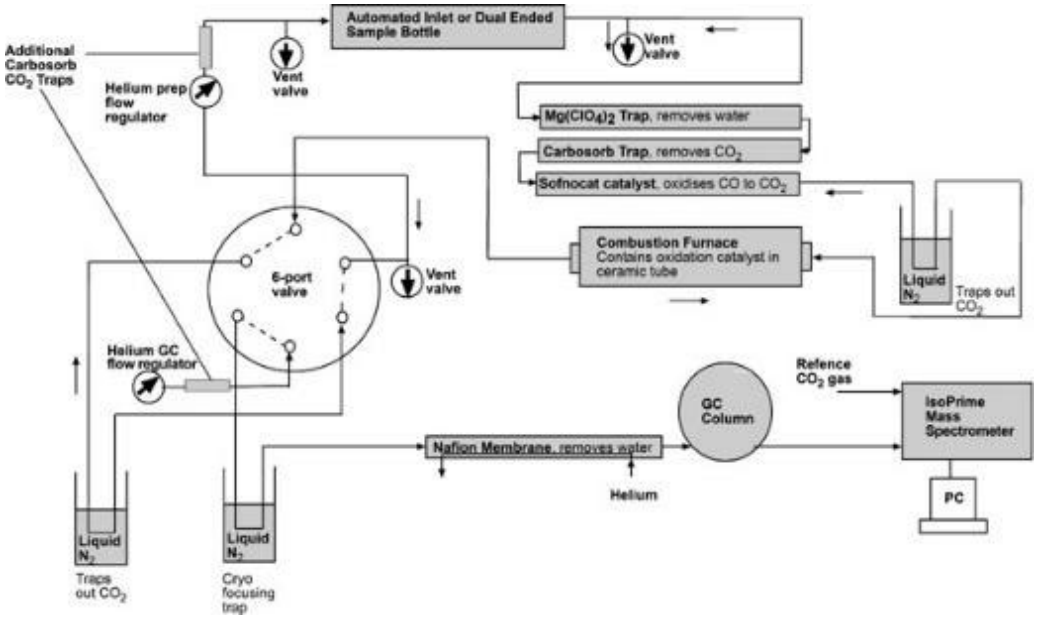


Figure 16: Diagram of the sampling equipment for CH_4 analysis set-up at RHUL. Reproduced from Fisher *et al.* (2006).

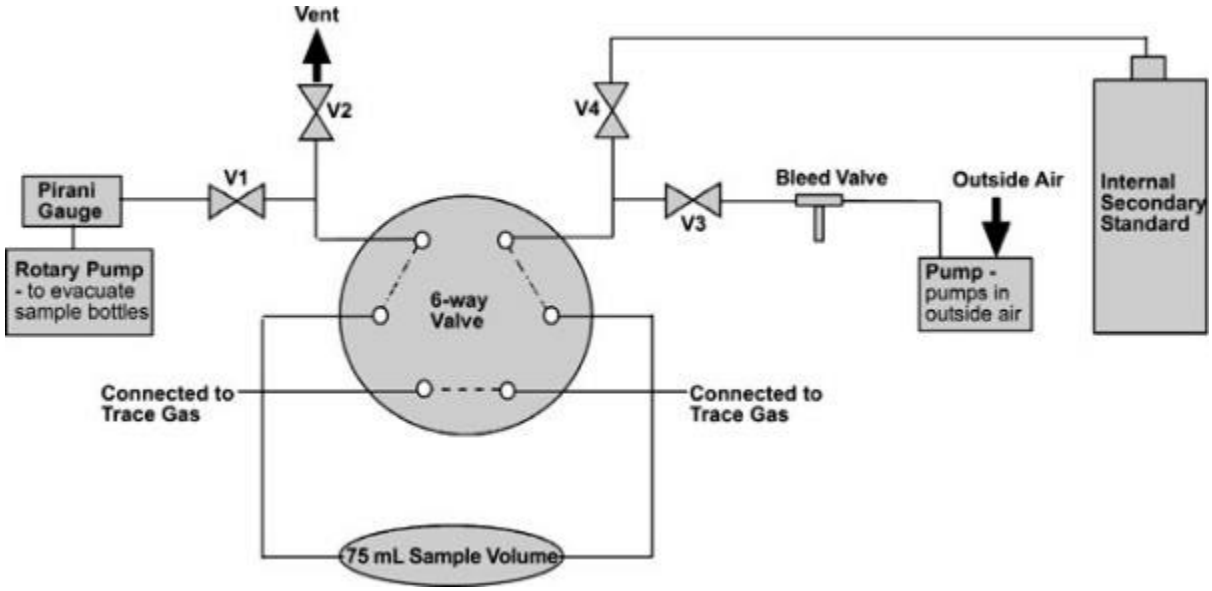


Figure 17: Diagram of the sampling equipment for CH_4 analysis set-up at RHUL. Reproduced from Fisher *et al.* (2006).



Figure 18: Image showing the CH_4 analyser during sample analysis. Reproduced from Fisher *et al.* (2006).

3.13. Determination of isotopic source signatures using the Keeling plot technique.

The Keeling plot regression (Keeling, 1958) was utilised in the identification of source isotopic signatures of CH_4 in collected samples. A plot of the $\delta^{13}CH_4$ against the inverse of the CH_4 mole fraction and linear regression is utilised to calculate the isotopic source signature (see equation 2). The y-intercept in this graph gives the isotopic source signature which is responsible for the excess methane mole fraction over the background. A mathematical representation of this can be simplified as:

$$\delta^{13}C_a = C_b(\delta^{13}C_b - \delta^{13}C_s) \times (\frac{1}{C_a}) + \delta^{13}C_s \quad \text{(equation 2)}$$

- C_a: Measured atmospheric concentration of CH_4.
- C_b : Atmospheric background of CH_4.
- $\delta^{13}C_a$: Measured isotopic composition.
- $\delta^{13}C_b$: Background atmospheric isotopic composition.
- $\delta^{13}C_s$: The source isotopic composition.

3.14. Data analyses

3.15. Regression analysis for Keeling plot computation

It is imperative to acknowledge that the regression approach employed may introduce error on both the x and y axes. This acknowledgement is necessary to evaluate the uncertainty surrounding the Keeling plot intercept and, in turn, the inaccuracy in the $\delta^{13}C$ source signature (Brownlow *et al*., 2017). The Reduced Major Axis Regression (RMA) program was used in this investigation. When a variable that is independent in an experiment is measured with error, RMA is an efficient and straightforward application that is recommended over Ordinary Least Squares (OLS) regression (Sokal and Rohlf, 1981). Such examples typically show that the slope estimations will be skewed. McArdle (1988) states that when the error rate in the variable is greater than one-third of the error rate in the y variable, RMA should be used to estimate the true relationship.

The RMA slope, *b,* is calculated according to the following equation:

$$b_{\text{RMA}} = \pm\sqrt{\frac{SSy}{SSx}} = \pm \sqrt{\frac{\Sigma y^2 - \frac{(\Sigma y)^2}{2}}{\Sigma x^2 - \frac{(\Sigma x)^2}{2}}} \quad \text{(equation 3)}$$

As done in OLS regression, *a*, the intercept indicating where the straight line intersects the y-axis (i.e., the y-intercept indicating the source isotopic signature) is calculated as:

$a_{\text{RMA}} = \bar{y} - b_{\text{RMA}}\,\bar{x}$ equation 4

r^2, the coefficient of correlation is then calculated as follows:

$$r^2_{\text{RMA}} = {SSx}/{(SSx)(SSy)} \quad \text{(equation 5)}$$

The errors are calculated as:

$$b_{\text{RMA}}\,[\text{SE}] = \sqrt{\frac{MSE}{SSx}} \quad \text{(equation 6)}$$

$$a_{\text{RMA}}\,[\text{SE}] = \sqrt{MSE\left(\frac{1}{n} + \frac{(\bar{x})^2}{SSx}\right)} \qquad \text{(equation 7)}$$

SSx and SSy are the sum of squares for the x and y variables. MSE is the mean standard error. $\bar{x}$ is the standard deviation.

By using random sampling with replacement to create new data sets with n cases each, the software also enables the computation of confidence intervals (C.I.).

One-way analysis of variance (ANOVA) was the statistical technique used to compare variations in CH_4 concentrations among plant species after testing for normality. ANOVA is

designed to compare the means of three or more groups. If ANOVA finds a significant difference, one can perform a post-hoc test (like Tukey's HSD) to determine which specific plant species pairs have significant differences in CH_4 concentrations. The ANOVA was used as there were more than 3 species that were being compared and the data also passed the normality test thus the ANOVA was the most appropriate test for use.

R Studio was used to perform the ANOVA (RStudio Team, 2020). Using RStudio, a plot of the CH_4 concentration for each location and vegetation community was created.

3.16. Wakkerstroom weather station data

Weather data (wind, air temperature, and relative humidity) was measured at the HOBO weather station in Wakkerstroom and accessed through a CR300 series logger. The data was utilized to assess the predominating weather conditions seasonally and to also understand the meteorological conditions on the days of ground sampling, and days leading up to the ground sampling. The data was plotted in RStudio.

3.17. Measurement principles of the TROPOMI instrument

TROPOMI consists of various products, including the product of the column-averaged dry air volume mixing ratio of methane (XCH_4).

TROPOMI has seven bands, being UV-1 (270-300nm), UV-2 (300-370nm), VIS (370-500nm), NIR-1 (685-710nm), NIR-2 (745-773nm), SWIR-1 (1590-1675nm) and SWIR-3 (2305-2385nm). The instrument has a line of sensors arranged in a push broom configuration, such that the across track image width is 2600 km. Pixel resolution is 7 km along track and 3.5 km across track at nadir for all spectral bands with the exception of UV1 with an across track width of 28 km and the SWIR bands of 7 km width, but both still 7 km along track. The larger pixel size of TROPOMI means that its data inherently smooths out local variability and provides a regional average rather than a point-specific measurement. This averaging can obscure localized sources or sinks of CH_4 that might be captured in spot-sampled measurements.

Retrieving CH_4 from space-based SWIR data is difficult due to scattering from aerosols and cirrus. While optically thin scatterers are significantly difficult to spot yet nevertheless alter the light path of the observed backscattered sunlight, optically thick scatterers can be successfully filtered out. If not properly accounted for, this could result in an under- or overestimation of the genuine CH_4 column. Modifications to the settings of the TROPOMI instrument were made on the 6th of August 2019 (Apituley *et al.,* 2022). As of date, S5P flies in loose formation with the United States Suomi National Polar-orbiting Partnership (NPP) satellite. The intentions of pairing these two satellites were to achieve the high spatial resolution cloud observation capabilities of the Visible Infrared Imager Radiometer Suite instrument (VIIRS) housed aboard the Suomi NPP satellite. At an altitude of 824 kilometres, the S5P satellite travels in a sun-synchronous orbit daily at an equatorial overpass time 13:30 SAST along with VIIRS. VIIRS and TROPOMI have a temporal separation of less than 5 minutes.

TROPOMI provides CH_4 column concentrations with adequate spatial and temporal coverage, and sufficient accuracy for CH_4 source detection.

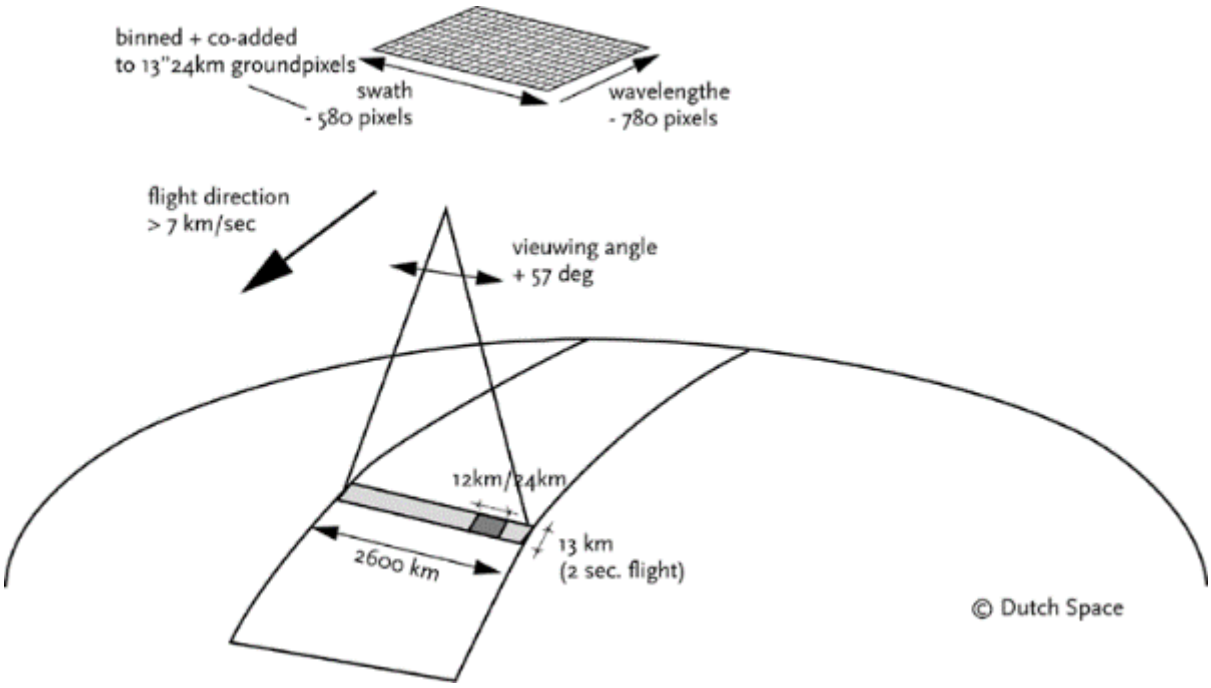


Figure 19: TROPOMI measurement principle (Apituley *et al.*, 2022).

3.18. TROPOMI CH_4 product

For the utilization of sufficiently accurate high-quality data, a selection of clear-sky scenes is made through the use of a filter from VIIRS which is housed in the Suomi-NPP satellite. There are various criteria of filtering in existence that are based on surface albedo, scattering properties, roughness of terrain, and fitting quality.

The CH_4 data product in TROPOMI is given as "total column averaged dry-air mole fraction (XCH_4)". The equation for calculation is denoted by:

total column averaged dry-air mole fraction of methane $= \sum_{i=0}^{n} \frac{x_i}{v_{air,dry}}$ → Equation 8

where x_i is the methane vertical sub-column, and $v_{air,dry}$ is the dry-air column. From this, based on retrieved data on surface albedo, a bias correction of the TROPOMI total column averaged dry-air mole fraction of methane is performed to ensure the accuracy of the data and suitability for utilization. Since the units for the methane product are '1e $^{-9}$ mol·mol^{-1} (ppb)', it should be noted that this is not the surface concentration but the total column-averaged dry-air mole fraction of CH_4 and thus is a representative of the complete atmospheric column. The Sentinel-

5P/TROPOMI mission is a crucial step toward the monitoring of CH_4 mole fractions, however in some instances its 7-km x 5.5 km pixel size does not generally allow sampling of individual point sources making it challenging to map and detect them.

3.19. TROPOMI data collection and processing

Sentinel-5P data were used in the analyses. The Level 3 offline (OFFL) CH_4 product, namely the "column-averaged dry-air mole fraction of CH_4 (in ppb - parts per billion) was accessed through the Google Earth Engine platform. The datasets for mapping were accessed from the "*COPERNICUS/S5P/OFFL/L3_CH4*" image collection. The dataset provides offline high-resolution imagery of CH_4 mole fractions. The S5P level 3 products are created through resampling of level 2 products into a common spatial and temporal grid. Level 2 data files with quality assurance (qa) value > 0.5 are utilized in the resampling process into a grid of $0.01^o \times 0.01^o$ resolution.

The Jupyter notebook was utilized to visualize the spatial imagery of the column-averaged dry-air mole fraction of CH_4. Earth Engine Python API, GEEMAP, seaborn, and matplotlib were utilized. A composite of the total column averaged dry-air mole fraction of methane was calculated by utilizing a start and end date to determine the range of images. Reducers are functions that are used to aggregate data across bands, arrays, time, space, and other data structures. Any basic statistic (e.g., minimum, maximum, mean, median, standard deviation, etc.) can be specified by the reducers to be used for the aggregation. The mean statistic was utilized in this study, and a data frame of date and the total column averaged dry-air mole fraction of methane over the time period "2022-08-01 to 2023-07-31" was produced. This time period was specifically used as it was inclusive of the dates ground sampling took place and covered all four seasons. Using the "GEEMAP" function, all map visualization parameters were then specified, and output maps were produced.

3.20. TROPOMI Data analyses

There is an objective to calculate and present the total column averaged dry-air mole fraction of CH_4 (ppb) as measured by the Tropospheric Monitoring Instrument (TROPOMI) at the Wakkerstroom wetland and Majuba power station to assess seasonal variations. The data frame produced for each site (Wakkerstroom wetland and Majuba power station) in terms of date and the mean total column averaged dry-air mole fraction of methane over the time period "2022-08-01 to 2023-07-31" was imported in RStudio. Each day, one image from TROPOMI was obtained for the specified Wakkerstroom wetland and Majuba power station co-ordinates (i.e., a single pixel for each image). In RStudio within this selected data collection time period, the months were separated into seasons with August, September, and October as spring , November, December, January as summer, February, March, April as autumn, May, June, July as winter. The average of all the daily datasets was calculated for each season and mapped. An

unpaired two-samples t-test was done to assess the difference between the sites in terms of their mean total column averaged dry-air mole fraction of methane. The t-statistic, degrees of freedom (df), confidence interval, and p-values were reported. The data had some days with missing measurements for each of the sites, thus for the Wakkerstroom wetland only 78 days had measurements and for the Majuba power station only 89 days had measurements. A boxplot was graphed for both sites.

3.21. The Cape Point Global Atmospheric Watch (GAW) station.

The Cape Point GAW monitoring station (34.3567° S, 18.4968° E) is located in the Western Cape, South Africa (Figure 20).

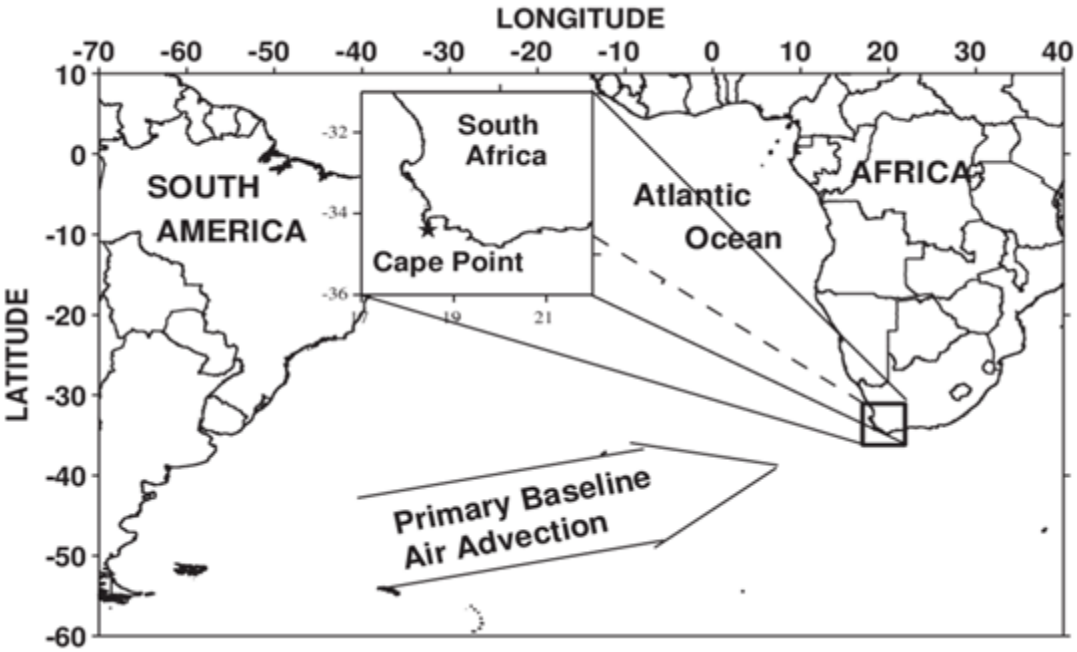


Figure 20:Map showing the location of the Cape Point GAW station (Labuschagne *et al.*, 2018).

3.22. Methane (CH_4) mole fraction measurement at Cape Point.

From the year 2012, the Cavity Ringdown Spectroscopy (CRDS) method was used for CH_4 mole fraction measurement when the gas chromatograph (GC) system was discontinued. This method allows for an increased frequency of measurements, at one minute instead of five-minute intervals as the instrument utilizes less calibration gas allowing the calibration gas to last several years where in the past it would last only for a year. CRDS is also oblivious to

water vapour, eliminating the requirement to strip out water from the collected sample.



Figure 21: Cape Point GAW station sampling instrumentation (source: Alban Thollot: "https://www.ige-grenoble.fr/Cape-Point-South-Africa").

Various trace gas data is collected at the Cape Point GAW station, and the focus of this study is the reported mole fraction of CH_4 (in ppb). Two datasets (accessed at: "https://gaw.kishou.go.jp/") were collected for the mole fraction of CH_4 at Cape Point- the filtered (background) and unfiltered datasets. The filtered dataset refers to data that has undergone some processing to eliminate noise, outliers, or artifacts. These data are representative of the background air conditions at Cape Point, meaning that it does not include the episodes of urban pollution and/or anthropogenic sources. The GAW mandate is that only background atmospheric levels are of interest thus this study focused on that data only and not the unfiltered dataset.

3.23. Data analyses for the Cape Point GAW data.

The filtered (background) data was plotted for the years 1983 - 2021. Post- 2021, the instruments at the station had a slight malfunction and thus have been excluded in this study. For each year, the data was aggregated into monthly measurements to assess the seasonal variations in the data and graphs were plotted using RStudio.

Weather data (wind, temperature, and relative humidity) for the Cape Point region was also accessed for the years 2020 -2022 from the South African Weather Service (SAWS). The

primary atmospheric transport channels to Cape Point were calculated using the Hybrid Single-Particle Lagrangian Integrated Trajectory (HYSPLIT) model which can be accessed at "https://www.ready.noaa.gov/HYSPLIT_traj.php". The trajectory shows the temporal and spatial motion of atmospheric trace gases. Backward trajectories are used to identify the source region of atmospheric components. Five-day backward trajectories were utilized to assess the origin/source of air masses to Cape Point.

4. RESULTS

In this section, a structured and comprehensive analysis of the collected data and findings will be presented. The chapter will be divided into three sections- Section A presents the results from field collected data consisting of carbon isotope measurements and CH_4 concentration measurements. Section B presents the satellite measurements from TROPOMI, and SECTION C presents data from the Global Atmospheric Watch (GAW) station at Cape Point, South Africa. To provide a coherent framework, each section of results begins with an overview of the research objective and a brief description of the dataset used. The analysis includes statistical tests and measures, if applicable, to support the interpretation of the data. The core findings will be dealt with in detail using relevant tables, figures, and text.

4.1. SECTION A: Ground field concentrations and isotope data from the Wakkerstroom wetland plant communities and the Majuba power station coal stockpile.

Research objective 1: An assessment of the seasonal concentrations (ppm) of CH_4 from the Wakkerstroom wetland and the coal stockpile at the Majuba Power Station.

The Wakkerstroom wetlands total CH_4 concentrations were calculated in spring (0.383 ± 0.110 ppm, n = 12), summer (0.429 ± 0.163 ppm, n = 14), autumn (1.198 ± 0.744 ppm, n = 20), and winter (0.226 ± 0.110 ppm, n = 18) (Figure 22, Table 2). In the CH_4 concentration analysis (Figure 22), *Phragmites* consistently exhibited the highest concentration amongst all species sampled in three out of the four seasons namely spring (0.209 ± 0.076 ppm), autumn (0.537 ± 0.239 ppm), and winter (0.132 ± 0.065 ppm). The coal stockpiles had the lowest CH_4 concentration amongst all species in three out of the four seasons namely in summer (0.022±0.021 ppm), autumn (0.014±0.053 ppm), and winter (0.002±0.004). Significant differences in CH_4 concentrations among plant species were found using a one-way ANOVA in each season ($p < 0.01$). Post-hoc tests (Tukey HSD) revealed that *Phragmites* had a CH_4 concentration 0.074 ppm (95% CI: -0.031 – (0.179)) higher than the coal stockpiles in summer. The water *Phragmites* had significantly higher CH_4 concentrations compared to coal stockpiles by 0.523 ppm (95% CI: -0.073 – (-0.972)) in autumn and by 0.130 ppm (95% CI: 0.043 – 0.217) in winter. Lastly, water depth did not significantly affect CH_4 concentrations during the autumn and winter sampling when water *Phragmites* and *Phragmites* had no significant differences, and *Typha* water compared to *Typha* also had no significant differences.

Phragmites had a higher concentration than *Typha* in both seasons when water depth assessments were conducted.

The *Phragmites* site in spring and summer had higher concentrations than *Typha* and Mixed. However, the soil surface of *Typha* and Mixed were drier than that of *Phragmites*. This led to the question of whether water depth was the governing factor of this high CH_4 concentration seen in *Phragmites*. Only in autumn and winter then were measurements of CH_4 concentration for the *Phragmites* and *Typha* within the wetlands water column taken.

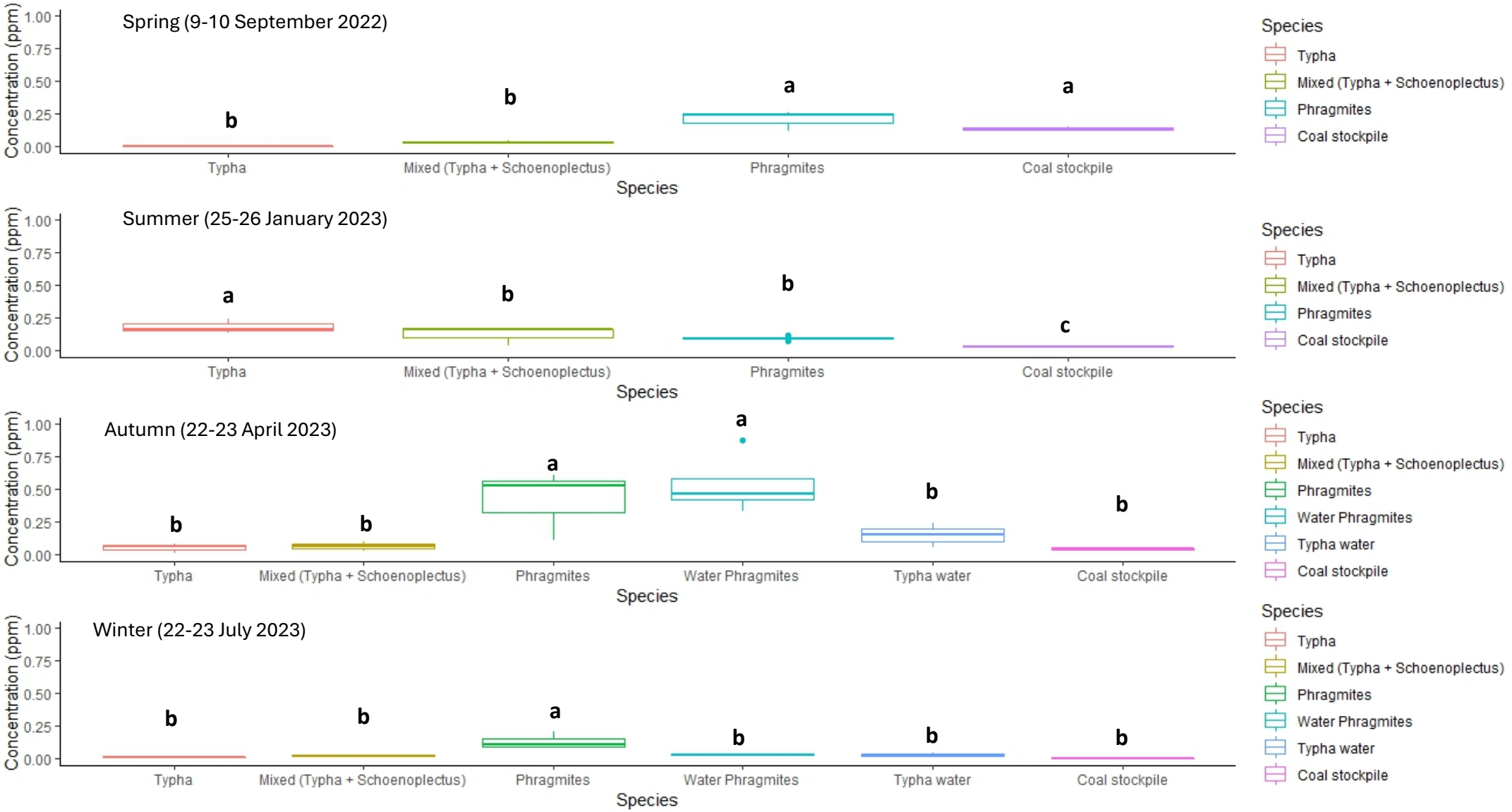


Figure 22: Concentration (ppm) measurements collected from various plant communities at the Wakkerstroom wetland and coal stockpiles at the Majuba power station in the spring (9-10 September 2022), summer (25-26 January 2023), autumn (22-23 April 2023) and winter(22-23 July 2023)

Table 2: Mean and standard deviation table for seasonal methane concentration (ppm) data.

Season	Species	Number of gas samples (n)	mean (ppm)	std. deviation
	Mixed (*Typha* + *Schoenoplectus*)	3	0.035	0.012
Spring	*Typha*	3	0.002	0.003
	Phragmites	3	0.209	0.076
	Coal stockpile	3	0.137	0.019
	TOTAL		0.383	0.110
Summer	*Typha*	3	0.185	0.056
	Mixed	3	0.122	0.072
	Phragmites	5	0.100	0.014
	Coal stockpile	3	0.022	0.021
	TOTAL		0.429	0.163
Autumn	Mixed (*Typha* + *Schoenoplectus*)	3	0.065	0.035
	Typha	3	0.055	0.038
	Phragmites	3	0.416	0.269
	water *Phragmites*	4	0.537	0.239
	Typha water	4	0.111	0.110
	Coal stockpile	3	0.014	0.053
	TOTAL		1.198	0.744
Winter	Mixed (*Typha* + *Schoenoplectus*)	3	0.022	0.011
	Typha	3	0.012	0.005
	Phragmites	3	0.132	0.065
	water *Phragmites*	3	0.032	0.008
	Typha water	3	0.026	0.017
	Coal stockpile	3	0.002	0.004
	TOTAL		0.226	0.110

Research objective 2: An assessment of the seasonal source isotopic signatures from the Wakkerstroom wetland and the coal stockpile at the Majuba Power Station.

In order to distinguish the carbon isotopic source signatures of CH_4 at both sites, the Keeling method was utilized by plotting the $\delta^{13}C$ against the inverse of the concentration (ppm^{-1}). For both the Wakkerstroom wetland and the Majuba power station's coal stockpiles, the source isotopic signature was determined. The source isotopic signature for the Wakkerstroom wetland was calculated using all the vegetation communities' inverse concentrations and $\delta^{13}C$. The isotopic signature ($\delta^{13}CH_4$) across the four seasons show that the Wakkerstroom wetland generally had an isotopic signature that was light (^{13}C depleted). The range in source isotopic signatures for the Wakkerstroom wetland was between -61.4‰ to -55.6‰. The trend and slope of the isotopic source signatures across the four seasons at the Wakkerstroom wetland varied over a small range (Figure 24).

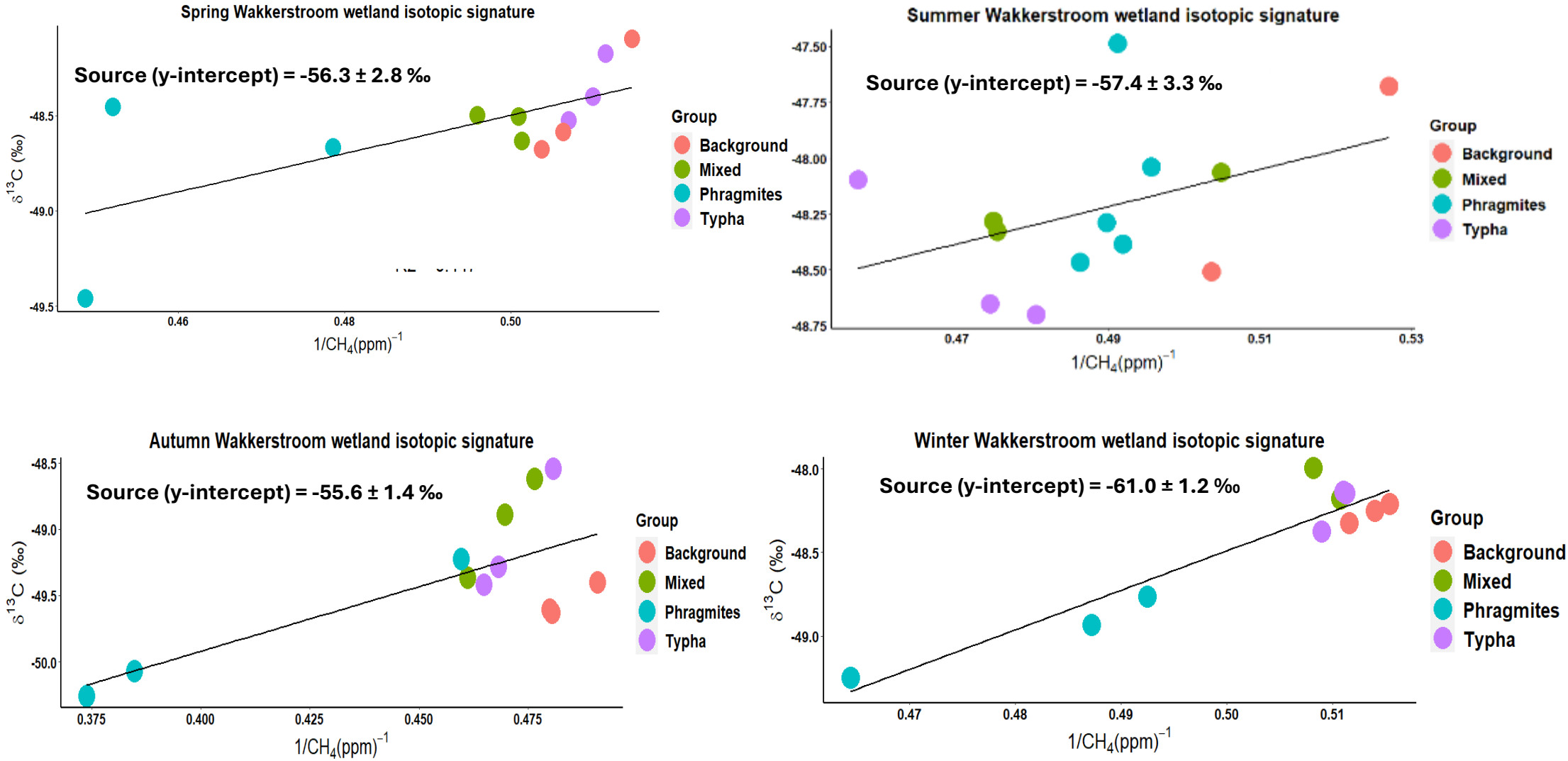


Figure 23: Keeling plots representing the source carbon isotopic source signatures of the Wakkerstroom wetland in the spring, summer, autumn, and winter seasons.

When assessing the source isotopic signature of the Majuba power station coal stockpiles, the results show that during the spring and summer seasons, the coal stockpiles had an isotopically heavier $\delta^{13}CH_4$ signature of -35.3 ± 1.0 ‰ and -43.5 ± 3.5 ‰ (Figure 24). In the autumn and winter seasons, the results show that the coal stockpiles had an isotopically lighter $\delta^{13}CH_4$ signature of - 62.0 ± 1.6 ‰ and - 87.0 ± 10.3 ‰. Thus, across the sampling period of four seasons, the source isotopic signatures of the Majuba power station coal stockpiles varied considerably over a large range. For the spring and summer seasons, the Majuba power station coal stockpiles had heavier (less depleted) isotopic values than the Wakkerstroom wetland. For the autumn and winter seasons, the Majuba power station coal stockpiles had lighter (more depleted) isotopic values than the Wakkerstroom wetland.

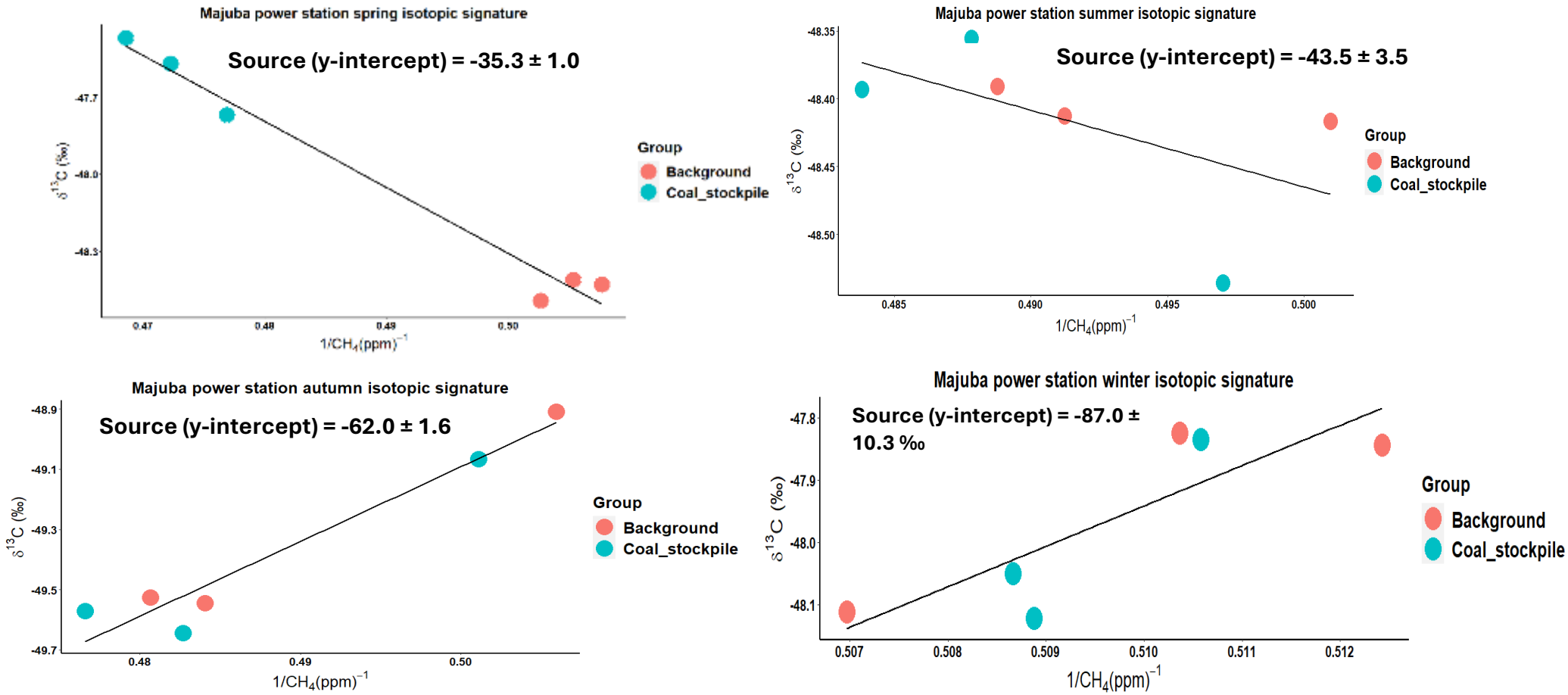


Figure 24: Keeling plots representing the carbon isotopic source signatures of the Majuba power station in the spring, summer, autumn, and winter seasons.

4.2. Meteorological variables at the Wakkerstroom wetland.

Meteorological variables are vital when analysing CH_4 concentrations for several reasons. Wind patterns play a crucial role in the dispersion of CH_4 in the atmosphere (Britter, 1989). Firstly, understanding wind direction is important to assess where the emitted CH_4 may be transported (for ground measurement purposes). Additionally, temperature can affect microbial activity in natural sites of CH_4 emission such as wetlands. Lastly, relative humidity affects the transport and chemical reactions of CH_4 in the atmosphere. High humidity can promote chemical reactions that can remove CH_4 from the atmosphere, while low humidity can slow down these reactions.

Meteorological data were accessed for the Wakkerstroom region in order to assess whether changing weather conditions could have affected CH_4 production at the wetland. The wind direction, air temperature, relative humidity, and air temperature data was accessed and graphed.

4.3. Seasonal wind patterns at the Wakkerstroom wetland

The wind roses for the Wakkerstroom region showed that in the spring (September, October, November), summer (December, January, February), and autumn (March, April, May) the wind blows from the north and the north easterly areas (> 40 %) for the majority of the time (Figure 25). There was also a flow of wind from the south westerly areas (≤ 10 %) and it was also shown that the wind rarely blew from the southeast. However, during the winter season (June, July, August), the wind rose showed a prevalent wind direction from the northeast (> 20 %) and the south westerly regions (> 20 %).

For three of the four seasons the dominant wind direction was quite constant according to the wind rose plots, blowing from the north and north easterly direction.

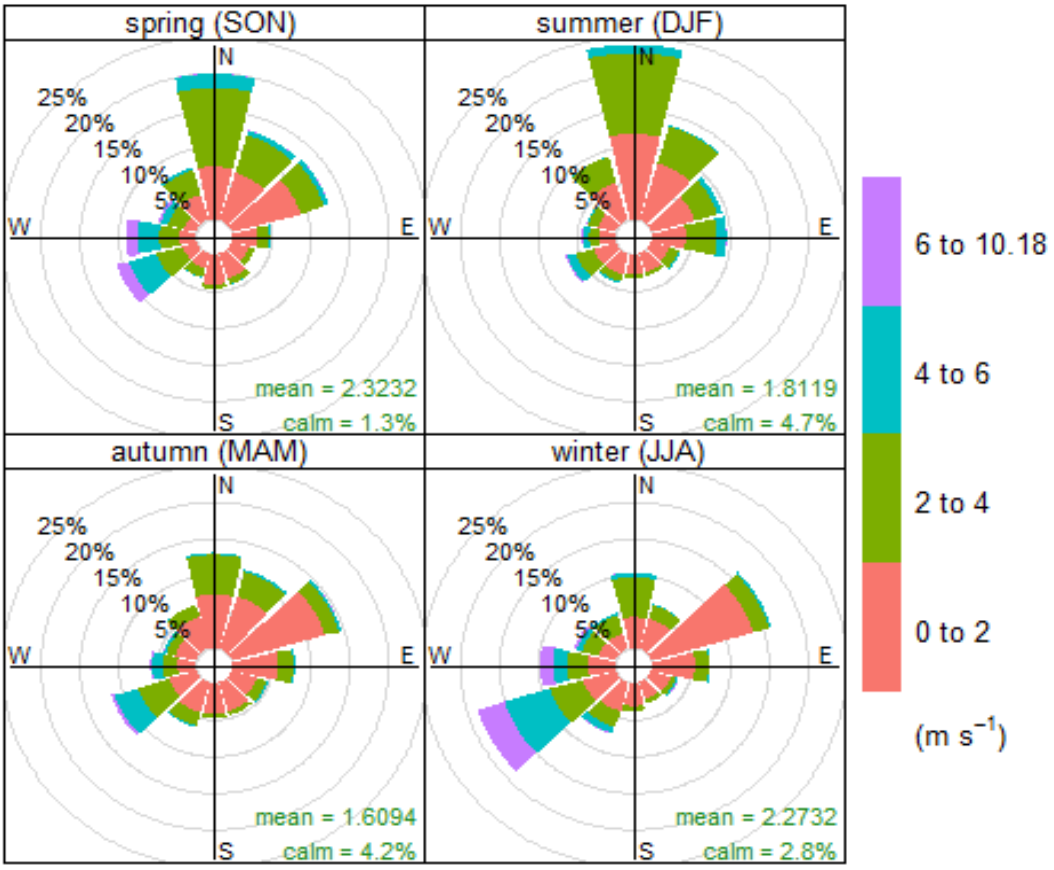


Figure 25:Seasonal wind rose plots at Wakkerstroom, Mpumalanga (SON: September, October, November; DJF: December, January, February; MAM: March, April, May; JJA: June, July, August)

4.4. Temperature and rainfall data at Wakkerstroom, Mpumalanga.

The air temperature at Wakkerstroom was graphed for the period 01 January 2022 until 31 August 2023 (Figure 26). The highest day temperature (30.1 °C) was recorded on 4 October 2022, and the lowest day temperature (16.2 °C) was recorded on 15 June 2022. The sampling dates have been denoted by the red arrows in Figure 26. During the spring (9 September 2022) and summer (25 January 2023) field sampling days, sampling occurred at a time when temperatures were above the mean. These were also the two sampling seasons where there had been rainfall on the days leading up to sampling (Figure 27) at the site. During these sampling dates, warmer wetter ground conditions had persisted on the days leading up to the sampling day. During the autumn (22 April 2023) and winter (22 July 2023) sampling days, the samples were collected at times below the mean temperature and rainfall was minimal (Figure 27). Cold and dry conditions dominated on the days leading up to these sampling days. and on the sampling days themselves.

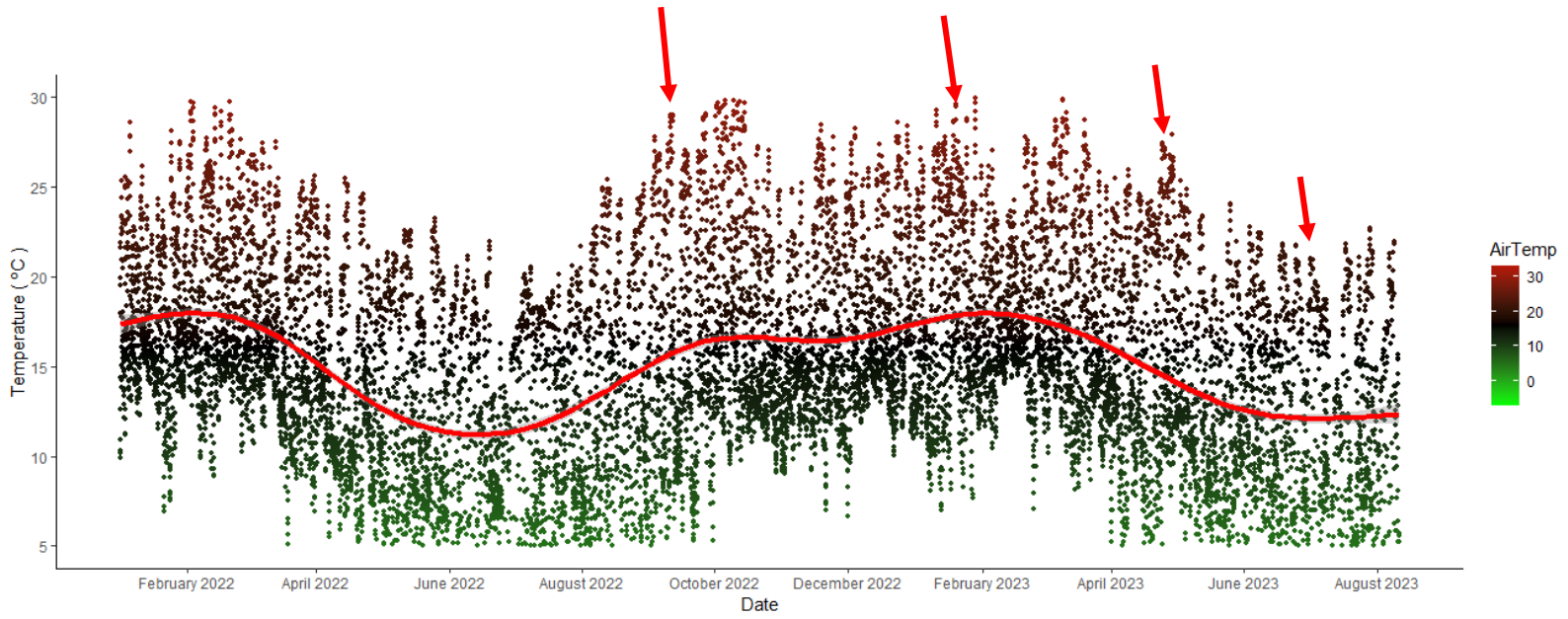


Figure 26:Seasonal temperature pattern (°C) at Wakkerstroom, Mpumalanga on January 2022 – August 2023 with red arrows indicating field sampling days in each season.

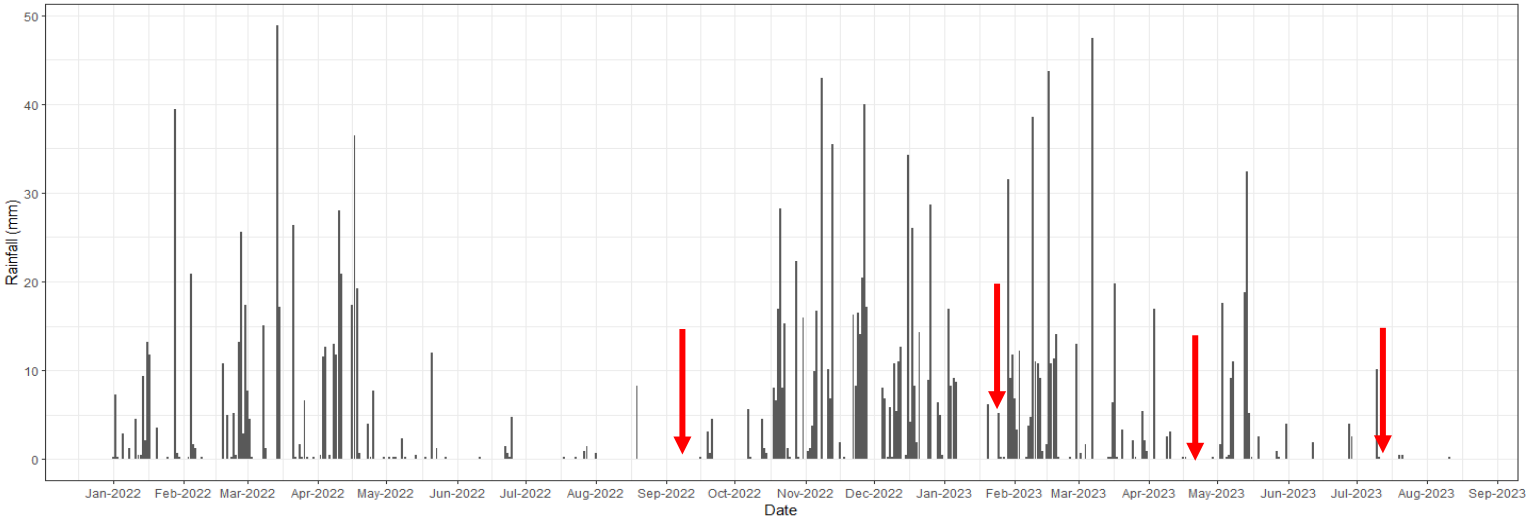


Figure 27:Seasonal rainfall pattern at Wakkerstroom, Mpumalanga from January 2022-August 2023 with red arrows indicating field sampling days in each season.

4.5. Relative humidity at Wakkerstroom, Mpumalanga.

The relative humidity of the air at the Wakkerstroom wetland (Figure 29), showed the highest percentages in the spring and summer months (December - April) when warmer, wetter conditions persisted, and the lowest values in the winter months (June – August) when cold, dry conditions persisted.

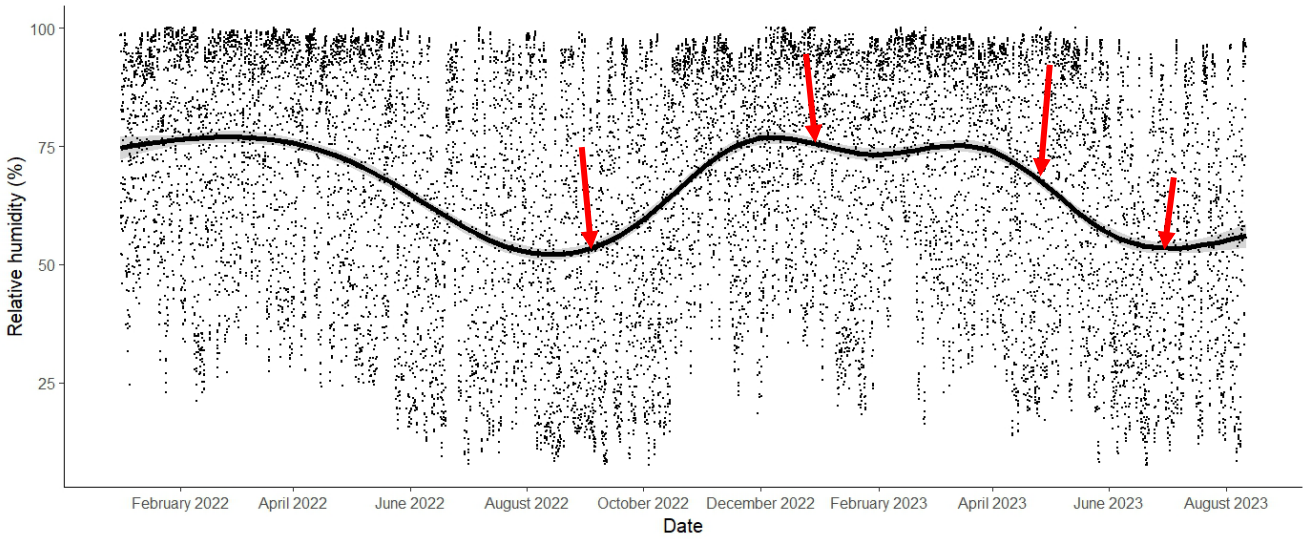


Figure 28:Relative humidity (%) at Wakkerstroom, Mpumalanga from January 2022-August 2023 with red arrows indicating field sampling days in each season.

4.6. SECTION B: TROPOMI measurements

Spatial and temporal scale differences should always be taken into consideration when assessing CH_4 concentrations. The field campaigns represented an aggregated mixed air sample within the near vicinity approximately 0-1 metres above the vegetation. The field campaigns also only represent a single point in time during each season. The field campaigns also quantified CH_4 concentrations by each source (vegetation community or power station) at a single point in time. Hence, to examine CH_4 mole fractions at greater temporal and spatial scales to provide a more comprehensive view of atmospheric CH_4 TROPOMI measurements of total column averaged dry-air mole fraction of methane (ppb) were obtained for Wakkerstroom wetland and Majuba power stations.

Research objective 3: An assessment of the total column averaged dry-air mole fraction of methane product as measured by TROPOMI at the Wakkerstroom wetland and Majuba power station.

Using TROPOMI, the total column averaged dry-air mole fraction of methane product was plotted (Figure 29) for the selected time period 01 August 2022 to 31 July 2023, which includes all the seasons – spring, summer, autumn, and winter. This period was chosen as it matches the field samples for concentrations and isotopic signatures. In RStudio within this selected data collection time period, the months were separated into seasons with August, September, and October as spring , November, December, January as summer, February, March, April as autumn, May, June, July as winter.

The data had some days with missing measurements for each of the sites, thus for the Wakkerstroom wetland only 78 days had measurements and for the Majuba power station only 89 days had measurements (Table 3). The results show that there was no statistically significant difference between the wetland site and the power station site. The Wakkerstroom wetland site had slightly lower values for the total column averaged dry-air mole fraction of methane (1855.4 ± 18.0 ppb) when compared to the Majuba power station site (1857.1 ± 22.9 ppb) across the specified time period. This is shown in Table 3. An unpaired two-samples t-test showed that the difference between the Wakkerstroom and the Majuba power station sites with respect to the mean total column averaged dry-air mole fraction of methane, was not significant, $t = 0.581$, $p = 0.562$, [95% CI: -4.415, - 8.099].

Table 3: Descriptive statistics of the total column averaged dry-air mole fraction of methane distribution at Majuba power station and Wakkerstroom.

Location	n	mean (ppb)	std. deviation	std. error mean
Wakkerstroom	78	1855.4	18.0	2.04
Majuba power station	89	1857.1	22.9	2.43

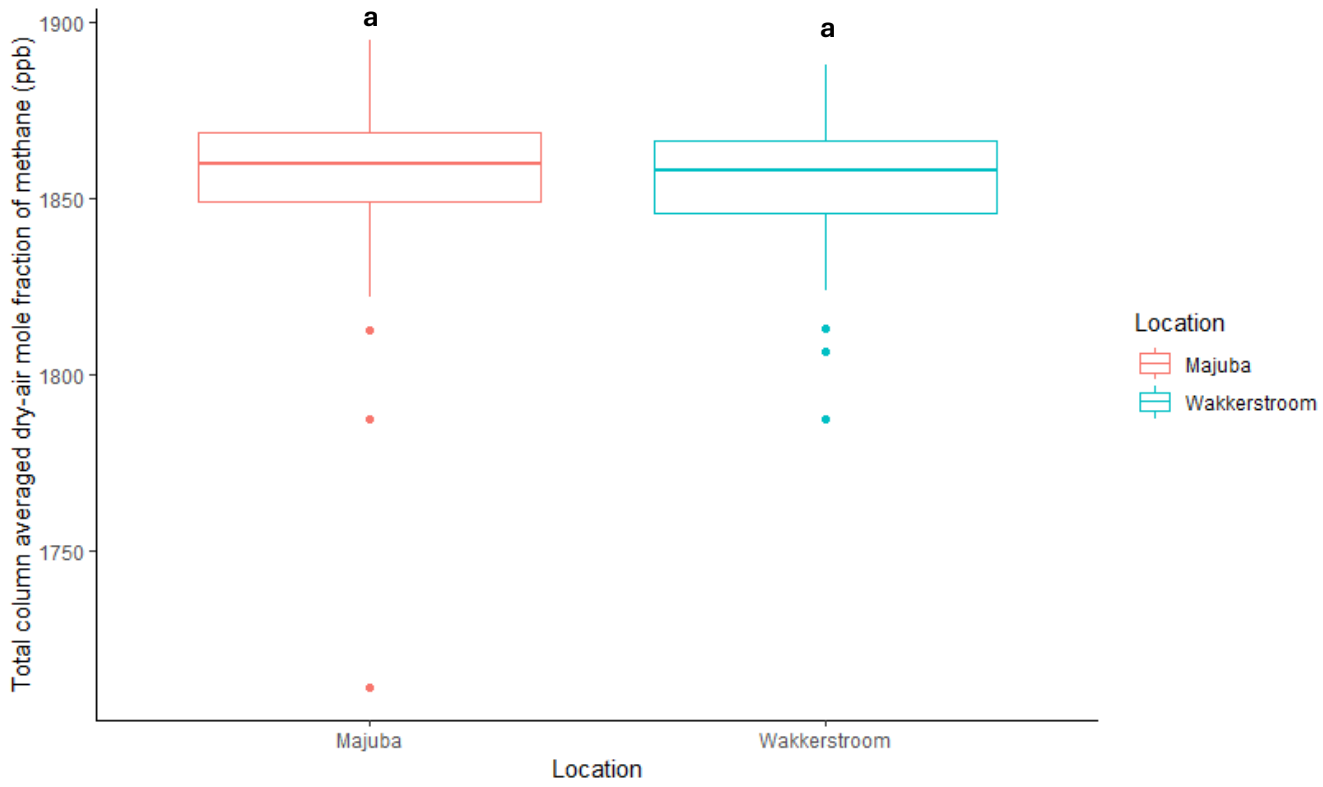
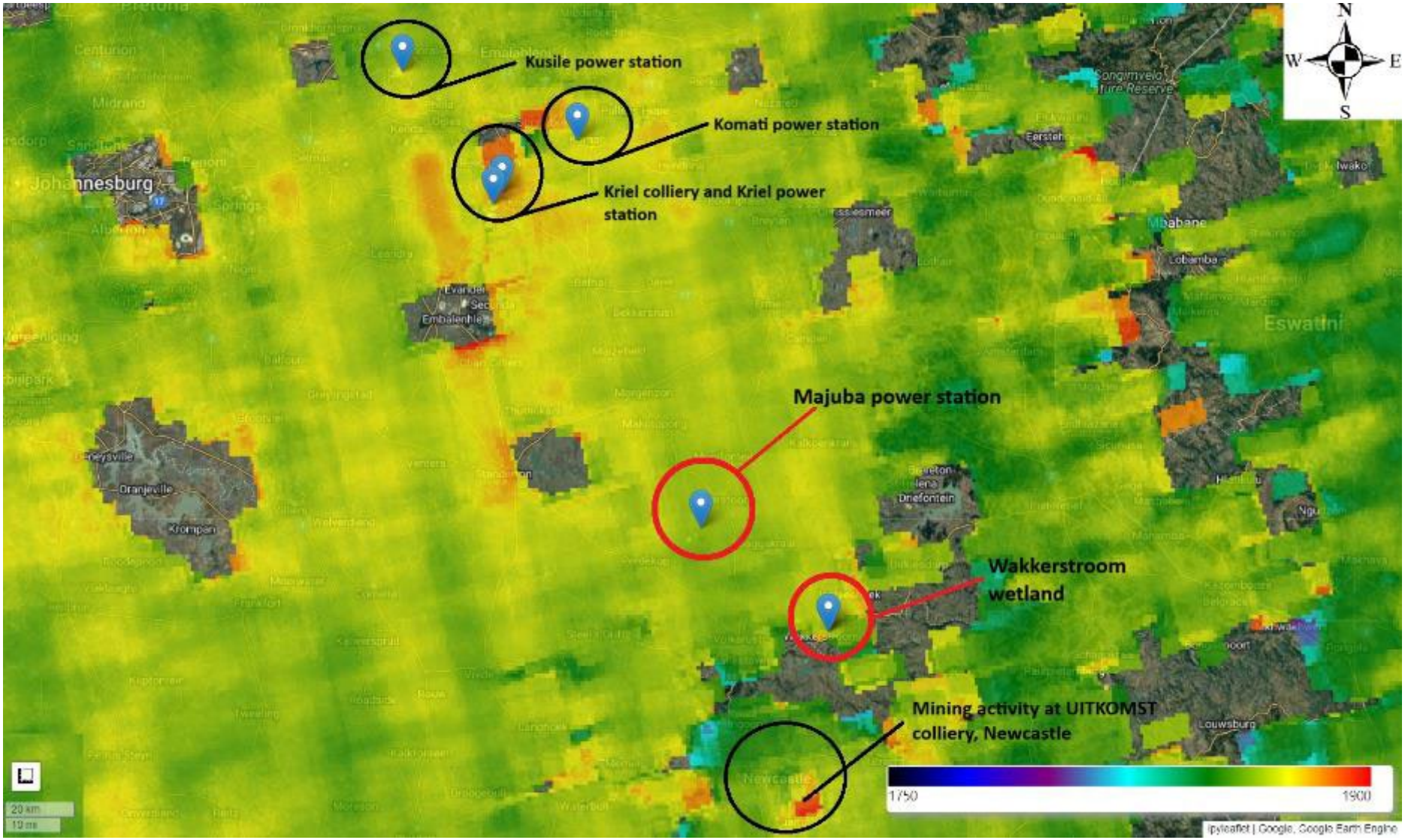


Figure 29: Boxplot showing the total column averaged dry-air mole fraction of methane at Wakkerstroom and Majuba power station in Mpumalanga province, South Africa as measured using TROPOMI.

Maps of the spatial distribution of CH_4 in Mpumalanga were produced. For the spring months (01 August 2022 – 30 October 2022), the total column averaged dry-air mole fraction of methane was mapped (Figure 30), and the Wakkerstroom wetland and Majuba power station locations were presented in the map (circled in red). When mapping the data, some power stations and collieries were also noticeable. Visual analysis of the maps across the selected time periods show that total column averaged dry-air mole fraction of methane does not show great differences when comparing the Wakkerstroom and Majuba power station regions as also observed through the t-test. In contrast to this, higher values were noticeable for other industrial activities such as the collieries when comparing them to the Majuba power station and the Wakkerstroom wetland.

In the summer (Figure 31) spatial distribution maps, there were notable disparities between collieries and power stations. Collieries yet again exhibited noticeably higher CH_4 levels compared to power stations and compared to the Wakkerstroom wetland. The Wakkerstroom wetland and Majuba power station had no noticeable differences in CH_4 mole fraction distributions. During the autumn (Figure 32) and winter (Figure 33) seasons however, the CH_4 distribution maps illustrate less noticeable disparities between collieries and power stations.



30: Map produced from TROPOMI total column averaged dry-air mole fraction of methane product (spring 2022)**.**

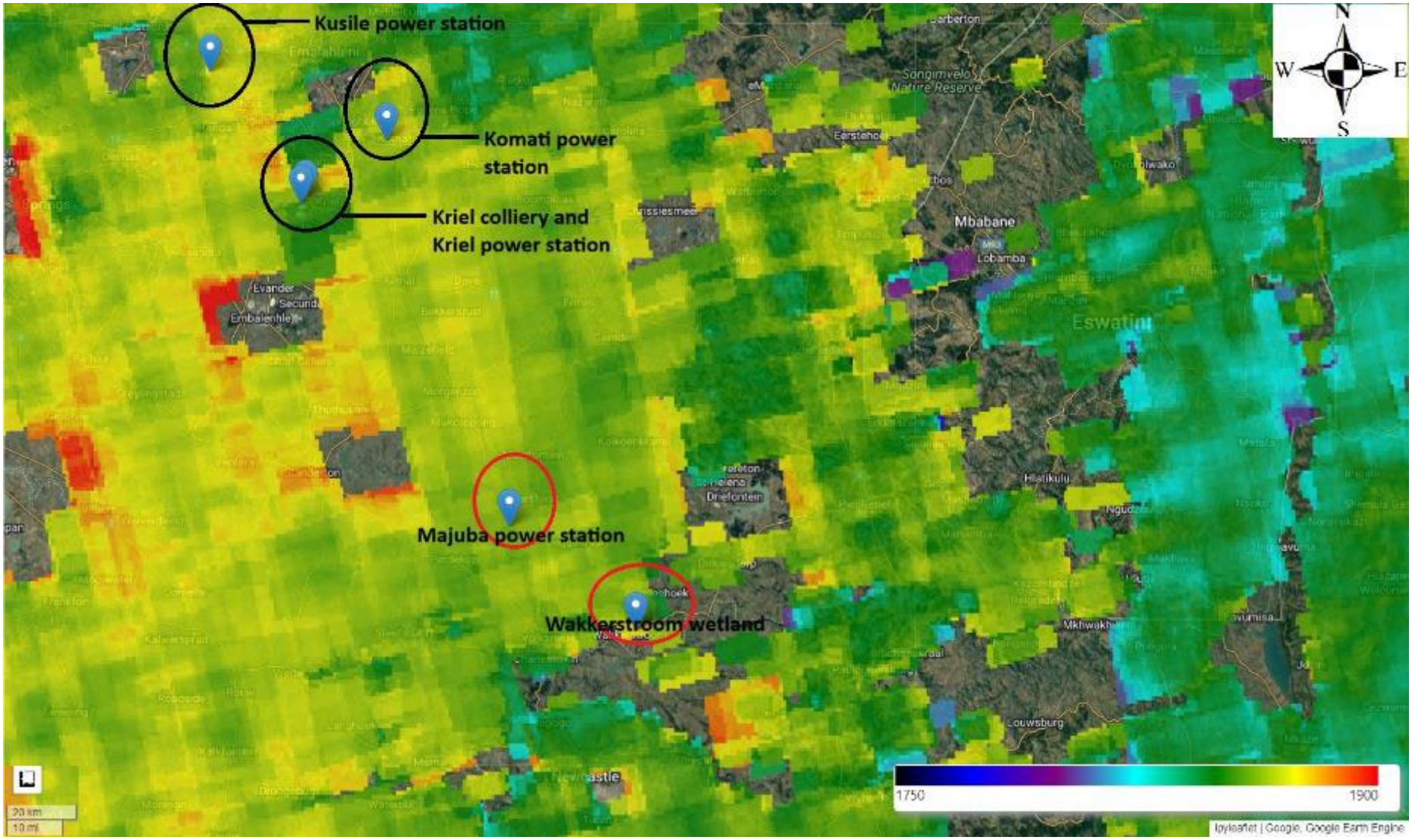


Figure 31: Map produced from TROPOMI total column averaged dry-air mole fraction of methane product (summer 2023).

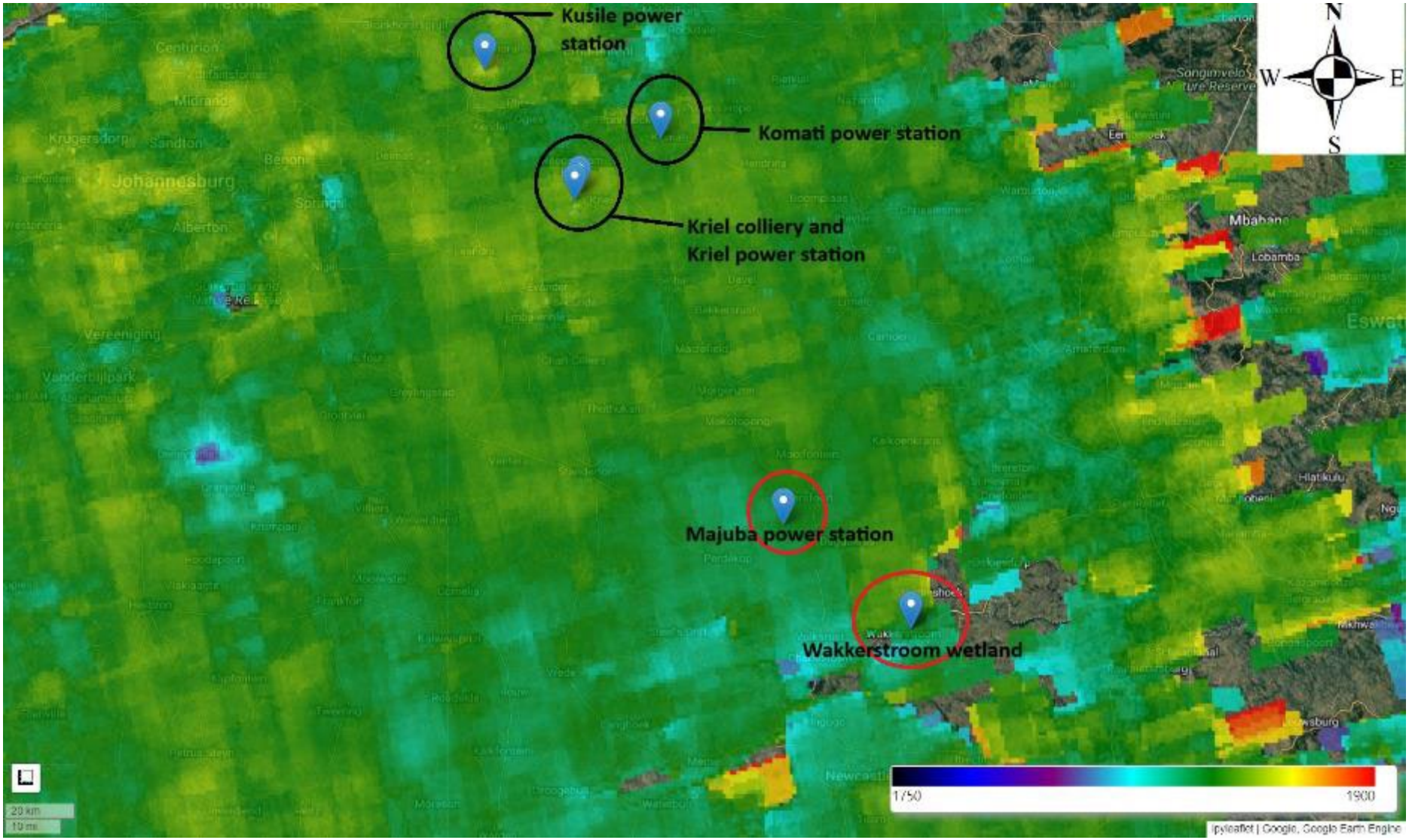


Figure 32: Map produced from TROPOMI total column averaged dry-air mole fraction of methane product (autumn 2023).

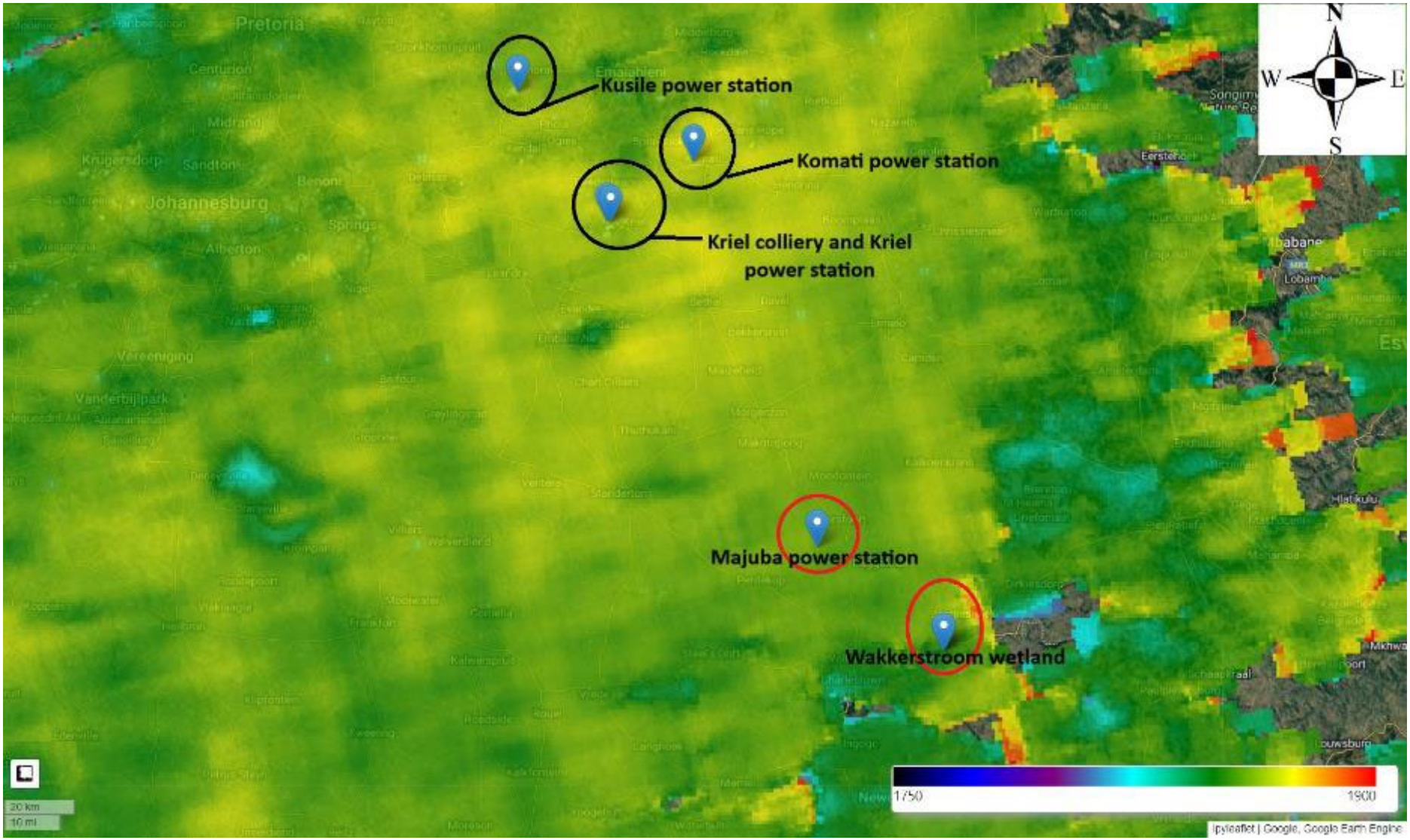


Figure 33: Map produced from TROPOMI total column averaged dry-air mole fraction of methane product (winter 2022).

From the mapping methane using TROPOMI, it is evident that regions with a high total column averaged dry-air mole fraction of methane can be visually identified. The collieries were seen with higher total column averaged dry-air mole fraction of methane in comparison to the power stations. The Wakkerstroom wetland was seen to not show great differences across seasons from the Majuba power station with respect to the total column averaged dry-air mole fraction of methane.

4.7. SECTION C: GAW measurements.

The Cape Point Global Atmospheric Watch station tracks regional changes in Southern African atmospheric composition and is representative of background/baseline conditions of the south Atlantic sector of the Southern Hemisphere. The long-term measurements at the station are important to capture regionally representative air masses. In contrast to short field campaigns, the station is able to capture atmospheric chemistry dynamics from greater spatial and temporal scales.

a) **Objective 4:** Analysis of the reported CH_4 mole fraction (ppb) in maritime (background) air as measured at the Cape Point Global Atmospheric Watch (GAW) station.

The annual data showing the reported mole fraction of CH_4 as measured by the Cape Point GAW station was calculated (Figure 35). The data were also aggregated monthly to assess whether seasonal patterns exist in the reported mole fraction of CH_4 at Cape Point. The GAW mandate is that only background atmospheric levels are of interest. Thus, the filtered (background) data was accessed and graphed monthly for the last 10 years (2014 – 2021) to assess the seasonal changes in the reported mole fraction of CH_4 (ppb) (Figure 34). These years were chosen specifically as instrument malfunction occurred at the station in 2021 leading to unavailability of data. The data show that during the winter season, when influences from local Cape Town conditions and influences from the greater interior of the country reach Cape Point, higher mole fractions of CH_4 are observed. This is in contrast to the other three seasons when the predominant air comes from the greater Southern Ocean and the mole fractions are lower.

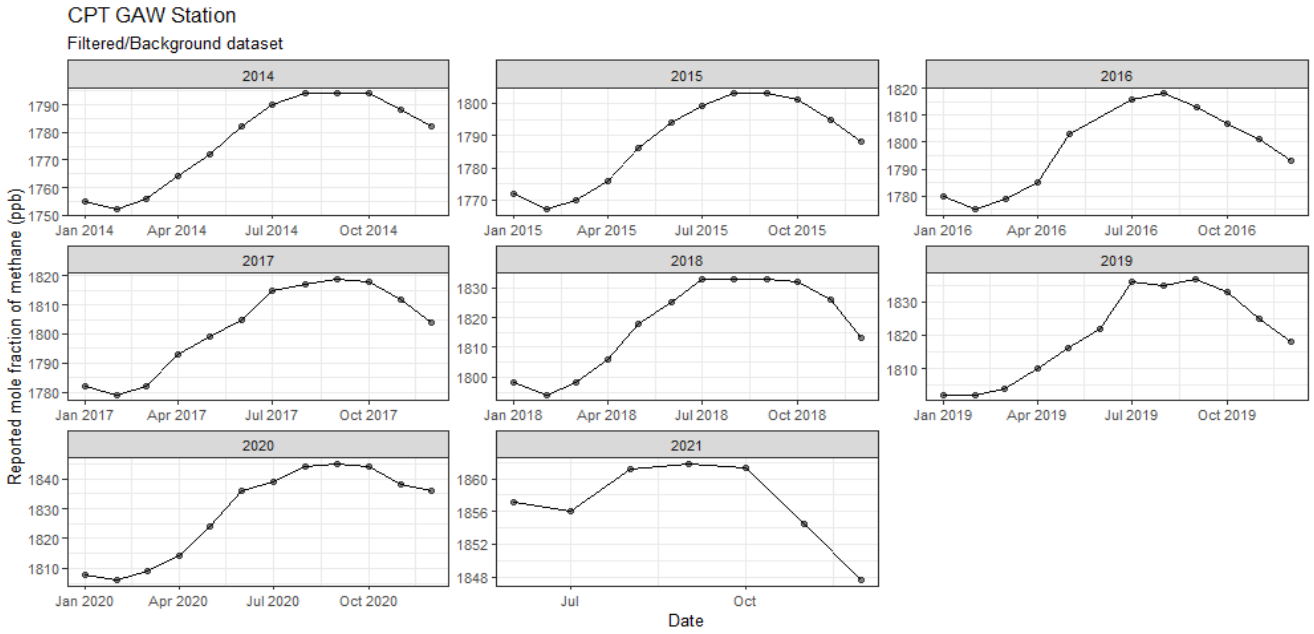


Figure 34: Mean monthly reported mole fraction of CH_4 at Cape Point GAW station during 2014-2021.

4.8. Annual reported mole fraction of CH_4 at Cape Point for 39 years (1983 - 2021).

The reported mole fraction of CH_4 (ppb) was graphed from 1983 -2021. The graph shows that over the entire time period, the mole fraction of CH_4 generally increased. However, it can be seen that the increase was at a higher rate from 1982 – 1990, and then had a slower rate of increase from 1990 – 2000. The trend started to stabilize in the years 2000 – 2010, and after 2010 started to increase at a high rate again. The reported mole fraction of CH_4 at Cape Point showed a great increase over the last 39 years as it went from 1570 ppb in 1983, to around 1856 ppb in 2021.

The Cape Point GAW data was an excellent way to assess the trend in the reported mole fraction of CH_4 of background Southern Hemisphere air masses. An overall increase in CH_4 mole fraction was observed for the Southern African region.

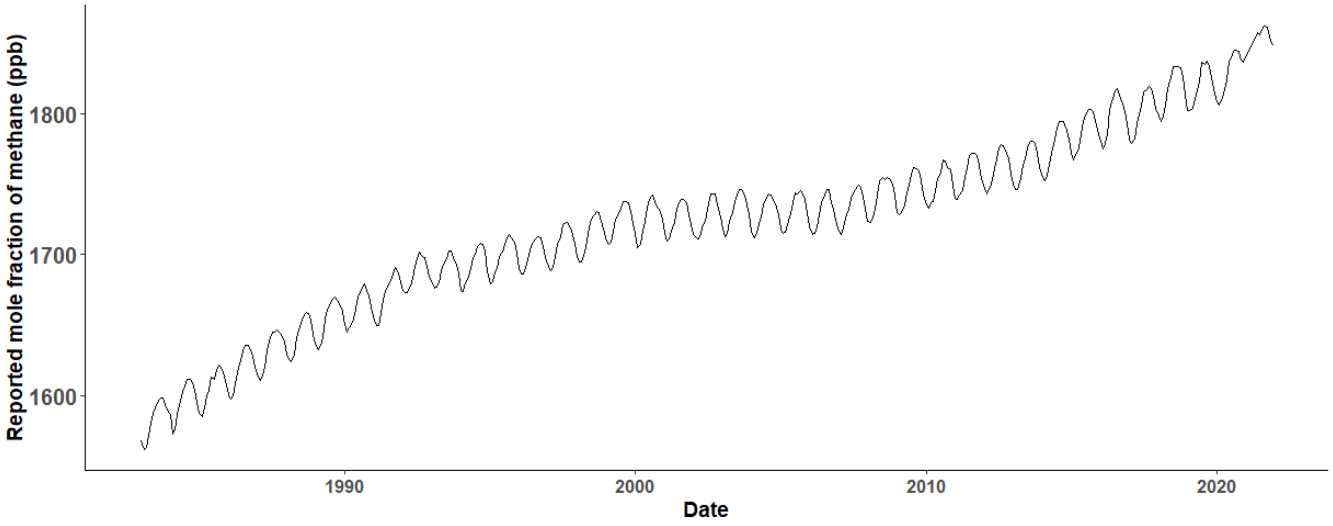


Figure 35:Reported mole fraction of methane (ppb) for each year at Cape Point for the years 1983 – 2021.

The seasonal weather data consisting of, wind roses, temperature, and relative humidity was also accessed from the South African Weather Service (SAWS) for the Cape Point site to aid in understanding the meteorological factors that characterize the environment annually and seasonally. The weather data that was accessible from the SAWS was only for the years 2020 – 2022. To assess whether or not the Cape Point data record possibly gets imprints from the South African interior, backward trajectory analyses were done for the warm summer season and the cold winter season using the HYSPLIT model.

4.9. Wind roses at Cape Point

Wind roses were graphed for all four seasons at the Cape Point GAW station (Figure 36). The wind rose reveals that the prevailing winds at Cape Point during spring predominantly blow from the southeast and east (> 40%). A similar observation is made in summer when the prevailing winds predominantly blow from the east and southeast (> 40%). The autumn wind rose plot also showed a predominant wind direction from the east and southeast (> 30%). The winter wind rose plot had quite a different pattern from the other three seasons in that the prevailing winds predominantly blew from the north and north westerly direction (> 40%). In summary, during spring, summer and autumn, the prevailing winds predominantly blew from the greater Southern Ocean (southeast) in contrast to winter when the prevailing winds predominantly blew from the north and north westerly continental source regions.

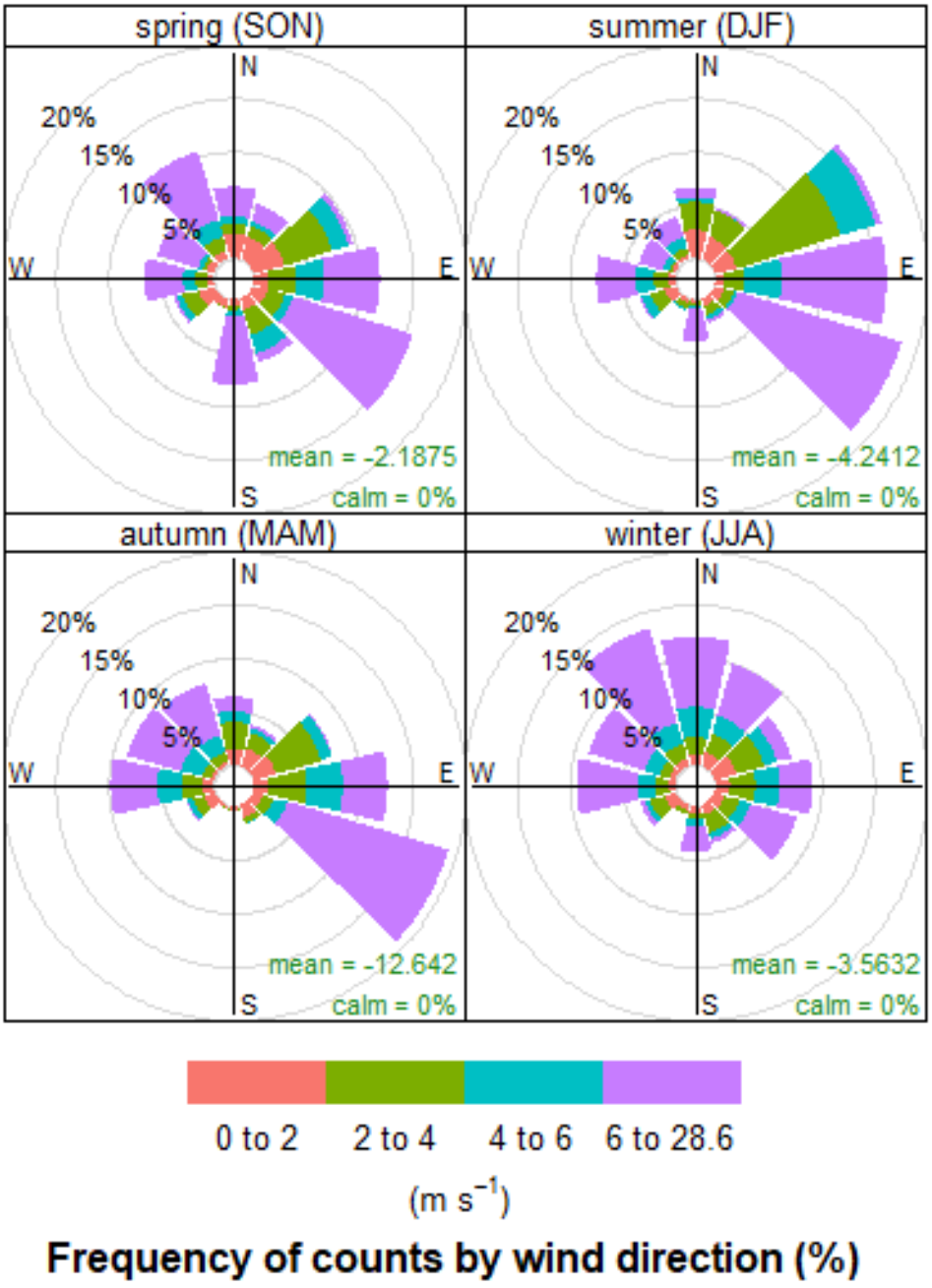


Figure 36: Seasonal wind rose plots for Cape Point GAW station (SON: September, October, November; DJF: December, January, February; MAM: March, April, May; JJA: June, July, August)

The Cape Point data is useful as it represents the southern hemispheric background concentrations of methane.

4.10. Atmospheric transport to Cape Point, South Africa.

The atmospheric transport patterns for Cape Point were computed using the HYSPLIT trajectory model (Figure 37). The trajectory analysis during the summer day (chosen as 20 January 2021) shows that much of the air travelled from the greater Southern Ocean towards Cape Point (Figure 37). On the winter day (chosen as 15 August 2021), much of the air travelled from further north of the City of Cape Town and also north of South Africa. Any polluted air from further north and northeast of the country could have been carried toward Cape Point.

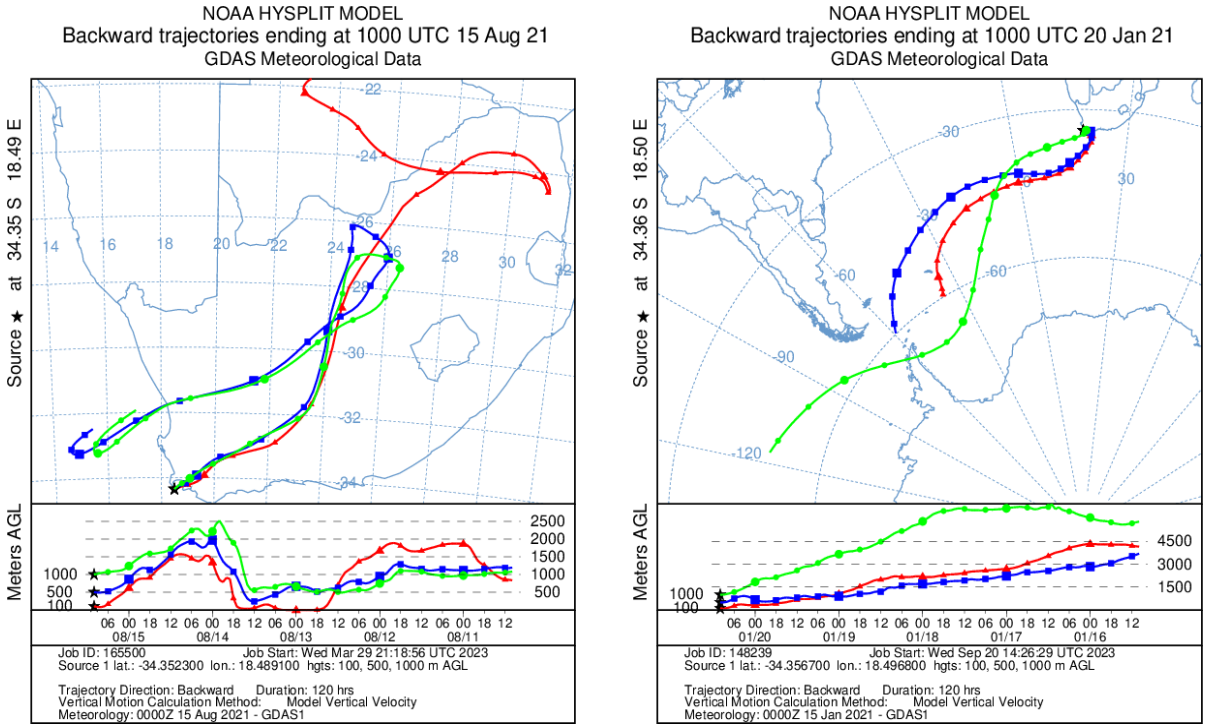


Figure 37: HYSPLIT backward trajectory analysis for the summer (20 January 2021) and winter (15 August 2021) representative days at Cape Point, South Africa.

4.11. Air temperature at Cape Point.

Temperature affects the solubility of gases in water (Britter, 1989; Jansen *et al*., 2022). In maritime air, the proximity to the ocean means that temperature changes can influence the solubility of CH_4 in seawater. When the water temperature rises, it can release CH_4 into the atmosphere, increasing its mole fraction in the surrounding air. For Cape Point then, the air temperature data was accessed and graphed for the years 2020, 2021, and 2022 (Figure 38). The data shows that at Cape Point, the highest temperatures were during the summer months (with highest temperatures between 33.10 °C to 34.20 °C during the summer months of the years 2020-2022) and the lowest temperatures were during the winter months (with lowest temperatures between 6.10 °C – 8.10 °C during the winter months of the years 2020-2022). The red trend line shows the mean monthly temperatures at Cape Point.

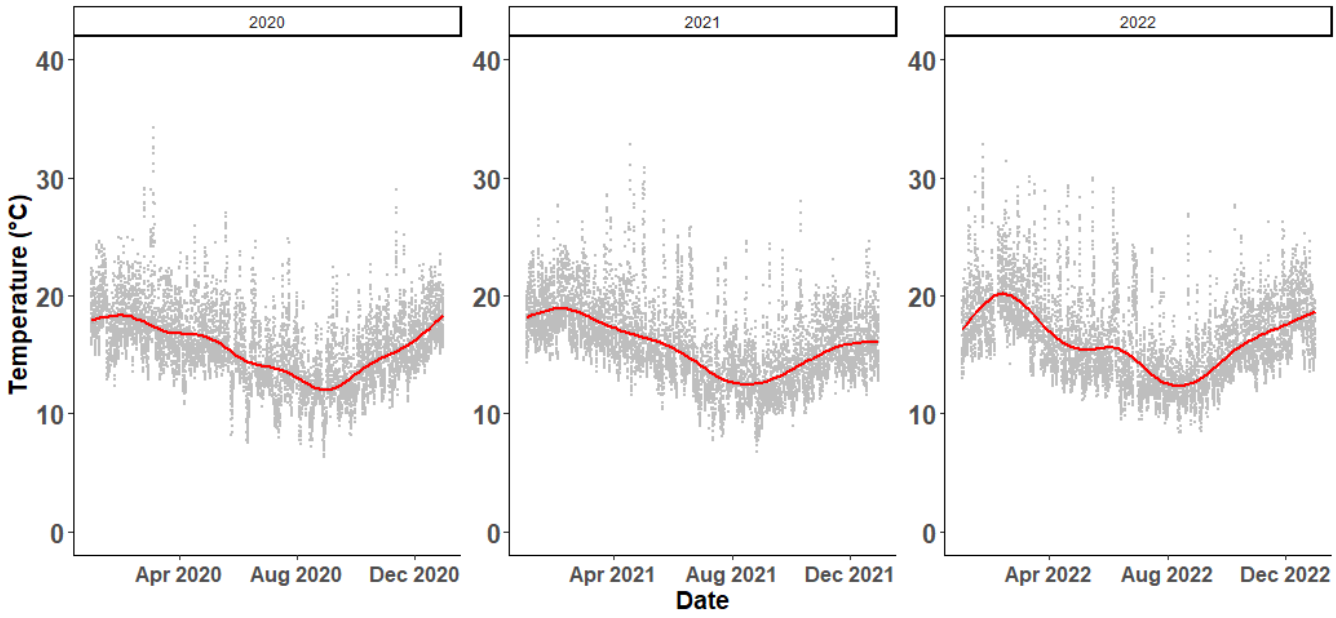


Figure 38:Seasonal air temperature graph for the Cape Point GAW station in Cape Town, South Africa for the years 2020 - 2022**.**

4.12. Relative humidity (%) at Cape Point.

CH_4 is naturally removed from the atmosphere by oxidation reactions involving hydroxyl radicals (OH). High relative humidity and high-water vapour, particularly in the summer, can indirectly influence CH_4 concentrations by altering the abundance and activity of OH radicals.

More water vapor in the air can enhance OH radical production and the subsequent removal of methane, leading to lower methane mole fractions in warmer seasons. The relative humidity seasonal graph was thus plotted for the Cape Point GAW station during the years 2020, 2021, and 2022. and showed that the relative humidity percentage was highest during the spring and summer months (October – February) and lowest during the autumn and winter months (April – September). The red trend line shows the mean monthly relative humidity pattern at Cape Point (Figure 39).

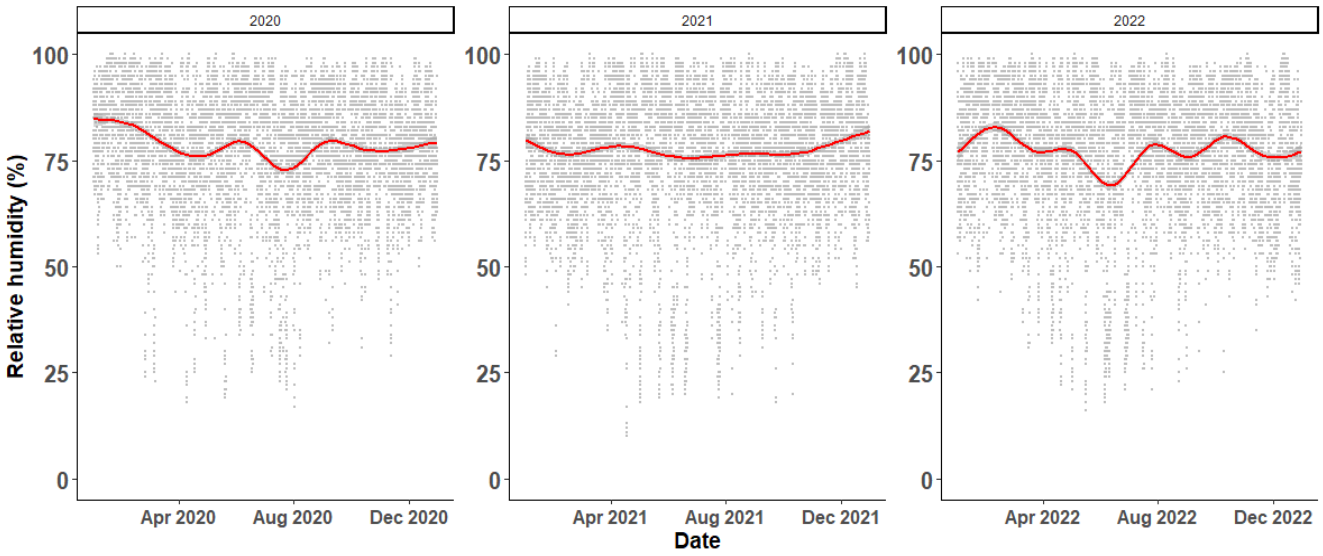


Figure 39: Seasonal/monthly relative humidity (%) patterns at Cape Point GAW station, South Africa.

The GAW data has thus shown an upward trend in CH_4 in its 39-year measurement period. This is an indicator of rising southern African trends in CH_4 mole fractions as maritime (background) air observations track regional changes in Southern African atmospheric composition. In maritime environments such as Cape Point, the complex interactions between temperature, humidity, oceanic processes, atmospheric transport, and regional methane sources and sinks make it challenging to predict the exact relationship between all variables and CH_4 mole fractions. It is thus essential to consider these factors holistically when studying the dynamics of CH_4 in maritime air. Detailed measurements and models are often necessary to understand the specific effects in a given region or under particular conditions.

5. DISCUSSION

Throughout this study, the CH_4 concentrations from Wakkerstroom wetland and Majuba power station have been assessed using various techniques. In this chapter, the results of the study are interpreted in context of the research questions. The significance and implications of the results are further discussed. Additionally, the findings are compared in the context of the literature. Limitations and conclusions are found at the end of this chapter.

5.1. Methane concentrations from the Wakkerstroom wetland and coal stockpile at the Majuba power station.

The aim of this study was to compare CH_4 concentrations from the Wakkerstroom wetland and Majuba power station coal stockpiles. Gas samples from these sites were collected in 3-Litre flexfoil bags, isotopically analysed seasonally, and their isotopic signatures were calculated.

Extensive academic research has been dedicated to the investigation of CH_4 emissions from wetlands. Some studies (Whiting and Chanton, 1992; Van Der Gon and Neue, 1995; Van Der Nat *et al.*, 1998; Otter and Scholes, 2000; Krüger *et al.*, 2012; Schultz and Pett *et al.*, 2018; Yang *et al.,* 2020) have utilized the chamber method to obtain CH_4 flux measurements whereas others have utilized the flexfoil bag method to assess CH_4 concentration measurements (Sriskantharajah *et al.*, 2012; Juszczak and Augustin, 2013; Gatland *et al.*, 2014; Fisher *et al.*, 2017; France *et al.*, 2022a; Shaw *et al.*, 2022) in wetlands. It is worthy to mention that the utilization of different measuring units (flux and concentration) to quantify emissions makes it slightly difficult to compare findings from various studies but allow a comprehensive view of CH_4 emissions.

The Wakkerstroom wetlands total CH_4 concentrations showed slightly lower concentrations in spring (0.383 ± 0.110 ppm), summer (0.429 ± 0.163 ppm), autumn (1.198 ± 0.744 ppm), winter (0.226 ± 0.110 ppm) when compared to the 1.85 – 1.94 ppm range seen at the Fennoscandian Artic wetlands (Fisher *et al.*, 2017), 1.8 – 2.4 ppm range observed at the Finnish subarctic wetlands (Sriskantharajah *et al.*, 2012), 1.9 – 2.4 ppm range seen at the Zambian wetlands (Shaw *et al.*, 2022), and 1.8 – 2.3 ppm range observed at the Bolivian wetlands (France *et al.*, 2022b). These studies (Sriskantharajah *et al.*, 2012; Fisher *et al.*, 2017; France *et al.*, 2022b; Shaw *et al.*, 2022) form part of those that utilised the flexfoil bag technique to quantify CH_4 concentrations as done in this study.

Factors such as the presence of varied vegetation communities and environmental variables such as water depth and weather play a role in the diffusion of CH_4 from wetlands. The

composition and structure of various vegetation communities play a crucial role in CH_4 concentrations in wetland ecosystems. There were three identified plant species at the Wakkerstroom wetland, each with unique vascular gas transport systems. Ground measurements showed that for three out of the four seasons, the *Phragmites* vegetation community at the Wakkerstroom wetland had the highest CH_4 concentration [spring (0.209 ± 0.076 ppm), autumn (0.537 ± 0.239 ppm), and winter (0.132 ± 0.065 ppm)] when compared to all other vegetation communities and coal stockpiles at the Majuba power station. These observations could be a result of gas transport of *Phragmites australis,* which has been stated to be notably efficient (van den Berg *et al.*, 2016; Kim *et al.*, 2020; van den Berg *et al.*, 2020). *Phragmites* generates a pressure gradient within the leaf sheaths, driven by humidity, resulting in airflow from the leaf sheaths to the rhizomes. Expelled through old and damaged stems, this airflow is controlled by stomata in the leaf sheaths and occurs more than five times faster than diffusion (Armstrong and Armstrong, 1991; Afreen *et al*., 2007; van den Berg *et al*., 2020). These stomata allow gas to move through diffusion, even though pressure differences prevent gas from moving. O_2 and N_2 concentrations are diluted by the increased humidity in the internal culm, which leads them to migrate from the atmosphere into the sheaths and increase internal pressure. This process begins after sunrise, peaks at noon with optimal photosynthetic rates, and decreases by sunset. It is dependent upon stomatal conductance. CH_4 concentrations from *Phragmites* wetlands during the growing season are indicative of these 24-hour cycles. *Phragmites* helps move O_2 into the soil, which improves CH_4 oxidation, but, it also helps move CH_4 from the soil to the atmosphere, avoiding the oxic soil-water layer (Figure 40).

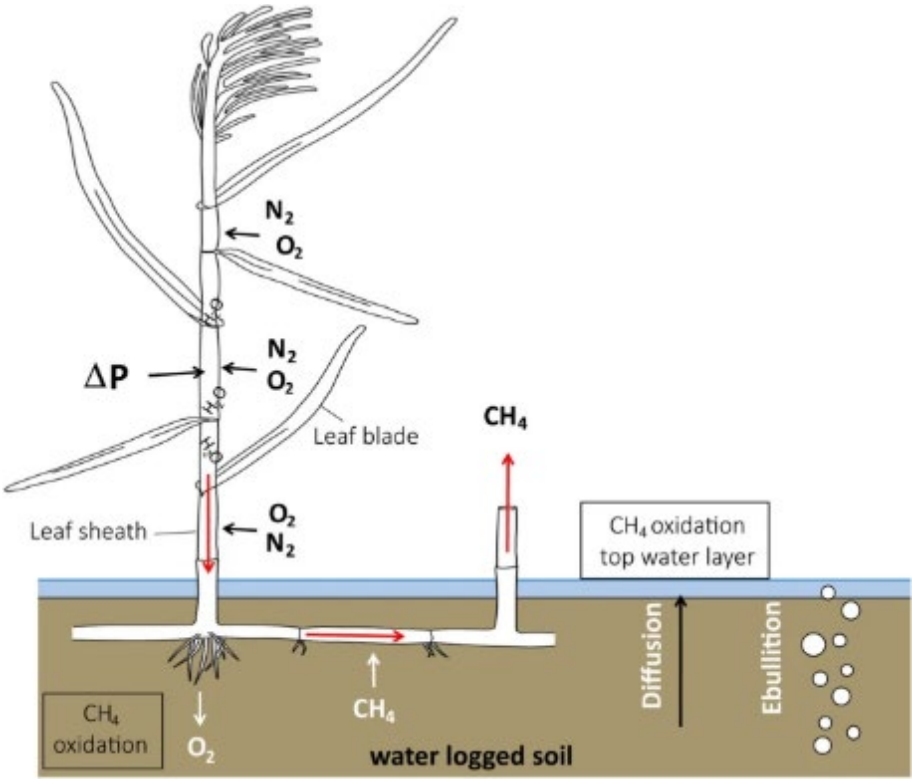


Figure 40: Diagram illustrating humidity-induced convection in *Phragmites* plants (van den Berg *et al.*, 2020). N_2 and O_2 move through stomata in the leaf sheath, driven by the diffusion gradient. Living plants generate higher pressure in the stem (ΔP), causing airflow towards the rhizome, venting through old and damaged stems (red arrows). O_2 is conveyed to the soil, while CH_4 diffusing into the rhizome is transported to the atmosphere. Where O_2 and CH_4 coexist, CH_4 oxidation takes place.

The results of this study can be analysed alongside those of Inamori *et al.* (2007), who found lower CH_4 fluxes (summer = 25 $mg.m^2.h^{-1}$, autumn = 10 $mg.m^2.h^{-1}$, winter = 9 $mg.m^2.h^{-1}$, spring =20 $mg.m^2.h^{-1}$) from *Phragmites* seasonally when compared to *Zizania. latifolia* (summer = 35 $mg.m^2.h^{-1}$, autumn: 20 $mg.m^2.h^{-1}$, winter = 9 $mg.m^2.h^{-1}$, spring= 65 $mg.m^2.h^{-1}$). Although the authors measured methane fluxes and not methane concentrations, their findings can be compared to this study as these are closely related concepts. The authors stated that *Phragmites* tends to reduce the activity of CH_4-producing bacteria due to its complex, deep root zone that oxidizes CH_4 to a greater depth when compared to *Z. latifolia's* shallow root system whereby the primary location of methanotroph activity is predominantly at the upper section of the soil (Inamori *et al.*, 2007). At the Wakkerstroom wetland however, *Phragmites* having the highest observed CH_4 concentration could potentially indicate that its root system rather promoted the activity of CH_4-producing bacteria. Varying environmental conditions such

as soil temperature, pH, and root systems of *Phragmites* could be a strong regulator of CH_4 concentrations from *Phragmites* (Inamori *et al.*, 2007; van den Berg *et al.*, 2020) and could have led to the CH_4 concentrations observed at the Wakkerstroom wetland.

Methane concentrations from *Typha Capensis* were also assessed in this study. In a study, Whiting and Chanton (2001) found CH_4 fluxes from *Typha latifolia* dominated wetlands to be lower (4.3 – 6.8 $mol.m^{-2}.yr^{-1}$) than those from *Peltandra virginica* (6.8 – 11.0 $mol.m^{-2}.yr^{-1}$). One of the research questions in this study was to assess how the water depth affected the observed CH_4 concentration at the Wakkerstroom wetland. The water depths of "*Typha* water" and "water *Phragmites"* was 50 cm above the soil surface. The effect of water depth was found to be negligible in our study during autumn because when "water *Phragmites"* (0.537±0.239 ppm) was compared to "*Phragmites"* on the wetland bank (0.416±0.269 ppm) no significant differences in terms of CH_4 concentrations were found, and when "*Typha* water" (0.111±0.110 ppm) was compared to "*Typha"* on the wetland bank (0.055±0.038 ppm) again no significant differences were found in terms of CH_4 concentration. The exception occurred in winter when "water *Phragmites*" (0.032±0.008 ppm) was significantly lower than "*Phragmites*" on the wetland bank (0.132±0.065 ppm). In both autumn and winter seasons however, the *Phragmites* community had a significantly higher CH_4 concentration when compared to "*Typha* water*"* and *"Typha"* on the wetland bank.

The results of this study during autumn are in agreement with Otter and Scholes (2000) who found that CH_4 concentrations for dry (water level > 10 cm below the soil surface) and moist (water level > 40 cm above the soil surface) floodplains had no significant differences. The results of this study can further be compared alongside the findings made by Were *et al.* (2021), who found that during the dry season-winter (Feb, March and April), CH_4 fluxes from *Typha* (13.5 ± 1.2 $mg.C.m^{-2}.h^{-1}$) were significantly higher ($p < 0.05$), than those observed from *Phragmites* (8.7 ± 0.5 $mg.C.m^{-2}.h^{-1}$). The results of this study showed the opposite of those by Were *et al.* (2021) because in the dry season- winter, CH_4 concentrations from "water *Phragmites*" were significantly higher than both "*Typha* water" and *Typha* on the wetland bank. The observation of a significant difference in CH_4 fluxes during the dry season was attributed to water level (Were *et al.*, 2021). In the dry season, the water level within the *Phragmites* vegetation community was markedly lower (1.9 ± 0.8 cm) compared to the *Typha* vegetation community (7.1 ± 3.2 cm). The water depth at which plants were rooted as reported by Were *et al.* (2021) was lower than that at which plants were rooted at Wakkerstroom (50 cm) which could have led to the contrasting results. However, results by Lawrence *et al.* (2017) had similar

levels to the water levels assessed at the Wakkerstroom wetland. Lawrence *et al.* (2017) showed that under high water levels (level greater than 10 cm above the soil surface), *Typha glauca* CH_4 fluxes were triple (mean: 45.9 ± 16.7 mg.CH_4-C.m^{-2}.h^{-1}) that of native wet meadow vegetation (15.0 ± 10.5 mg CH_4-C.m^{-2}.h^{-1}) indicating a definite impact of water level on *Typha* CH_4 fluxes. The water depth in wetland ecosystems thus can be stated to play a role in CH_4 emissions, but this differs in various individual wetlands according to exactly how deeply rooted the plants are. High water levels enhance soil anaerobicity by filling soil pore spaces, as documented by Marín-Muñiz *et al.* (2015). Subsequently, under anaerobic conditions, methanogenesis is promoted, leading to increased CH_4 emissions (Brooker *et al.*, 2014).

The Majuba power station coal stockpiles had the lowest CH_4 concentrations for three out of four seasons, [summer (0.022 ± 0.021 ppm), autumn (0.014 ± 0.053 ppm), and winter (0.002 ± 0.004)] when compared to the vegetation communities at the Wakkerstroom wetland. Studies on CH_4 concentrations from coal stockpiles are limited (Kozinc *et al.*, 2004; Zhang, 2013). The results of this study are in agreement with Kozinc *et al.* (2004) who measured CH_4 concentrations at the Velenje coal stockpiles, their results indicate that, aside from June and July 2001, the concentration of CH_4 was typically below the quantification limit (< 100 ppm). In their study, Kozinc *et al.* (2004) further emphasized that in circumstances where the coal utilized has a greater CH_4 content, the desorption process is primarily responsible for CH_4 concentrations from a coal power station. Coal is frequently stockpiled after mining before being utilized to generate electricity, and stockpiles may produce favourable circumstances for CH_4 desorption - lower pressures and high temperatures (Kozinc *et al.,* 2004; Zhang, 2013), resulting in CH_4 to escape from the coal matrix (Kozinc *et al.,* 2004; Zhang, 2013) and could serve as the explanation for CH_4 concentrations observed at Majuba power station.

The meteorological data showed high temperatures in the summer seasons particularly the months of January and February, and the lowest temperatures in the winter season, particularly June and July at the Wakkerstroom wetland. Since sampling was done during the afternoon (13h00 – 17h00) on the sampling days when temperatures and production at the wetland were at their peak, it is possible that temperature affected the CH 4 measurements by stimulating microbial enzyme activity as observed by other studies (Inglett *et al*, 2012; Yavitt et al., 2019). Persistent high temperatures, in the spring and summer seasons particularly, may have also influenced lability of available carbon from plant litter at each of the wetland, affecting CH_4 production.

5.2. Source carbon isotopic signatures in CH_4 ($\delta^{13}CH_4$) at the Wakkerstroom wetland and Majuba power station coal stockpiles.

The CH_4 concentration measurements were crucial in that they were utilised to calculate the source isotopic signature of each site seasonally using the Keeling plot method. When comparing the source isotopic signatures of the two sites, the Wakkerstroom wetland had an overall signature that was consistently light, ^{13}C depleted isotopic signatures seasonally ranging between -61.4 ‰ to -55.6 ‰. In contrast to this, the Majuba power station had inconsistent isotopic signatures through the sampling seasons - heavier isotopic signatures with ^{13}C enrichment during spring and summer at -35.3 ± 1.0 ‰ and -43.5 ± 3.5 ‰ respectively, and lighter signatures with ^{13}C depletion during autumn and winter of -62.0 ± 1.6 ‰ and -87.0 ± 10.3 ‰ respectively.

The isotopic signatures of the Wakkerstroom wetland are similar to those reported by MOYA/ZWAMPS Team *et al.* (2022) showing that emissions from the equatorial Nile wetlands and the agricultural regions ranged from -55 to -49 ‰, and from the Upper Congo and Zambezi wetlands were around -60 ± 1 ‰. MOYA/ZWAMPS Team *et al.* (2022) attributed their findings to plant metabolic pathways, within different plant functional types. The metabolic composition of the local vegetation plays a crucial role in generating unique isotopic signatures ($\delta^{13}CH_4$) at the regional level. In warm tropical grasslands, farms, and wetlands, the prevalence of C_4 plants such as maize, sugar, papyrus, and various pastoral grasses contributes to higher carbon content enriched in ^{13}C (Fisher *et al.*, 2017). In contrast, trees, bushes, and vegetation such as reeds with C_3 metabolisms exhibit significant discrimination against ^{13}C (MOYA/ZWAMPS Team *et al.* 2022). This distinction in plant metabolic pathways significantly influences the isotopic composition of CH_4 and could have led to the observed ^{13}C depleted isotopic signatures seen at the Wakkerstroom wetland since the vegetation communities (*Typha* and *Phragmites*) consist of a C_3 metabolic pathway. *Phragmites* utilises the C_3 photosynthetic pathway (Hough and Wetzel, 1977; Mal and Narine, 2004; Kiviat, 2013; Get *et al.*, 2014), although its photosynthetic rates and the existence of mature chloroplasts in the bundle sheath exhibit some similarities to the C_4 pathway (Antonielli *et al.*, 2002; Milke *et al.*, 2020; Srivastava *et al.*, 2014; Raghuvanshi *et al.* 2023). *Typha* is also a C_3 monocot that inhabits both brackish and freshwater tidal marshes (Farnsworth and Meyerson, 2003; Jones, 1988; Schweingruber *et al.*, 2020; Musara and Aladejana, 2020). The results of this study also differ with France *et al.* (2022a) who showed that $\delta^{13}CH_4$ signature of papyrus-rich tropical wetlands in Uganda had a bulk wetland signature of about -52 ± 2 ‰. They also attributed their

findings to the prevalence of C_4 plants which are associated with ^{13}C enriched isotopic signatures, as opposed to the C_3 vegetation prevalent at the Wakkerstroom wetland. In their study, France *et al.*, (2022a) further stated that variations in source isotopic signatures seasonally can also be related to differences in CH_4 production mechanisms. Greater amounts of ^{13}C-enriched CH_4 are anticipated in settings where acetoclastic methanogenesis is prevalent, while environments characterized by nutrient scarcity, where CO_2 reduction (hydrogenotrophic methanogenesis) is dominant, are likely to exhibit more ^{13}C depleted CH_4. However, wetland isotopic signatures generally range between -80 ‰ to -40 ‰ as reported by Moritz Schroll *et al. (*2020) and the Wakkerstroom wetland fell with this range.

The source isotopic signatures from coal mines are more widely reported in literature than signatures from coalbeds/coal stockpiles but the two cannot be directly compared as these are two distinct coal environments. The source isotopic signatures of the Majuba power station coal stockpiles were however slightly similar with those by Zazzeri *et al.* (2016), who found that the source isotopic signatures in deep and anthracite opencast mines ranged between -40 and -30 ‰. The isotopic composition of CH_4 generated during the coalification process is influenced by the methane's origin pathway (Whiticar, 1996). The thermogenic generation of CH_4 from coal takes place during the coalification process, where rising temperature and pressure lead to the devolatilization of CH_4, CO_2, water, and other gases from the coal. Thermogenic CH_4 has a higher isotopic enrichment in ^{13}C ($\delta^{13}C > -50$ ‰) compared to biogenic methane because methanogens preferentially utilize the lightest isotopes due to the lower bond energy (Rice, 1993). This could be one of the factors that led to the observed isotopic signatures at Majuba power station particularly during spring and summer when signatures were ^{13}C enriched compared to the lighter signatures of the Wakkerstroom wetland. However, Rice (1993) demonstrated, based on information from Australian, Chinese, and German coalbeds, that shallow coalbeds generally have CH_4 with a comparatively lighter isotopic composition compared to deeper ones. When meteoric water intrudes, secondary biogenic methane, characterized by a lighter isotopic signature, can be produced and blend with the thermogenic gas previously generated. During autumn and winter, temperatures are generally lower, leading to reduced evaporation rates. This means that any meteoric water that infiltrates the coal stockpile is more likely to remain there, potentially increasing the moisture content of the coal. This could have also been the explanation for the lighter isotopic signatures at the Majuba power station particularly during autumn and winter seasons. Coal isotopic signatures generally

range between -40 ‰ and -30 ‰ as reported by Moritz Schroll *et al.* (2020), however in this study the results from Majuba did not fit into this range.

There are other factors that could have affected the isotopic signatures (and even the CH_4 concentration) of coal from the Majuba power station. The first factor considered was the presence of coal trucks to continuously stockpile the coal. On some sampling days, there were many trucks (spring and summer) as seen in figure 3, which could lead to the assumption that there was coal being stockpiled during the time of sampling. However, on other days, there were none which could have affected the observed concentrations of CH_4 at Majuba power station and subsequently the source signatures (since signatures are calculated from the concentrations). The downwind location of sampling at the Majuba power station varied depending on wind direction (1.71 km from the stockpile in spring, 6.8 km from the coal stockpile in summer, 2.65 km from the stockpile in autumn). Wind can disperse CH_4 emissions, causing the emissions to rapidly dissipate and reduce in terms of concentration levels at the sampling collection point especially if the gas is allowed to spread over a wide area. Lastly, as we had to measure from a distance, other biological features (grasslands and small streams/wetland) between the stockpile and the sample points could have led to the mixed signal in observed signature of the coal.

5.3. Satellite based measurements of CH_4 mole fractions using TROPOMI.

On a higher spatial and temporal scale, this study compared TROPOMI measurements of CH_4 mole fractions from the emission sites (Wakkerstroom wetland region and Majuba power station) for the period 1 August 2022, to 31 July 2023. For this selected time period, no significant differences were found between the Wakkerstroom wetland (1855.4 ± 18.0 ppb) and Majuba power station (1857.1 ± 22.9 ppb) in terms of the total column averaged dry-air mole fraction of methane. The results are similar to those found by Karoff and Vara-Vela (2023) who reported total column averaged dry-air mole fraction of methane for each continent in terms of land cover type. Africa's permanent wetlands and water bodies were reported to be at 1852 ppb and 1861 ppb respectively whilst urban/built up lands were at 1853 ppb. They substantiated their findings by stating that the limited spatial resolution of total column averaged dry-air mole fraction of methane observations from TROPOMI may result in the exclusion and inaccurate reporting of numerous small permanent wetlands from the assessed wetlands. The Wakkerstroom wetland also had limitations in terms of spatial resolution as it was too small in size (only a few pixels on TROPOMI) for accurate detection and measurement by TROPOMI

– thus measurements taken were not only of the wetland but also included the larger area surrounding the wetland in Wakkerstroom which could have affected the recorded total column averaged dry-air mole fraction of methane. This limitation also existed with TROPOMI measurement over the Majuba power station.

When observing results of wetlands in South Sudan, the lowest mole fractions were at 1050 - 2600 ppb and the highest mole fractions at 1870 - 2930 ppb (Pandey *et al.*, 2022). They found the lowest mole fractions during the season with the highest precipitation and lowest temperatures (June, July, August) and propose that temperature could exert a more significant influence on mole fractions from the wetlands in South Sudan. The measurements in the study by Pandey *et al.* (2022) were higher than those seen at the Wakkerstroom wetland. The disagreement in measurements could be due to the Wakkerstroom wetland being in a temperate climate and not a tropical zone and temperatures are not as high to lead to the higher mole fractions of CH_4 observed in Sudanese wetlands (Zeleke *et al.*, 2024).

TROPOMI allows CH_4 measurements in locations that are difficult to access physically. To the best of our knowledge, there are currently no studies using TROPOMI to measure CH_4 from coal stockpiles specifically, and this could be due to the spatial resolution limitation. On a national scale however, the results of this study are in agreement with Shikwambana *et al.* (2022) who found that the interior and northern regions of South Africa had concentrations of CH_4, ranging between 1826–1850 ppb which are the locations where power stations are located as well. However as seen in figure 31 and figure 32, collieries had higher total column averaged dry-air mole fraction of methane than the Majuba power station. The greater CH_4 mole fractions from coal mines compared to coal power stations can be attributed to the inherent presence of methane in coal deposits. Mining operations release this CH_4 into the air, as it is commonly trapped within coal seams during geological processes. Extraction activities, particularly in deeper coal seams, can lead to the substantial release of CH_4 when coal is mined.

TROPOMI's global coverage, frequent observations, and ability to capture large-scale patterns contribute significantly to our understanding of CH_4 concentrations in the atmosphere, however there are limitations that should be considered when dealing with data from this satellite instrument. TROPOMI assessed the differences in mole fractions from the entire Wakkerstroom wetland and Majuba power station tropospheric columns. This vertical averaging makes it difficult to differentiate between emissions occurring near the surface and those at higher elevations within the troposphere. For example, emissions from the coal

stockpiles near the surface of the Majuba power station may mix with biogenic emissions from vegetation or ruminants, and TROPOMI might observe an integrated signal without the ability to attribute it to specific sources.

5.4. Cape Point GAW CH_4 data.

Methane data from the Cape Point GAW station is an extensive and unique resource that provides in-depth understanding of trends and atmospheric concentrations of CH_4. This study had an objective to assess the trends in the reported mole fraction of CH_4 in maritime (background) air as measured at the Cape Point GAW station. Long-term monitoring of the composition of atmospheric trace gases is made possible by the observational continuity at Cape Point. Long-term datasets, like those from the Cape Point GAW station, are essential for identifying patterns and modifications that take place over protracted periods of time and offer important insights into how the climate is changing on Earth.

Over the 39-year period, the results showed an increasing trend in the reported mole fraction of CH_4 (in ppb) as measured at the Cape Point GAW station with the highest mole fractions observed during the cold winter months (July - September) and lowest mole fractions observed in the spring and summer months (November – April). Lower CH_4 mole fractions were observed during the summer months (November to April) as this is when strong winds from the southeast to the southwest buffet the Cape Peninsula and the air is mostly clean maritime (Preston-Whyte and Tyson, 1988). On the other hand, during the winter months, when the primary wind direction shifts and the north westerly winds carry the pollution from the city of Cape Town southward (Preston-Whyte and Tyson, 1988), greater CH_4 mole fractions were recorded. The results of the trend in mole fraction of CH_4 at Cape Point further showed a large deviation in 2016 in both the annual and monthly graphs, followed by similar winter-time deviations in 2019 and 2020. While this phenomenon is not yet fully understood and currently still under investigation, it might be associated with an undefined local source near the station too. The results of our study can be compared to those from other GAW stations in different continents. Fang *et al*. (2013) observed an increase in CH_4 mole fractions of 77 ± 35 ppb at the Lin'an WMO GAW stations in China. The authors stated surface winds as an enhancer to the observed mole fractions, particularly because Lin'an is situated in an economically developed region. Surface winds play a crucial role in the mole fractions of methane.

The transport of atmospheric of a gas is influenced by its atmospheric residence time. A trace gas such as CH_4 with a long atmospheric lifetime of approximately 10 years could have major transport effects. Since the inter-hemispheric exchange is approximately one year and CH_4 atmospheric residence time is longer than this, if there are emission pulses from the Northern Hemisphere these emissions can be detected in the GAW records at Cape Point causing high mole fractions of CH_4 to be observed (Preston-Whyte and Tyson, 1988; Labuschagne *et al.*, 2018). Atmospheric transport effects were shown by the HYSPLIT backward trajectory analysis done for the one winter and one summer day. Microbial and fossil fuel emissions through emission sources like the Wakkerstroom wetland and Majuba power station might also have a small but noticeable imprint on the Cape Point record through atmospheric transport effects.

At the WLG GAW station in Eurasia, China, Liu *et al*. (2021) reported in a study that atmospheric CH_4 levels exhibited a primarily constant ascent. The average CH_4 mole fraction was just 1799.0±0.4 ppb in 1994. By 2019, however, it had increased by almost 133 ppb to a record high of 1932.0±0.1 ppb. Seasonal averages of CH_4 levels at WLG (from 1994 to 2018) were shown, with summer having the highest levels (1861.7±0.4 ppb), winter coming in second (1856.7±0.3 ppb), autumn coming in third (1855.9±0.4 ppb), and spring coming in fourth (1853.1±0.3 ppb). These seasonal results by Liu *et al.* (2021) are slightly higher than those from the Cape Point GAW station which were around 1825 ppb in 2021. However, seasonal analysis at GAW showed higher CH_4 mole fractions in winter months and not summer as presented by Liu *et al.* (2021). The lower CH_4 mole fraction in summer is at times a result of more oxidation of CH_4 by the hydroxyl (OH) radical when there is more ultraviolet (UV) radiation producing more OH (Dorn *et al.*, 1988).

5.5. Limitations and suggestions for future work.

- In this study, daytime ground measurements were recorded at a particular day in each season for each vegetation community. Future studies should investigate diurnal patterns of CH_4 concentrations to understand how environmental factors such as temperature, water level, and microbial activity influence CH_4 release. Continuous measurements over 24-hour cycles and across different seasons can provide valuable data on temporal variability.
- Explore advanced monitoring techniques such as drone-based monitoring, or sensor networks for continuous and real-time ground monitoring of CH_4 concentrations from the wetland and coal stockpiles. These techniques can provide an integrated signal and valuable insights into emission patterns and trends of CH_4 from the wetland coal stockpiles throughout the day.
- It was difficult to deduce whether meteorological conditions had noticeable effects on CH_4 concentrations as air temperatures data was assessed and not soil temperature and associated soil conditions such as pH levels. Future studies should consider variables in pH and soil temperature in analyses.

6. CONCLUSION

This study showed that differences exist between CH_4 concentrations from the microbial source-the Wakkerstroom wetland and the anthropogenic source - the Majuba power station. The two sources' methane concentrations differed, indicating probable differences in the size of concentrations, as well as their isotopic signatures. The *Phragmites* vegetation community at the Wakkerstroom wetland was responsible for the highest CH_4 concentration for three of four seasons whereas coal stockpiles at the Majuba power station had the lowest concentrations. Wetlands dominated by *Phragmites australis* could emit more CH_4 than *Typha* dominated wetlands. The Wakkerstroom wetland had consistently light, ^{13}C depleted isotopic signatures seasonally ranging between -61.4 ‰ to -55.6 ‰, when compared with the Majuba power station which had inconsistent isotopic signatures through the sampling seasons with heavier isotopic signatures with ^{13}C enrichment during spring and summer at -35.3 ± 1.0 ‰ and -43.5 ± 3.5 ‰ respectively, and lighter signatures with ^{13}C depletion during autumn and winter of -62.0 ± 1.6 ‰ and -87.0 ± 10.3 ‰ respectively.

This study revealed that both satellite (TROPOMI) and ground measurement methods are useful for an improved understanding of methane concentrations. Combining these two approaches enhances the accuracy and effectiveness of the analysis, addressing limitations in temporal frequency and spatial coverage associated with ground sampling. While ground measurements offer detailed insights into specific locations, such as concentrations from wetland vegetation communities or coal stockpiles at Majuba power station, TROPOMI provides broader spatial coverage and temporal monitoring capabilities. However, TROPOMI may have less single-source point accuracy. To overcome these challenges and improve source identification, researchers should use complementary data and methods, including ground-based measurements and satellites with higher spatial resolution. Integrating these diverse data sources provides a more thorough understanding of CH_4 emissions. Furthermore, since the trend in the CH_4 mole fraction as measured at the Cape Point GAW station over the 39-year period is seen to be rising, there is a requirement for the direct monitoring of fossil fuel and microbial sources such as wetlands to be assessed for their CH_4 emissions and effects on the atmospheric chemistry signature.

Methane is a highly effective greenhouse gas, possessing a considerably higher Global Warming Potential than CO_2 over shorter durations. This indicates that methane has a greater capacity to retain heat in the atmosphere, resulting in a more pronounced contribution to global warming per unit of mass compared to carbon dioxide within a particular timeframe. Hence, mitigating methane emissions can result in more immediate and substantial reductions in the pace of global warming, due to the greater warming potential of methane than carbon dioxide. To mitigate CH_4 emissions, studies such as this one that are multifaceted in measurement methods and provide comprehensive assessments of CH_4 emissions are vital. This is crucial particularly in South Africa where CH_4 emissions studies are limited.

7. REFERENCES

Abbass, K., Qasim, M. Z., Song, H., Murshed, M., Mahmood, H., & Younis, I., 2022. A review of the global climate change impacts, adaptation, and sustainable mitigation measures. *Environmental Science and Pollution Research*, 29(28), 42539-42559.

Adams, J. B., & Bate, G. C., 1999. Growth and photosynthetic performance of *Phragmites australis* in estuarine waters: a field and experimental evaluation. *Aquatic Botany*, 64(3-4), 359-367.

Afreen, F., Zobayed, S. M. A., Armstrong, J. & Armstrong, W., 2007. Pressure gradients along whole culms and leaf sheaths, and other aspects of humidity-induced gas transport in *Phragmites australis*. *Journal of experimental Bot*any 58, 1651–1662.

African Development Bank., 2022. Methane in Africa – A high-level assessment of anthropogenic methane emissions in Africa with case studies on potential Evolution and abatement. Available at:https://www.afdb.org/sites/default/files/documents/publications/afdb_-_methane_in_africa.pdf. Accessed: 12 February 2024.

AK-BHD, M., 2021. WMO Greenhouse Gas Bulletin. *World Meteorological Organization: Geneva, Switzerland*.

Antonielli, M., Pasqualini, S., Batini, P., Ederli, L., Massacci, A. and Loreto, F., 2002. Physiological and anatomical characterisation of *Phragmites australis* leaves. *Aquatic Botany*, *72*(1), 55-66.

Antonijević, D., Hoffmann, M., Prochnow, A., Krabbe, K., Weituschat, M., Couwenberg, J., Ehlert, S., Zak, D. and Augustin, J., 2023. The unexpected long period of elevated CH_4 emissions from an inundated fen meadow ended only with the occurrence of cattail (*Typha latifolia*). *Global change biology*, *29*(13), 3678-3691.

Armstrong, J. & Armstrong, W., 1991. A convective through-flow of gases in *Phragmites australis (Cav.) Trin. ex Steud*. *Aquat*ic *Bot*any, 39, 75–88.

Armstrong, J. & Armstrong, W., 1990. Light-enhanced convective throughflow increases oxygenation in rhizomes and rhizosphere of *Phragmites australis (Cav.)Trin. ex Steud*. *New Phytologist Foundation*, 114, 121–128.

Bakkaloglu, S., Lowry, D., Fisher, R.E., France, J.L. and Nisbet, E.G., 2021. Carbon isotopic characterisation and oxidation of UK landfill methane emissions by atmospheric measurements. *Waste Management*, 132, 162-175.

Bakkaloglu, S., Lowry, D., Fisher, R.E., Menoud, M., Lanoisellé, M., Chen, H., Röckmann, T. and Nisbet, E.G., 2022. Stable isotopic signatures of methane from waste sources through atmospheric measurements. *Atmospheric Environment*, 276, 119021.

Bandh, S. A., Shafi, S., Peerzada, M., Rehman, T., Bashir, S., Wani, S. A., & Dar, R., 2021. Multidimensional analysis of global climate change: a review. *Environmental Science and Pollution Research*, 28, 24872-24888.

Bansal, S., Johnson, O.F., Meier, J. and Zhu, X., 2020. Vegetation affects timing and location of wetland methane emissions. Journal of Geophysical Research: *Biogeosciences*, 125(9), 2020JG005777.

Bansal, S., Tangen, B. and Finocchiaro, R., 2016. Temperature and hydrology affect methane emissions from prairie pothole wetlands. *Wetlands,* 36(Suppl 2), 371-381.

Bastviken, D., Treat, C.C., Pangala, S.R., Gauci, V., Enrich-Prast, A., Karlson, M., Gålfalk, M., Romano, M.B. and Sawakuchi, H.O., 2023. The importance of plants for methane emission at the ecosystem scale. *Aquatic Botany*, 184, 103596.

BirdLife South Africa., 2006. Available at: http://www.birdlife.org.za/wakkerstroom/

Brantley, H.L., Thoma, E.D., Squier, W.C., Guven, B.B. and Lyon, D., 2014. Assessment of methane emissions from oil and gas production pads using mobile measurements. *Environmental science & technology*, 48(24), 14508-14515.

Brix, H., Sorrell, B. K. & Lorenzen, B. Are *Phragmites*-dominated wetlands a net source or net sink of greenhouse gases? 2001. *Aquatic Botany,* 69, 313–324.

Brooker, M.R., Bohrer. G., Mouser P.J., 2014. Variations in potential CH_4 fux and CO_2 respiration from freshwater wetland sediments that differ by microsite location, depth and temperature. *Ecological Engineering,* 72:84–94.

Browning, J. 1992. Studies in Cyperaceae in southern Africa. 20: Changed status of *Schoenoplectus corymbosus var. brachyceras* and report of hybrids. *South African Journal of Botany,* 58(6), 530-532.

Brownlow, R., Lowry, D., Fisher, R. E., France, J. L., Lanoisellé, M., White, B., Wooster, M. J., Zhang, T., and Nisbet, E. G., 2017. Isotopic Ratios of Tropical Methane Emissions by Atmospheric Measurement. *Global Biogeochem*ical *Cycle*, 31, 1408–1419.

Brownlow, R., Lowry, D., Fisher, R. E., France, J. L., Lanoisellé, M., White, B., Nisbet, E. G., 2017. Isotopic ratios of tropical methane emissions by atmospheric measurement. *Global Biogeochemical Cycles*, 31, 1408–1419.

Bruhl, J.J. and Wilson, K.L., 2007. Towards a comprehensive survey of C_3 and C_4 photosynthetic pathways in Cyperaceae. *Aliso: A Journal of Systematic and Floristic Botany*, *23*(1), 99-148.

Calabrese, S., Garcia, A., Wilmoth, J.L., Zhang, X. and Porporato, A., 2021. Critical inundation level for methane emissions from wetlands. *Environmental Research Letters*, 16(4), 044038.

Cao, X., Huang, W., Huang, D., Tian, Y., Jiang, X. and Zhang, J., 2017. Effects of plant species on CH_4 emission from integrated vertical subsurface flow constructed wetlands. *Desalination and Water Treatment*, 85, 358-364.

Center, A.R.C. and Eltschlager, K.K., 2001. Technical measures for the investigation and mitigation of fugitive methane hazards in areas of coal mining. *The Office of Surface Mining Reclamation and Enforcement,* 75-85.

Chang, T.C. and Yang, S.S., 2003. Methane emission from wetlands in Taiwan. *Atmospheric*

Environment, 37(32), 4551-4558.

Cohen, B. and Winkler, H., 2014. Greenhouse gas emissions from shale gas and coal for electricity generation in South Africa. *South African Journal of Science*, 110(3-4), 01-05.

Crutzen, P.J. & Lelieveld, J., 2001. Human impacts on atmospheric chemistry. *Annual Review of Earth and Planetary Sciences*, 29(1), 17– 45.

Dacey, J.W., 1981. Pressurized ventilation in the yellow waterlily. *Ecology*, 62(5), 1137-1147.

De Gouw, J.A., Veefkind, J.P., Roosenbrand, E., Dix, B., Lin, J.C., Landgraf, J. and Levelt, P.F., 2020. Daily satellite observations of methane from oil and gas production regions in the United States. *Scientific reports*, 10(1), 1379.

Deng, Y., Liu, P. and Conrad, R., 2019. Effect of temperature on the microbial community responsible for methane production in alkaline NamCo wetland soil. *Soil Biology and Biochemistry*, 132, 69-79.

Department of Forestry, Fisheries and the Environment (DFFE). 2023. South Africa's 5th Biennial Update Report (BUR-5) to the United Nations Framework Convention on Climate Change (UNFCCC). Republic of South Africa. Available at: https://www4.unfccc.int/sites/SubmissionsStaging/NationalReports/Documents/34185207_South%20Africa-BUR5-1-Fifth%20Biennial%20Update%20Report%20%20of%20South%20Africa%20Submission%20to%20UNFCCC.pdf (Accessed: 15 August 2024).

Dlugokencky, E. J., Bruhwiler, L., White, J. W. C., Emmons, L. K., Novelli, P. C., Montzka, S. A., *et al*., 2009. Observational constraints on recent increases in the atmospheric CH_4 burden. *Geophysical Research Letters*, 36(18).

Dlugokencky, E. J., Nisbet, E. G., Fisher, R., & Lowry, D., 2011. Global atmospheric methane: budget, changes, and dangers. *Philosophical Transactions of the Royal Society A: Mathematical, Physical and Engineering Sciences*, 369(1943), 2058-2072.

Fang, S., Tans, P.P., Yao, B., Luan, T., Wu, Y. and Yu, D. 2017. Study of atmospheric CO_2 and CH_4 at Longfengshan WMO/GAW regional station: The variations, trends, influence of local sources/sinks, and transport. *Science China Earth Sciences*, 60, 1886-1895.

Fang, S.X., Zhou, L.X., Masarie, K.A., Xu, L. and Rella, C.W., 2013. Study of atmospheric CH_4 mole fractions at three WMO/GAW stations in China. *Journal of Geophysical Research: Atmospheres*, 118(10), 4874-4886.

Farnsworth, E.J. and Meyerson, L.A., 2003. Comparative ecophysiology of four wetland plant species along a continuum of invasiveness. *Wetlands*, *23*(4), 750-762.

Feig, G.T., Mudau, T.E., Piketh, S. *et al*. 2016. Atmospheric Methane characterisation over the South African interior. *Proceedings of the 2016 Conference of the National Association for Clean Air (NACA), Nelspruit, South Africa*.

Fiehn, A., Eckl, M., Kostinek, J., Gałkowski, M., Gerbig, C., Rothe, M., Röckmann, T., Menoud, M., Maazallahi, H., Schmidt, M. and Korbeń, P., 2023. Source apportionment of methane emissions from the Upper Silesian Coal Basin using isotopic signatures. *Atmospheric Chemistry and Physics*, *23*(24), 15749-15765.

Fiehn, A., Eckl, M., Kostinek, J., Gałkowski, M., Gerbig, C., Rothe, M., Röckmann, T., Menoud, M., Maazallahi, H., Schmidt, M. and Korbeń, P., 2023. Source apportionment of methane emissions from the Upper Silesian Coal Basin using isotopic signatures. *Atmospheric Chemistry and Physics*, 23(24), 15749-15765.

Fisher, R. E., *et al*. 2017. Measurement of the ^{13}C isotopic signature of methane emissions from northern European wetlands, *Global Biogeochemical Cycles*, 31, 605–623.

Fisher, R., Lowry, D., Wilkin, O., Sriskantharajah, S., & Nisbet, E. G., 2006. High-precision, automated stable isotope analysis of atmospheric methane and carbon dioxide using continuous-flow isotope-ratio mass spectrometry. *Rapid Communications in Mass Spectrometry: An International Journal Devoted to the Rapid Dissemination of Up-to-the-Minute Research in Mass Spectrometry*, 20(2), 200-208.

Forrester, L., Lim, Y.H. and Usher, I., 2017. New advances in mine site gas analysis using gas chromatographs. *Proceedings of the 17th Coal Operators' Conference, Mining Engineering*, *University of Wollongong*, 314-325.

France, J.L., Fisher, R.E., Lowry, D., Allen, G., Andrade, M.F., Bauguitte, S.J.B., Bower, K., Broderick, T.J., Daly, M.C., Forster, G. and Gondwe, M., 2022a. $\delta^{13}C$ methane source signatures from tropical wetland and rice field emissions. *Philosophical Transactions of the Royal Society A*, 380(2215), p.20200449.

France, J.L., Lunt, M.F., Andrade, M., Moreno, I., Ganesan, A.L., Lachlan-Cope, T., Fisher, R.E., Lowry, D., Parker, R.J., Nisbet, E.G. and Jones, A.E., 2022b. Very large fluxes of methane measured above Bolivian seasonal wetlands. *Proceedings of the National Academy of Sciences*, 119(32), p.e2206345119.

Ganesan, A.L., Stell, A.C., Gedney, N., Comyn-Platt, E., Hayman, G., Rigby, M., Poulter, B. and Hornibrook, E.R.C., 2018. Spatially resolved isotopic source signatures of wetland methane emissions. *Geophysical Research Letters*, 45(8), 3737-3745.

Gatland, J.R., Santos, I.R., Maher, D.T., Duncan, T.M. and Erler, D.V., 2014. Carbon dioxide and methane emissions from an artificially drained coastal wetland during a flood: Implications for wetland global warming potential. *Journal of Geophysical Research: Biogeosciences*, *119*(8), 1698-1716.

Ge, Z.M., Zhang, L.Q., Yuan, L. and Zhang, C., 2014. Effects of salinity on temperature-dependent photosynthetic parameters of a native C_3 and a non-native C_4 marsh grass in the Yangtze Estuary, China. *Photosynthetica*, *52*(4), 484-492.

GÜLŞEN, H. and YAPICIOĞLU, P., 2021. Minimizing Greenhouse Gas Emissions from a Horizontal Subsurface Flow Constructed Wetland. *Turkish Journal of Water Science and Management*, *5*(2), 247-270.

Hardy, J. T. 2003. Climate change: causes, effects, and solutions. John Wiley & Sons.

Hegerl, G. C., Brönnimann, S., Cowan, T., Friedman, A. R., Hawkins, E., Iles, C., ... & Undorf, S., 2019. Causes of climate change over the historical record. *Environmental Research Letters*,

14(12), 123006.

Hornsey, M. J., & Fielding, K. S., 2020. Understanding (and reducing) inaction on climate change. *Social Issues and Policy Review*, 14(1), 3-35.

Hough, R.A. and Wetzel, R.G., 1977. Photosynthetic pathways of some aquatic plants. *Aquatic Botany*, *3*, pp.297-313.

Hu, H., Landgraf, J., Detmers, R.,Borsdorff, T., Aan de Brugh, J.,Aben, I., *et al*., 2018. Toward global mapping of methane with TROPOMI: First results and intersatellite comparison to GOSAT. *Geophysical Research Letters*, 45, 3682–3689.

Inamori, R., Gui, P., Dass, P., Matsumura, M., Xu, K.Q., Kondo, T., Ebie, Y. and Inamori, Y., 2007. Investigating CH_4 and N_2O emissions from eco-engineering wastewater treatment processes using constructed wetland microcosms. *Process Biochemistry*, 42(3), 363-373.

Inglett, K. S., Inglett, P. W., Reddy, K. R., & Osborne, T. Z., 2012. Temperature sensitivity of greenhouse gas production in wetland soils of different vegetation. *Biogeochemistry,* 108, 77-90.

IPCC, 2022. Climate Change 2022: Impacts, Adaptation, and Vulnerability. Contribution of Working Group II to the Sixth Assessment Report of the Intergovernmental Panel on Climate Change [H.-O. Pörtner, D.C. Roberts, M. Tignor, E.S. Poloczanska, K. Mintenbeck, A. Alegría, M. Craig, S. Langsdorf, S. Löschke, V. Möller, A. Okem, B. Rama (eds.)]. Cambridge University Press. In Press.

Jansen, J., Woolway, R.I., Kraemer, B.M., Albergel, C., Bastviken, D., Weyhenmeyer, G.A., Marce, R., Sharma, S., Sobek, S., Tranvik, L.J. and Perroud, M., 2022. Global increase in methane production under future warming of lake bottom waters. *Global change biology*, 28(18), 5427-5440.

Javadinejad, S., Eslamian, S. & Ostad-Ali-Askari, K., 2019. Investigation of monthly and seasonal changes of methane gas with respect to climate change using satellite data. *Applied Water Science,* 9, 180.

Jiménez-Mejías, P., Luceño, M. and Castroviejo, S., 2007. *Schoenoplectus corymbosus*: a tropical Old-World sedge (*Cyperaceae*) discovered in Spain and Morocco. *Nordic Journal of Botany*, 25: 70-74.

Johnson, O.F., Panda, A., Lishawa, S.C. and Lawrence, B.A., 2021. Repeated large-scale mechanical treatment of invasive *Typha* under increasing water levels promotes floating mat formation and wetland methane emissions. *Science of the Total Environment*, 790, 147920.

Jones, M.B., 1988. Photosynthetic responses of C_3 and C_4 wetland species in a tropical swamp. *The Journal of Ecology*, pp.253-262.

Juszczak, R. and Augustin, J., 2013. Exchange of the greenhouse gases methane and nitrous oxide between the atmosphere and a temperate peatland in central Europe. *Wetlands*, 33, 895-907.

Kammann, C., Hepp, S., Lenhart, K. and Müller, C., 2009. Stimulation of methane consumption by endogenous CH_4 production in aerobic grassland soil. *Soil Biology and Biochemistry*, 41(3), 622-629.

Karoff, C. and Vara-Vela, A.L., 2023. Data driven analysis of atmospheric methane concentrations as function of geographic, land cover type and season. *Frontiers in Earth Science*, *11*, 1119977.

Keeling, C. D., 1958. The concentration and isotopic abundances of atmospheric carbon dioxide in rural areas. *Geochimica et Cosmochim*ica *Acta*, 13, 322–334.

Keppler, F., Hamilton, J. T. G., Braß, M., and Röckmann, T., 2006. Methane emissions from terrestrial plants under aerobic conditions. *Nature*, 439, 187–191.

Keppler, F., Schiller, A., Ehehalt, R., Greule, M., Hartmann, J., and Polag, D., 2016. Stable isotope and high precision concentration measurements confirm that all humans produce and exhale methane. *Journal of Breath Research*, 10.

Kim, J., Lee, J., Yun, J., Yang, Y., Ding, W., Yuan, J. and Kang, H., 2020. Mechanisms of

enhanced methane emission due to introduction of *Spartina anglica* and *Phragmites australis* in a temperate tidal salt marsh. *Ecological Engineering*, 153, 105905.

Kirschke, S., Bousquet, P., Ciais, P. *et al.* 2013. Three decades of global methane sources and sinks. *Nature Geosci*ence, 6, 813–823.

Kiviat, E. 2013. Ecosystem services of *Phragmites* in North America with emphasis on habitat functions. *AoB plants*, *5*, p.plt008.

Knapp, A.K. and Yavitt, J.B., 1992. Evaluation of a closed-chamber method for estimating methane emissions from aquatic plants. *Tellus B*, 44(1), 63-71.

Korrensalo, A., Mammarella, I., Alekseychik, P., Vesala, T. and Tuittila, E.S., 2022. Plant mediated methane efflux from a boreal peatland complex. *Plant and Soil*, p1-18.

Kosmack, D., 2008. Capture and use of coal mine ventilation air methane. *Consol Energy Incorporated*.

Kotze, D.C., Breen, C.M. and Klug, J.R., 1994. A management plan for Wakkerstroom Vlei. In: Oellermann, R.G., Darroch, M.A.G., Klug, J.R. and Kotze, D.C. (eds), Wetland preservation valuation, and management practices applied to wetlands: South African case studies. WRC Report No. 501/5/94. Pretoria: *Water Research Commission*.

Kozinc, J., Zupančič-Kralj, L. and Zapušek, A., 2004. Evaluation of gas emissions from coal stockpile. *Chemosphere*, 55(8), 1121-1126.

Krüger, J.P., Gerold, G., Beckedahl, H. and Jungkunst, H.F., 2012. Effect of environmental conditions on methane and nitrous oxide fluxes of two South African wetlands. Geo-öko, 33(1-2), 66-88.

Kvenvolden, K. A., 1995. A review of the geochemistry of methane in natural gas hydrate. *Organic Geochemistry*, 23, 997–1008.

Labuschagne, C., Kuyper, B., Brunke, E. G., Mokolo, T., Van der Spuy, D., Martin, L., *et al* & Joubert, W., 2018. A review of four decades of atmospheric trace gas measurements at Cape

Point, South Africa. *Transactions of the Royal Society of South Africa*, 73(2), 113-132.

Laing, G. D., Tack, F. M. G., & Verloo, M. G., 2003. Performance of selected destruction methods for the determination of heavy metals in reed plant (*Phragmites australis*). *Analytica Chimica Acta*, 479, 191-198.

Lan, X., Nisbet, E. G., Dlugokencky, E. J., & Michel, S. E., 2021. What do we know about the global methane budget? Results from four decades of atmospheric CH_4 observations and the way forward. *Philosophical Transactions of the Royal Society A*, 379(2210), 20200440.

Lawrence, B.A., Lishawa, S.C., Hurst, N., Castillo, B.T. and Tuchman, N.C., 2017. Wetland invasion by *Typha* × *glauca* increases soil methane emissions. *Aquatic Botany*, 137, 80-87.

Liu, S., Fang, S., Liu, P., Liang, M., Guo, M. and Feng, Z., 2021. Measurement report: Changing characteristics of atmospheric CH_4 in the Tibetan Plateau: records from 1994 to 2019 at the Mount Waliguan station. *Atmospheric Chemistry and Physics*, *21*(1), 393-413.

Lu, X., Harris, S.J., Fisher, R.E., France, J.L., Nisbet, E.G., Lowry, D., Röckmann, T., van der Veen, C., Menoud, M., Schwietzke, S. and Kelly, B.F., 2021. Isotopic signatures of major methane sources in the coal seam gas fields and adjacent agricultural districts, Queensland, Australia. *Atmospheric chemistry and physics*, 21(13), 10527-10555.

MacDonald, J.A., Fowler, D., Hargreaves, K.J., Skiba, U., Leith, I.D. and Murray, M.B., 1998. Methane emission rates from a northern wetland; response to temperature, water table and transport. *Atmospheric Environment*, *32*(19), 3219-3227.

Makgetla, N. and Patel, M., 2021. The coal value chain in South Africa. *Trade & Industrial Policy Strat*egies Pretoria.

Mal, T.K. and Narine, L., 2004. The biology of Canadian weeds, *Phragmites australis (Cav.) Trin. ex Steud*. *Canadian Journal of Plant Science*, *84*(1), 365-396.

Marín-Muñiz J.L, Hernández ME, Moreno-Casasola P., 2015. Greenhouse gas emissions from coastal freshwater wetlands in Veracruz Mexico: effect of plant community and seasonal

dynamics. *Atmospheric Environment,* 107:107–117.

Masoko, P., Mokgotho, M. P., Mbazima, V. G., & Mampuru, L. J., 2008. Biological activities of *Typha capensis (Typhaceae)* from Limpopo Province (South Africa). *African Journal of Biotechnology*, 7(20).

McArdle, B.H., 1988. The structural relationship: regression in biology. *Canadian Journal of Zoology*, *66*(11), 2329-2339.

McCartney, M., Morardet, S., Rebelo, L.M., Finlayson, C.M. and Masiyandima, M., 2011. A study of wetland hydrology and ecosystem service provision: GaMampa wetland, South Africa. *Hydrological sciences journal*, 56(8), 1452-1466.

Mikhaylov, A., Moiseev, N., Aleshin, K., & Burkhardt, T., 2020. Global climate change and greenhouse effect. *Entrepreneurship and Sustainability Issues*, 7(4), 2897.

Milke, J., Gałczyńska, M. and Wróbel, J., 2020. The importance of biological and ecological properties of *Phragmites australis (Cav.) Trin. Ex Steud*., in phytoremendiation of aquatic ecosystems—the review. *Water*, *12*(6), 1770.

Moeletsi, M.E. and Tongwane, M.I. 2015. 2004 methane and nitrous oxide emissions from manure management in South Africa. *Animals,* 5(2), 193-205.

MOYA/ZWAMPS Team, Nisbet, E.G., Allen, G., Fisher, R.E., France, J.L., Lee, J.D., Lowry, D., Andrade, M.F., Bannan, T.J., Barker, P. and Bateson, P., 2022. Isotopic signatures of methane emissions from tropical fires, agriculture and wetlands: the MOYA and ZWAMPS flights. *Philosophical Transactions of the Royal Society A*, *380*(2215), 20210112.

Mu, J., Qi, J., Yu, H., Hu, C., Mu, Y. and Qu, J., 2022. Dynamic chamber as a more reliable technique for measuring methane emissions from aquatic ecosystems. *Science of The Total Environment*, 851, 158147.

Musara, C. and Aladejana, E.B., 2020. *Typha capensis (Rohrb.) NE Br.(Typhaceae)*: morphology, medicinal uses, biological and chemical properties. *Plant Science Today*, *7*(4), 578-583.

Nisbet, E. G., Dlugokencky, E. J., Manning, M. R., Lowry, D., Fisher, R. E., France, J. L., Michel, S. E., Miller, J. B., White, J. W. C., Vaughn, B., Bousquet, P., Pyle, J. A., Warwick, N. J., Cain, M., Brownlow, R., Zazzeri, G., Lanoisellé, M., Manning, A. C., Gloor, E., Worthy, D. E. J., Brunke, E. G., Labuschagne, C., Wolff, E. W., and Ganesan, A. L.: Rising atmospheric methane: 2007–2014 growth and isotopic shift. 2016. *Global Biogeochemical Cycles*, 30, 1356–1370.

Nisbet, E. G., Dlugokencky, E. J., Manning, M. R., Lowry, D., Fisher, R. E., France, J. L., Ganesan, A. L. 2016. Rising atmospheric methane: 2007–2014 growth and isotopic shift. *Global Biogeochemical Cycles*, 30(9), 1356-1370.

Nisbet, E.G., M.R. Manning *et al*., 2019. Very strong atmospheric methane growth in the 4 years 2014–2017: Implications for the Paris Agreement. *Global Biogeochemical Cycles*, 33, 318–342.

Otter, L.B. and Scholes, M.C., 2000. Methane sources and sinks in a periodically flooded South African savanna. *Global Biogeochemical Cycles*, *14*(1), 97-111.

Pandey, S., Houweling, S., Lorente, A., Borsdorff, T., Tsivlidou, M., Bloom, A.A., Poulter, B., Zhang, Z. and Aben, I., 2021. Using satellite data to identify the methane emission controls of South Sudan's wetlands. *Biogeosciences*, 18(2), 557-572.

Plant, G., Kort, E.A., Murray, L.T., Maasakkers, J.D. and Aben, I., 2022. Evaluating urban methane emissions from space using TROPOMI methane and carbon monoxide observations. *Remote Sensing of Environment*, 268, 112756.

Preston-Whyte, R. A., & Tyson, P. D., 1988. Atmosphere and weather of southern Africa. Oxford University Press.

Quay, P., Stutsman, J., Wilbur, D., Snover, A., Dlugokencky, E., and Brown, T.: The isotopic composition of atmospheric methane. 1999. *Global Biogeochemical Cycles,* 13, 445–461.

Raghuvanshi, M.S., Sawal, R.K., Landol, S., Dorje, N., Pandey, L., Enoch, S., Raza, M. and Saxena, A., 2023. Invasive Common Reed (*Phragmites australis (Cav.) Trin. ex Steud.)*: A Serious Ecological Threat to Ladakh Tethys Himalayan Biodiversity in Changing Climate. *American Journal of Climate Change*, 12(3), 321-334.

Reagan, M. T., & Moridis, G. J. 2008. Dynamic response of oceanic hydrate deposits to ocean temperature change. *Journal of Geophysical Research: Oceans*, 113(C12).

Rey-Sanchez, A. C., Morin, T. H., Stefanik, K. C., Wrighton, K., & Bohrer, G., 2018. Determining total emissions and environmental drivers of methane flux in a Lake Erie estuarine marsh. *Ecological Engineering*, 114, 7-15.

Rice, D., 1993. Composition and origins of coalbed gas. *Hydrocarbons from coal, AAPG Studies in Geology*, 38, 159–184.

RStudio., 2020. Integrated Development for R. RStudio, PBC, Boston, MA URL http://www.rstudio.com/

Rubino, M., D.M. Etheridge *et al*., 2019. Revised records of atmospheric trace gases CO_2, CH_4, N_2O, and $\delta^{13}C$-CO_2 over the last 2000 years from Law Dome, Antarctica. *Earth System Science Data*, 11(2), 473–492,

Sadavarte, P., Pandey, S., Maasakkers, J.D., Lorente, A., Borsdorff, T., Denier van der Gon, H., Houweling, S. and Aben, I., 2021. Methane emissions from superemitting coal mines in Australia quantified using TROPOMI satellite observations. *Environmental Science & Technology*, 55(24), 16573-16580.

Saunois, M., Bousquet, P., Poulter, B., Peregon, A., Ciais, P., Canadell, J. G., Zhu, Q., 2016. The global methane budget: 2000–2012. *Earth System Science Data Discussions*, 1-79.

Saunois, M., Stavert, A.R., Poulter, B., Bousquet, P., Canadell, J.G., Jackson, R.B., Raymond, P.A., Dlugokencky, E.J., Houweling, S., Patra, P.K. and Ciais, P., 2020. The global methane

budget 2000–2017. *Earth system science data*, 12(3), 1561-1623.

Schipper, L.A. and Reddy, K.R., 1994. Methane production and emissions from four reclaimed and pristine wetlands of southeastern United States. *Soil Science Society of America Journal*, *58*(4), 1270-1275.

Schroll, M., Keppler, F., Greule, M., Eckhardt, C., Zorn, H. and Lenhart, K., 2020. The stable carbon isotope signature of methane produced by saprotrophic fungi. *Biogeosciences*, 17(14), 3891-3901.

Schultz, R.E. and Pett, L., 2018. Plant community effects on CH_4 fluxes, root surface area, and carbon storage in experimental wetlands. *Ecological engineering*, *114*, 96-103.

Schweingruber, F.H., Kučerová, A., Adamec, L. and Doležal, J., 2020. Anatomic atlas of aquatic and wetland plant stems. *Springer Nature*.

Shaw, J. T., Allen, G., Barker, P., Pitt, J. R., Pasternak, D., Bauguitte, S. J.-B., *et al*., 2022. Large methane emission fluxes observed from tropical wetlands in Zambia. *Global Biogeochemical Cycles,* 36, e2021GB007261.

Shen, L., Zavala-Araiza, D., Gautam, R., Omara, M., Scarpelli, T., Sheng, J., Sulprizio, M.P., Zhuang, J., Zhang, Y., Qu, Z. and Lu, X., 2021. Unravelling a large methane emission discrepancy in Mexico using satellite observations. *Remote Sensing of Environment*, 260, 112461.

Shikwambana, L.; Mokgoja, B.; Mhangara, P., 2022. A Qualitative Assessment of the Trends, Distribution and Sources of Methane in South Africa. *Sustainability,* 14, 3528.

Shode, F. O., Mahomed, A. S., & Rogers, C. B., 2002. Typhaphthalide and typharin, two phenolic compounds from *Typha capensis*. *Phytochemistry*, 61(8), 955-957.

Silva, R., Pires, M., Azevedo, C.M., Fagundes, L., Garavaglia, L. and Gomes, C.J., 2010. Monitoring light hydrocarbons in Brazilian coal mines and in confined coal samples. *International journal of coal geology*, 84(3-4), 269-275.

Snowden, G.E., 2009. Population Level Variation in Growth of the C_3 Salt Marsh Sedge, *Schoenoplectus americanus*, and Its Potential Effects on Ecosystem Function (Master's thesis). University of Notre Dame.

Sokal, R.R. and Rohlf, F.J., 1981. Taxonomic congruence in the *Leptopodomorpha* re-examined. *Systematic Zoology*, *30*(3), 309-325.

Sriskantharajah, S., Fisher, R.E., Lowry, D., Aalto, T., Hatakka, J., Aurela, M., Laurila, T., Lohila, A., Kuitunen, E. and Nisbet, E.G., 2012. Stable carbon isotope signatures of methane from a Finnish subarctic wetland. Tellus B: *Chemical and Physical Meteorology*, 64(1), 18818.

Srivastava, J., Kalra, S.J. and Naraian, R., 2014. Environmental perspectives of *Phragmites australis (Cav.) Trin. Ex. Steudel*. *Applied Water Science*, *4*(3), 193-202.

Stern, D. I., & Kaufmann, R. K., 2014. Anthropogenic and natural causes of climate change. *Climatic change*, 122, 257-269.

Stockdale, V.A., Furniss, D.G. and Scholes, M.C., 2021. An Assessment of Wakkerstroom Wetland and Its Vegetation Communities from 1938 to 2019. *Journal of Water Resource and Protection*, 13, 807-821. https://doi.org/10.4236/jwarp.2021.1310043

Svensson, B.H. and Rosswall, T., 1984. In situ methane production from acid peat in plant communities with different moisture regimes in a subarctic mire. *Oikos*, 341-350.

Tongwane, M.I. and Moeletsi, M.E., 2020. Emission factors and carbon emissions of methane from enteric fermentation of cattle produced under different management systems in South Africa. *Journal of Cleaner Production*, 265, 121931.

Turner, A.J., Jacob, D.J., Benmergui, J., Brandman, J., White, L. and Randles, C.A., 2018. Assessing the capability of different satellite observing configurations to resolve the distribution of methane emissions at kilometer scales. *Atmospheric Chemistry and Physics*, 18(11), 8265-8278.

van den Berg, M., Ingwersen, J., Lamers, M. and Streck, T., 2016. The role of *Phragmites* in

the CH_4 and CO_2 fluxes in a minerotrophic peatland in southwest Germany. *Biogeosciences*, 13(21), 6107-6119.

van den Berg, M., van den Elzen, E., Ingwersen, J., Kosten, S., Lamers, L. P., & Streck, T., 2020. Contribution of plant-induced pressurized flow to CH_4 emission from a *Phragmites* fen. *Scientific reports*, 10(1), 12304.

Van Der Gon, H.D. and Neue, H.U., 1995. Influence of organic matter incorporation on the methane emission from a wetland rice field. *Global biogeochemical cycles*, *9*(1), 11-22.

Van Der Nat, F.F.W., Middelburg*, J.J., Van Meteren, D. and Wielemakers, A. 1998. Diel methane emission patterns from *Scirpus lacustris* and *Phragmites australis*. *Biogeochemistry*, *41*, pp.1-22.

Van Deventer, H., & Cho, M. A., 2014. Assessing leaf spectral properties of *Phragmites australis* impacted by acid mine drainage. *South African Journal of Science*, 110(7-8), 1-12.

Van Wyk, B. E., Oudtshoorn, B. V., & Gericke, N., 1997. Medicinal Plants of South Africa. Briza.

Vigano, I., Röckmann, T., Holzinger, R., van Dijk, A., Keppler, F., Greule, M., Brand, W. A., Geilmann, H., and van Weelden, H., 2009. The stable isotope signature of methane emitted from plant material under UV irradiation. *Atmospheric Environ*ment, 43, 5637–5646, https://doi.org/10.1016/j.atmosenv.2009.07.046.
wakkerstroom.cfm.

Wali, S.U., 2022. Methane emissions and soil carbon in floodplain wetlands of the Macquarie Marshes (Doctoral dissertation, Macquarie University).

Wang, Z., Li, K., Shen, X., Yan, F., Zhao, X., Xin, Y., Ji, L., Xiang, Q., Xu, X., Li, D. and Ran, J., 2023. Soil nitrogen substances and denitrifying communities regulate the anaerobic oxidation of methane in wetlands of Yellow River Delta, China. *Science of the Total*

Environment, 857, 159439.

Weber, E.U. and Stern, P.C., 2011. Public understanding of climate change in the United States. *American Psychologis*t, 66(4), 315.

Were, D., Kansiime, F., Fetahi, T. and Hein, T., 2021. Carbon dioxide and methane fluxes from various vegetation communities of a natural tropical freshwater wetland in different seasons. *Environmental Processes*, 8, 553-571.

Were, D., Kansiime, F., Fetahi, T., Cooper, A. and Jjuuko, C., 2019. Carbon sequestration by wetlands: a critical review of enhancement measures for climate change mitigation. *Earth Systems and Environment*, *3*, 327-340.

Wesley, D., Dallimore, S., MacLeod, R., Sachs, T. and Risk, D., 2023. Characterization of atmospheric methane release in the outer Mackenzie River delta from biogenic and thermogenic sources. *The Cryosphere*, 17(12), 5283-5297.

Whigham, D.F., Kudoh, A., Megonigal, J.P., Langley, J.A., Noyce, G.L. and Sakai, T., 2023. Reproductive responses to increased density and global change drivers in a widespread clonal wetland species, *Schoenoplectus americanus*. *Research Square*.

Whiticar, M. J., 1996. Stable isotope geochemistry of coals, humic kerogens and related natural gases. *International J*ournal of *Coal Geol*ogy, 32, 191–215.

Whiting, G.J. and Chanton, J.P., 2001. Greenhouse carbon balance of wetlands: methane emission versus carbon sequestration. *Tellus B*, *53*(5), 521-528.

Whiting, G.J. and Chanton, J.P., 1992. Plant-dependent CH_4 emission in a subarctic Canadian fen. *Global biogeochemical cycles*, *6*(3), 225-231.

Yang, H., Tang, J., Zhang, C., Dai, Y., Zhou, C., Xu, P., Perry, D.C. and Chen, X. 2020. Enhanced carbon uptake and reduced methane emissions in a newly restored wetland. *Journal of Geophysical Research: Biogeosciences*, *125*(1), p.e2019JG005222.

Yavitt, J. B., Kryczka, A. K., Huber, M. E., Pipes, G. T., & Rodriguez, A. M., 2019. Inferring methane production by decomposing tree, shrub, and grass leaf litter in bog and rich fen peatlands. *Frontiers in Environmental Science*, 7, 182.

Yu, K., Hiscox, A. and DeLaune, R.D., 2013. Greenhouse gas emission by static chamber and eddy flux methods. *Methods in biogeochemistry of wetlands*, 10, 427-437.

Zazzeri, G., Lowry, D., Fisher, R.E., France, J.L., Lanoisellé, M. and Nisbet, E.G., 2015. Plume mapping and isotopic characterisation of anthropogenic methane sources. *Atmospheric Environment*, *110*, 151-162.

Zeleke, T.T., Lukwasa, A.Z.W., Beketie, K.T. and Ayal, D.Y., 2024. Analysis of spatio-temporal precipitation and temperature variability and trend over Sudd-Wetland, Republic of South Sudan. *Climate Services*, *34*, 100451.

Zhang, J., Han, G., Mao, H., Pei, Z., Ma, X., Jia, W. and Gong, W. 2022. The spatial and temporal distribution patterns of total column averaged dry-air mole fraction of methane in China: New observations from TROPOMI. *Atmosphere*, 13(2), 177.

Zhu, T., Bian, W., Zhang, S., Di, P. and Nie, B., 2017. An improved approach to estimate methane emissions from coal mining in China. *Environmental science & technology*, 51(21), 12072-12080.